

DISSERTATION

In vitro investigation of the role of *Helicobacter pylori* urease in repair mechanisms of gastric epithelial cells and cytokine release by monocyte derived dendritic cells

Ausgeführt zum Zwecke der Erlangung des akademischen Grades eines
Doktors der Naturwissenschaften unter der Leitung von

Univ.-Prof. Dipl.-Ing. Dr. techn. Peter Christian Kubicek

Inst. f. Verfahrenstechnik, Umwelttechnik und Techn. Biowissenschaften

Eingereicht an der Technischen Universität Wien

Fakultät für Technische Chemie

von

Zsuzsanna Kovách

Matrikelnummer 0126765

Wien, Februar 2006.

Content

1	KURZFASSUNG	1
2	ABSTRACT.....	4
3	INTRODUCTION	7
3.1	HELICOBACTER PYLORI.....	7
3.1.1	<i>Epidemiology and transmission.....</i>	7
3.1.2	<i>Morphology.....</i>	8
3.1.3	<i>Genomics.....</i>	8
3.1.4	<i>Pathophysiology.....</i>	9
3.1.4.1	<i>Mucosal wound repair mechanisms.....</i>	11
3.1.4.2	<i>Transforming growth factor (TGF-β).....</i>	12
3.1.4.3	<i>Heparin binding epidermal growth factor-like growth factor.....</i>	13
3.1.5	<i>Adaptation to acidic environment.....</i>	13
3.1.6	<i>Motility and chemotaxis.....</i>	14
3.1.7	<i>Virulence factors.....</i>	16
3.1.8	<i>Adhesion to host cells.....</i>	19
3.2	UREASE.....	20
3.2.1	<i>Genetic and molecular assembly.....</i>	22
3.2.2	<i>Native protein structure.....</i>	24
3.2.3	<i>Localization.....</i>	25
3.3	CYTOKINES.....	26
3.3.1	<i>Genetic predisposition.....</i>	30
3.4	IMMUNE RESPONSE.....	30
3.4.1	<i>The gastric mucosa as the first line of defense.....</i>	30
3.4.2	<i>Humoral immune response.....</i>	31
3.4.3	<i>Cellular immune response.....</i>	31
3.5	DENDRITIC CELLS.....	32
3.5.1	<i>DC-T cell Interaction.....</i>	35
3.5.2	<i>Antigen uptake.....</i>	37
3.5.3	<i>Helicobacter pylori and Dendritic cell interaction.....</i>	37
3.5.4	<i>Role in peripheral tolerance mechanisms.....</i>	38
3.6	PERSISTENCE OF INFECTION.....	39
4	AIM OF THE STUDY.....	42
5	MATERIALS AND METHODS.....	43
5.1	BACTERIA AND CULTURE CONDITIONS.....	43
5.2	GENETIC COMPLEMENTATION OF MUTANT N6UREB::TNKM.....	44
5.2.1.1	<i>Electroporation.....</i>	45
5.2.1.2	<i>Characterization of complemented clones.....</i>	45
5.3	SDS-PAGE AND WESTERN BLOTTING TO DETECT H. PYLORI UREASE.....	46
5.4	MODIFIED LOWRY PROTEIN ASSAY.....	47
5.5	UREASE ACTIVITY.....	48
5.5.1	<i>Semiquantitative urease test.....</i>	48
5.5.2	<i>Urease specific activity using the Berthelot and Lowry method.....</i>	48
5.6	PURIFICATION OF SURFACE ASSOCIATED H. PYLORI UREASE.....	49
5.6.1	<i>Preparation of water extract of H. pylori.....</i>	49
5.6.2	<i>Column chromatography.....</i>	49
5.7	PURIFICATION OF RECOMBINANT UREASE.....	51
5.7.1	<i>Culture media and overexpression conditions.....</i>	52

5.7.2	<i>Purification of the His-tagged proteins</i>	53
5.8	HB-EGF EXPRESSION BY KATO III CELLS	55
5.8.1	<i>Tissue culture cell line Kato III</i>	55
5.8.1.1	Stimulation of Kato III cells	55
5.8.2	<i>RNA isolation</i>	55
5.8.3	<i>cDNA synthesis</i>	56
5.8.4	<i>Quantitative Real-time RT-PCR</i>	56
5.8.4.1	Theoretical basis	56
5.8.4.2	Primers and TaqMan probes for real-time RT-PCR	58
5.8.4.3	PCR conditions	58
5.8.4.4	Normalization	59
5.8.5	<i>Detection of soluble HB-EGF protein by Western blot analysis</i>	59
5.8.6	<i>Detection of mitogen activated protein-kinases (MAPKs) by Western blot analysis</i>	60
5.8.7	<i>Cell proliferation assay</i>	61
5.9	STIMULATION OF PBMCS	62
5.9.1	<i>Isolation of PBMCS from peripheral blood</i>	62
5.9.2	<i>Cytokine secretion assay and flow cytometry</i>	63
5.9.3	<i>Intracellular cytokine detection by flow cytometry</i>	64
5.10	STIMULATION OF MONOCYTE DERIVED DENDRITIC CELLS	66
5.10.1	<i>Monocyte isolation from PBMCS</i>	66
5.10.1.1	Monocyte isolation using gelatin coated culture dishes and stimulation of DCs	66
5.10.1.2	Monocyte isolation using anti-CD14 MicroBeads.....	67
5.10.2	<i>Analysis of the maturation state of DCs by flow cytometry</i>	69
5.10.3	<i>Quantitation of cytokines in cell culture supernatants</i>	70
5.10.4	<i>Flow cytometry</i>	72
5.11	BUFFERS	73
6	RESULTS	77
6.1	CHARACTERIZATION OF COMPLEMENTED CLONES	77
6.1.1	<i>Insert orientation</i>	77
6.1.2	<i>Protein Expression</i>	77
6.2	UREASE ACTIVITY	78
6.2.1	<i>Semiquantitative test</i>	78
6.2.2	<i>Urease specific activity using the Berthelot and Lowry method</i>	79
6.3	PURIFICATION OF SURFACE ASSOCIATED H. PYLORI UREASE	79
6.3.1	<i>Protein analysis of samples after each purification step</i>	80
6.4	PURIFICATION OF RECOMBINANT UREASE SUBUNITS	81
6.5	EXPRESSION OF THE HB-EGF BY KATO III CELLS AFTER H. PYLORI INFECTION	82
6.5.1	<i>Quantitation of HB-EGF polyA⁺-RNA</i>	82
6.5.2	<i>Detection of soluble HB-EGF protein release by Western blot analysis</i>	84
6.5.3	<i>Effect of MAPK inhibitors on HB-EGF gene expression</i>	85
6.5.4	<i>Effect of H. pylori urease on MAP kinases activation</i>	86
6.5.5	<i>Cell proliferation assay</i>	87
6.6	STIMULATION OF PBMCS	88
6.6.1	<i>Extracellular cytokine measurement - cytokine secretion assay</i>	88
6.6.2	<i>Intracellular cytokine detection</i>	89
6.6.3	<i>Extracellular cytokine detection</i>	92
6.7	MONOCYTE DERIVED DENDRITIC CELLS	93
6.7.1	<i>Surface staining of dendritic cells</i>	94
6.7.2	<i>Cytokine production by dendritic cells</i>	96
7	DISCUSSION	103
8	REFERENCES	110

1 Kurzfassung

H. pylori ist der Verursacher von Gastritis und Magengeschwüren. Die Infektion selbst verläuft zumeist symptomlos, ist aber durch eine lebenslange Persistenz des Erregers charakterisiert.

In der Literatur wurde schon gezeigt, dass einige bakterielle Faktoren aufgrund ihrer apoptotischen oder Th1-Zell-assoziierten, gewebeschädigenden Wirkungen mit einer Erkrankung assoziiert sind. Es wurde jedoch auch gezeigt, dass andere Faktoren diesen Wirkungen entgegenwirken können und dadurch zum Persistieren der Infektion beitragen. In früheren Studien wurde gezeigt, dass *H. pylori* die heparin-binding epidermal-growth-factor-like growth factor (HB-EGF) Produktion in Epithelzellen induzieren kann. Die dafür verantwortlichen bakteriellen Faktoren konnten jedoch nicht identifiziert werden.

In der hier vorliegenden Studie wurde die Rolle der *H. pylori*-Urease bei der HB-EGF-Expression auf transkriptioneller, sekretorischer und funktioneller Ebene unter Verwendung der Kato III Epithelzelllinie untersucht. Ebenso wurde der Einfluss der *H. pylori*-Urease auf die Th1/Th2-Immunantwort mittels Stimulation von PBMCs analysiert. Die CD4⁺-T-Zell-Aktivierung und die intrazelluläre und extrazelluläre Zytokinproduktion (IL-10, IFN γ , IL-4) wurden gemessen. Es wurden auch die Effekte der Urease auf die Reifung von Dendritischen Zellen (Ursprung aus Monozyten) und deren Zytokinsekretion untersucht, da die von Dendritischen Zellen freigesetzten Zytokine den Typ der Immunantwort beeinflussen können. Freigesetztes TGF- β 1, welches ebenso wie HB-EGF bei der Ulkus-Heilung mitwirkt und außerdem bei der Induktion der Immuntoleranz eine Rolle spielen kann, wurde ebenfalls analysiert. In allen Experimenten wurden lebende Bakterien (Wildtypstamm N6, Mutante N6*ureB*::TnKm mit fehlender Ureaseproduktion, Mutante N6*ureG*::TnKm mit Produktion von enzymatisch inaktivem Apoprotein und K8 als genetisch komplementierter Klon), deren jeweilige Lysate, gereinigte oberflächliche Urease oder rekombinante strukturelle Untereinheiten als Stimulus in den entsprechenden Zellkulturen verwendet.

Die Quantifizierung der HB-EGF-Transkripte mittels RT-PCR (Real-time reverse PCR) zeigte eine statistisch signifikant gesteigerte Expression ($P < 0,05$) der HB-EGF-mRNA in den Zellen wenn sie der Urease exponiert wurden. Dies konnte auch auf Proteinebene mittels Westernblot bestätigt werden. Weiterhin hat die Urease einen beträchtlichen Anstieg der Zellproliferation ausgelöst ($P < 0,05$). Im Gegensatz zu p38- und p54/46-MAP-Kinasen wurden die p44/p42-Kinasen durch die Urease aktiviert. Durch die Verwendung von spezifischen p44/p42-MAP-Kinase-Inhibitoren wurde dieser Effekt der Urease auf die HB-EGF-Genexpression als auch auf die Zellproliferation unterbunden. Die ähnlichen Ergebnisse des mutierten Stammes (N6*ureG*::TnKm) und des Wildtypstamm N6 lassen darauf schließen, dass dieser Effekt großteils unabhängig von der enzymatischen Aktivität ist.

Die Stimulierung der PBMCs erfolgte über eine längere Inkubationsperiode, um die Induktion und Proliferation von Th1/Th2-spezifischen Klonen zu ermöglichen. Nach Restimulierung der PBMCs konnte die Produktion von intrazellulären Zytokinen in CD4⁺-T-Zellen nur nach Zugabe von PMA/Ionomycin mittels Durchflusszytometrie ausreichend detektiert werden. Interessanterweise waren die Werte wesentlich niedriger bei jenen Proben, welche mit der Positivkontrolle (anti-CD3/anti-CD28) oder mit lebenden Bakterien stimuliert wurden, als bei den unbehandelten Proben (Negativkontrolle). Dieses deutet darauf hin, dass eventuell eine stärkere erste Stimulus zu einer Desensibilisierung der Zellen führte. Die Analyse des Zytokingehaltes der Zellüberstände mittels ELISA bestätigte die durchflusszytometrischen Ergebnisse.

Bei der Analyse der Zelloberflächenmarker mittels Durchflusszytometrie konnte gezeigt werden, dass sowohl lebende als auch lysierte Bakterien innerhalb von 48 Stunden eine starke Reifung der Dendritischen Zellen (DCs) induzieren können, vergleichbar mit dem Effekt von LPS. Im Gegensatz zu anderen Stimuli führte N6*ureB*::TnKm schon innerhalb von 6 Stunden zu einem Rückgang der Exposition von Mannose Rezeptoren, als Zeichen der Reifung. Im Vergleich zu LPS induzierte *H. pylori* eine wesentlich niedrigere IL-12- und höhere IL-10-Konzentration. Dies deutet an, dass deren Interaktion mit den DCs eine Polarisierung der Immunantwort in Richtung Th2 bewirken kann. Überdies induzierte der Wildtypstamm N6 48 Stunden nach Stimulation höhere IL-10 Werte als

die Mutante N6*ureB*:TnKm. Dieser Effekt war im Fall von MCP-1, welches die Th2-Effektorzell-Differenzierung induziert noch deutlicher. Die Werte für MIP-1 β , welches ein Effektormolekül für Th1-Zellen ist, waren bei Versuchen mit N6*ureB*:TnKm bemerkenswert höher als jene Werte, welche mit N6 oder K8 (komplementierter Klon, produziert die gleiche Menge Urease wie N6) erzielt wurden.

Diese Ergebnisse deuten erneut an, dass die Urease die Th2-vermittelte Immunantwort verstärken kann. Von besonderer Bedeutung ist die Tatsache, dass intakte *H. pylori*-Bakterien (aber nicht deren Lysate) eine hohe TGF- β 1-Produktion induzierten. Im Vergleich zu N6*ureB*:TnKm rufen Urease-produzierende Stämme signifikant ($P < 0.05$) höhere Konzentrationen von diesem Chemokin hervor, welches in der gastrointestinalen, mukosalen Heilung, u.a. aufgrund der Inhibition der gewebeschädlichen Th1-vermittelten Immunantwort, eine wichtige Rolle spielt.

Auf diese Weise wurde gezeigt, dass die *H. pylori*-Urease *in vitro* die verstärkte Expression von HB-EGF und die Zellproliferation über die Aktivierung des p44/p42 vermittelten MAP-Kinase-Weges in Kato III Zellen induziert. Diese Beobachtung, zusammen mit der vermuteten Rolle der Urease bei der Induktion der TGF- β 1-Produktion bei Dendritischen Zellen, ist möglicherweise von besonderer Bedeutung bezüglich der Ulkus-Heilung. Darüber hinaus scheint Urease bis zu einem gewissen Grad die Freisetzung von wesentlichen Zytokinen und Chemokinen wie IL-10, MCP-1 und MIP-1 β aus Dendritischen Zellen zu beeinflussen, welche *in vivo* die Th2-Immunantwort begünstigen.

2 Abstract

H. pylori causes gastritis and peptic ulceration. However, infection is characterized by generally low level of disease and lifelong persistence. Whereas some bacterial factors were shown to be associated with disease due to their apoptotic or Th1-related tissue damaging properties, some others may counteract these effects, thus contributing to the persistent nature of the infection.

In previous studies, *H. pylori* was shown to induce heparin-binding epidermal-growth-factor-like growth factor (HB-EGF) production by gastric epithelial cells, but the bacterial factors being responsible for this effect were not identified. In the present study, the role of *H. pylori* urease in induction of HB-EGF was investigated at the transcriptional, secretional, and functional level using the gastric epithelial cell line Kato III. Furthermore, the possible influence of *H. pylori* urease on the type of immune response (Th1/Th2) was investigated by stimulation of PBMCs and determination of CD4⁺ T cell activation and intracellular and extracellular cytokine production (IL-10, IFN γ , IL-4). Finally, the effect of urease on maturation of monocyte derived dendritic cells and cytokine secretion by these cells was also investigated, since cytokines released by dendritic cells may also determine the type of immune response. Release of TGF- β 1, which like HB-EGF may contribute to ulcer healing and, furthermore may play a role in the induction of immune tolerance, was also assessed. In all experiments, isogenic live bacteria (parental strain N6, mutant N6ureB::TnKm lacking urease, mutant N6ureG::TnKm producing an enzymatically inactive apoprotein, and genetically complemented clones), the respective bacterial lysates, purified surface-associated urease or the recombinant structural subunits were used to stimulate the appropriate cell cultures.

Quantitation of HB-EGF transcripts by real time RT-PCR revealed a statistically significant upregulation of HB-EGF due to urease ($P < 0.05$), which was further confirmed at the protein level by Western-blot analysis. Furthermore, urease caused a considerable increase in cell proliferation ($P < 0.05$). In contrast to p38 and p54/p46 MAP kinases, p44/p42 MAP kinases were activated in response to urease and the use of specific p44/p42 inhibitors abolished the effect of urease in both HB-EGF gene expression and cell proliferation. Results with N6ureG::TnKm were similar to those

obtained with wild-type N6 suggesting that these effects were largely independent of enzymatic activity.

Stimulation of PBMCs was followed by incubation over a longer period of time in order to allow for the induction of Th1- or Th2-type specific T cell clones and their proliferation. After restimulation of PBMCs, intracellular cytokine production by CD4⁺ T cells could sufficiently be detected by flow cytometry only through additional activation by PMA/Ionomycin. Interestingly, values were considerably lower in samples stimulated with the positive control (anti-CD3/anti-CD28) or live bacteria than in untreated negative control samples suggesting that stronger stimuli may have caused desensitization of cells upon the first stimulation. Analysis of the cytokine content of the supernatants by ELISA confirmed to a large extent flow cytometric findings.

As shown by flow cytometric analysis of surface markers, *H. pylori* both live bacteria and bacterial lysates induced within 48 h strong maturation of immature DCs, which was comparable to that induced by LPS. However, in contrast to other stimuli, N6*ureB*::TnKm caused mannose receptor loss as sign of maturation as soon as within 6 h of stimulation. Compared to LPS, *H. pylori* induced considerably lower IL-12 and higher IL-10 levels suggesting that its interaction with DCs may induce polarization towards Th2 immune response. Moreover, N6 induced after 48 h of stimulation higher IL-10 values than those by N6*ureB*::TnKm. This effect was more prominent in case of MCP-1, which promotes Th2 effector cell development. Values of MIP-1 β , which is an effector molecule for Th1 cells, obtained with N6*ureB*::TnKm were considerably higher than those obtained with N6 or K8 (complemented clone producing similar amounts of urease to N6). Again, this finding suggests that urease may promote Th2 immune response. Most importantly, intact *H. pylori* bacteria but not lysates induced significant amounts of TGF- β 1. In comparison to N6*ureB*::TnKm, urease producing bacteria induced significantly higher levels of this chemokine ($P < 0.05$), which has a special role in gastrointestinal mucosal healing downregulating the tissue damaging Th1 response.

Thus, *H. pylori* urease was shown to induce HB-EGF upregulation and cell proliferation via activation of the p44/p42 MAP kinases pathway in Kato III cells in-vitro. This finding together with the possible role of urease in the induction of TGF- β 1 by dendritic cells

may be of particular interest in terms of ulcer healing. Furthermore, urease may at least to some extent influence the release of key cytokines and chemokines by dendritic cells such as IL-10, MCP-1, and MIP-1 β , which may favor the Th2 immune response in the in-vivo situation.

3 Introduction

3.1 *Helicobacter pylori*

3.1.1 Epidemiology and transmission

Helicobacter pylori (*H. pylori*) is a Gram-negative bacterium that colonizes the epithelium of the human stomach and infection is associated with the development of chronic gastritis, ulceration, adenocarcinoma and mucosal lymphoma but the pathogenic mechanisms that determine the clinical outcome remain poorly understood. It was isolated for the first time in 1982 by accidental extended incubation and the discovery was rewarded with medical Nobel-price in 2005. Today, *H. pylori* is well-recognized as an important human pathogen and has been classified as class 1 carcinogen by the WHO. Worldwide, more than 50% of the population is infected whereas particularly in developing countries the prevalence of the infection exceeds 95% (Figure 1). In developed countries, prevalence becomes higher with the age, which is due to a cohort phenomenon. As no significant non-human or environmental source for this infection has been identified, person to person spread is almost certainly the main mode of transmission. Moreover, since *H. pylori* infection has been shown to be typically acquired in early childhood, a predominantly intrafamilial transmission has been postulated. Having an infected mother has been suggested to be the most prominent risk factor [1]. Possible transmission routes are fecal-oral, oral-oral, or gastro-oral, but firm evidence is lacking. However, the most conceivable mode of transmission is the gastro-oral route (reflux or belching). In most infected individuals *H. pylori* infection persists for a lifetime. Approximately 10% of infected individuals will develop gastric hyperacidity and peptic ulcers. On the other hand, approximately 30% develop hypochlorhydria which leads to corpus gastritis. These patients are at high risk to develop atrophic gastritis and carcinoma.

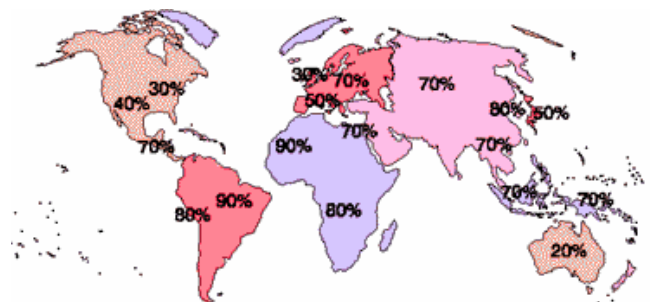


Figure 1 Worldwide prevalence of *H. pylori* infection

3.1.2 Morphology

H. pylori is highly variable and may exhibit different morphological features during varying environmental conditions [2]. The bacteria can be observed in the logarithmic growth phase as long, thin spirals with up to three turns in the body shape with several unipolar flagella (Figure 2). In the late stationary phase bacteria have a rounded coccoid form [3]. *H. pylori* can also show morphology similar to *H. heilmannii*, having four or more turns in the helical form [4].

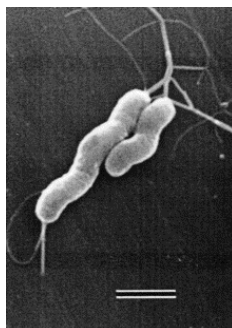


Figure 2 Electron micrograph picture of *H. pylori*. Spiral bacterial bodies with a bundle of sheathed flagella. Bar=1 μ m.

3.1.3 Genomics

From the microbiological point of view, *H. pylori* is a highly host adapted organism. Typical for bacterial species specialized to survive only in a single environment, *H. pylori* has a small genome (1.67Mbp-1500 genes) containing only a minimal set of metabolic pathways and regulatory protein genes. The genomes of *H. pylori* isolates are also divergent [5], [6] with some genes at different locations and order in different strains [7]. Approximately 5% of the genes are strain specific [8]. However many proteins are

conserved between *H. pylori* strains, like flagellins, some adhesins and the urease enzyme [9], [10], [11], [12], [13], [14], [15], [16].

3.1.4 Pathophysiology

In physiologic terms, the stomach could be divided into two main compartments which differ in glands, marker cells and acidity. The acidic proximal corpus that contains the acid producer parietal cells, the histamine producer enterochromaffin-like (ECL) cells and the pepsinogen producer chief-cells, and a less acidic distal antrum that does not have parietal cells but contains the endocrine somatostatin-producing D cells and gastrin-producing G cells and control acid secretion; somatostatin negatively regulates gastrin, gastrin enhances acid secretion in parietal cells. Neck cells are in both part and produce glycoprotein. A cross-section of the gastric mucosa (inner side facing) shows a thick mucus-layer consisting of mucopolysaccharides, an epithelial cell monolayer, the basement membrane and the mucus layer with glands located in a matrix of reticular connective tissue (lamina propria mucosae). Changes concomitant with *H. pylori* infection develop mainly in these parts of the stomach tissue. Environmental conditions within the mucus layer include high viscosity, low oxygen tension, depletion of certain substrates and metal ions.

Infection with *H. pylori* is believed to elicit an acute inflammatory response referred to as “acute gastritis” of short duration and little if any clinical manifestations. Although a cellular and humoral immune response is generated upon infection only a minority of patients develop clinical symptoms and ulcer which could be interpreted as somehow disturbed balance between colonization and parasitism. In the acute phase of the infection, approximately 10-14 days after *H. pylori* infection, in most cases hypochlorhydria will develop. Thereafter, the infection progresses to a chronic state with a wide range of histopathologic findings and clinical symptoms. During the inflammatory process IL-1 β is produced which suppress acid production. After few days in normal case acid secretion will be normalized, the majority of patients have both antral and corpus gastritis resulting no changes in gastric secretion. However, in some cases the acid secretion balancing fails. The acid homeostasis and disease depend crucially on the topographic distribution in the stomach of the *H. pylori*-induced inflammation

(Figure 3). If the acid producer parietal cells are extremely damaged, like in the case of pangastritis or corpus predominant gastritis, where *H. pylori* induced inflammation suppresses parietal cell function. Reduced acid secretion further augments gastrin levels, which, while ineffective in raising acid production from the inflamed gastric corpus, provide an ongoing proliferative stimulus to gastric epithelial cells and lead to progressive loss of gastric glands (Figure 4b). Also, high level of IL-1 β production (which suppresses the somatostatin production of the D cells) is associated with reduced acid production and this may lead to gastric atrophy and intestinal metaplasia which are part of the multi-step model of gastric carcinogenesis [17]. Such atrophic changes, because of lowered acid production, are protective against duodenal ulceration and probably against acid-induced complications of gastroesophageal reflux [18], [19]. On the other hand, in antral-predominant gastritis, the long lasting enhanced acid production is associated with a high risk of duodenal ulcer disease [20] (Figure 4a). There are many reasons for developing high acid secretion such as the low inflammatory genetic makeup, increased gastrin secretion [21] or environmental factors like smoking.

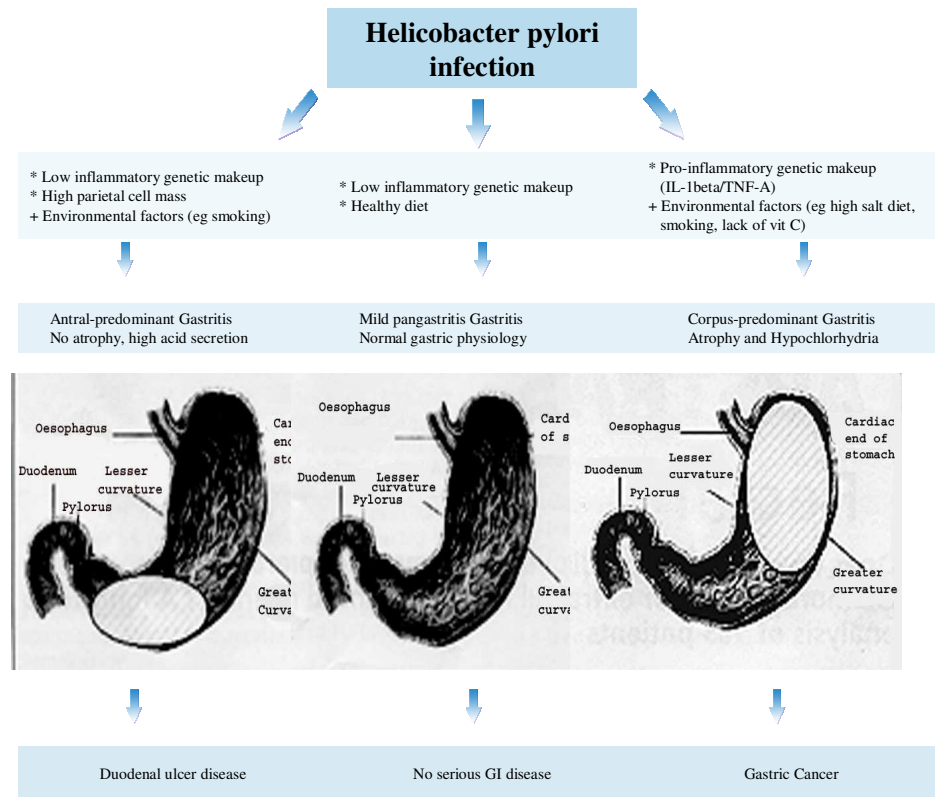


Figure 3 Relation of topography of inflammation to gastric physiology and clinical outcome. GI: gastrointestinal.

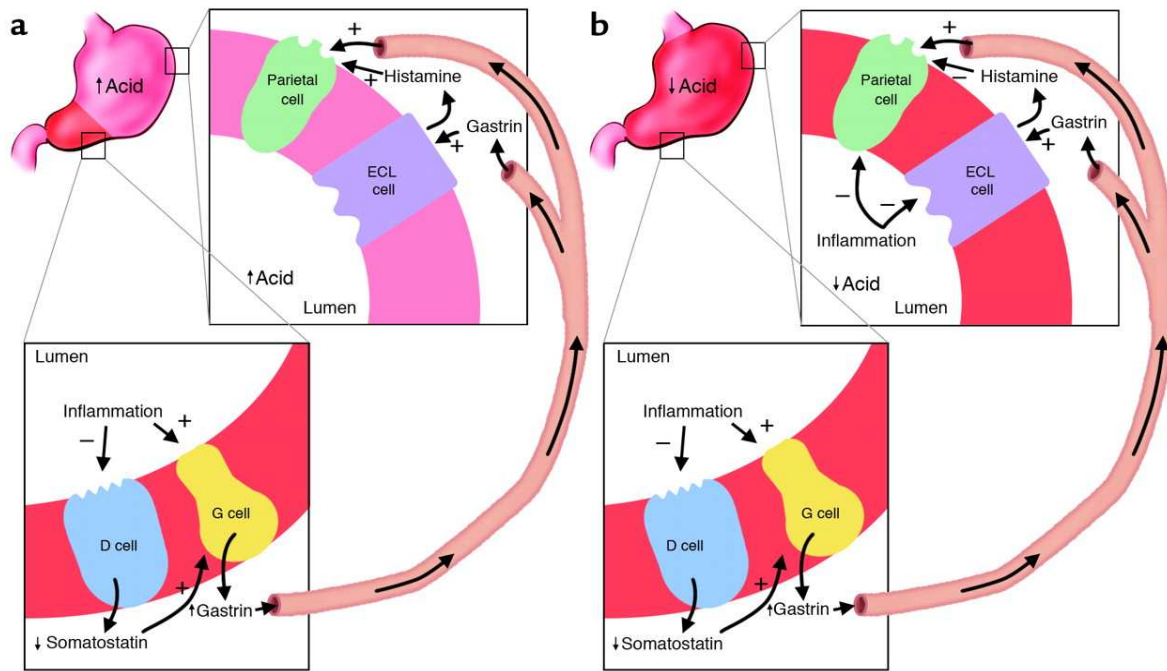


Figure 4 Relation of topography of inflammation to gastric physiology and clinical outcome (a) *H. pylori*-induced antral-predominant inflammation. (b) *H. pylori*-induced pan-gastritis.

3.1.4.1 Mucosal wound repair mechanisms

Well-coordinated mechanisms have evolved that provide both innate protection against gastrointestinal mucosal injury and facilitation of rapid mucosal repair following mucosal damage. Repair of intestinal mucosa after injury occurs through the aggregate effect of coordinated processes whose relative contributions are likely dependent on the depth rather than the extent of damage. Ultimate repair of injury requires both proliferative replacement of damaged epithelial cells and remodeling of extracellular matrix and deeper cell populations to restore normal architecture and a fully functional mucosa. Many of the regulatory peptides are products of the immune and other lamina propria cell populations, which are activated following disruption of the mucosal barrier. Thus efforts to repair the epithelium follow inherently from inflammatory effects after initial damage; the repair process in turn may allow abrogation of further inflammation [22].

3.1.4.1.1 Role of growth factors

Transforming growth factor alpha ($TGF\alpha$) and epidermal growth factor (EGF) control cell proliferation. $TGF\alpha$ predominantly plays this role under normal conditions and after

acute injury, while EGF exerts its actions mainly during healing of chronic ulcers. During healing of chronic ulcers, a new epithelial lineage secreting EGF and other growth peptides develops and the majority of cells lining the ulcer margin overexpress the EGF receptor. Granulation connective tissue, which grows under the stimulation of basic fibroblast growth factor (bFGF) and venous epidermal growth factor (VEGF), is the major source for regeneration of connective tissue lamina propria and microvessels within the ulcer scar. Other growth factors such as insulin-like growth factor, keratinocyte growth factor, hepatocyte growth factor and trefoil peptides have been implicated in gastrointestinal (gastric ulcers, colitis) regeneration following injury [23]. These growth factors trigger mitogenic, motogenic and survival pathways utilizing Ras, MAPK, PI-3K/Akt, PLC-gamma and Rho/Rac/actin signalling [24]. Inhibition of these signaling pathways dramatically delays ulcer healing. Variety of cytokines (interleukin (IL)-1, IL-2, IL-4, IL-15, and interferon gamma) play also important role in mucosal wound healing. These growth factors and cytokines appear to promote restitution through a transforming growth factor- β (TGF- β)-dependent pathway and act to both enhance expression of TGF- β and to entrance its bioactivation [25]. Indeed, in *H. pylori* induced gastritis activated TGF β -1 is abundant in the mucosa [26].

3.1.4.2 Transforming growth factor (TGF- β)

TGF- β is a multifocal cytokine, which regulates many diverse cellular processes including proliferation, apoptosis and differentiation. Although TGF- β inhibits epithelial and endothelial cell proliferation, it has special role in gastrointestinal mucosal healing as it stimulates fibroblasts [27], induces cell migration, angiogenesis and enhances cellular matrix production and downregulates the ongoing tissue damaging Th1 response [26]. TGF- β is a 25-kDa disulfide-linked homodimeric peptide. Three mammalian isoforms (TGF- β 1, TGF- β 2 and TGF- β 3) have been identified. TGF- β 1 is the prevalent form and found almost ubiquitously [28] other isoforms are expressed in a more limited variety of cells and tissues. In the stomach, TGF- β 2 is present in chief cells, TGF- β 3 in parietal, chief and mucus cells [29]. Immunoreactive TGF- β 1 is produced by the parietal and neck cells, but not by epithelial cells [30]. TGF- β is synthesized as a

large precursor that is subsequently cleaved. The cleaved pro-region known as the latency-associated peptide (LAP) remains non-covalently associated with the mature peptide to form a latent TGF- β 1 complex. This small latent complex will be secreted and undergoes further processing in the extracellular matrix. TGF- β exerts its action by binding to its transmembrane serin/threonine kinase receptors, which in turn triggers activation of various intracellular signaling (Smad, TAK, MAPK, p53) pathways resulting in distinct effects [31].

3.1.4.3 Heparin binding epidermal growth factor-like growth factor

Heparin binding epidermal growth factor-like growth factor (HB-EGF) is TGF- β -regulated in intestinal epithelial cells [32]. HB-EGF is a member of the epidermal growth factor receptor (EGF-r) related peptides including EGF and TGF α and is a potent stimulus for cell proliferation and migration. HB-EGF is synthesized as a transmembrane protein (proHB-EGF) and cleaved on the cytoplasmic membrane to yield soluble HB-EGF of 19 – 23 kDa [33]. However, a considerable amount of proHB-EGF remains uncleaved on the cell surface. HB-EGF is an early response peptide that plays an important role in mediating the earliest cellular response for proliferative stimuli and cellular injury thus contributing to the process of cell renewal. In the stomach, HB-EGF is synthesized in parietal and gastrin producer cells and acts in autocrine or paracrine manner to regulate proliferation and differentiation of gastric mucosal cells [34]. Interestingly, *H. pylori* was shown to induce expression of HB-EGF in MKN 28 gastric mucosal cells [35]. However, the bacterial antigen responsible for this effect has not been yet identified.

3.1.5 Adaptation to acidic environment

H. pylori has a unique way of adapting in the harsh environment of the stomach. Inside the stomach the gastric juice is composed of digestive enzymes and concentrated hydrochloric acid. It used to be thought that the stomach contained no bacteria and was actually sterile, but discovery of *H. pylori* changed that hypothesis.

The stomach is protected from its own gastric juice by a thick layer of mucus that covers the stomach lining and *H. pylori* takes advantage of this protection by living in the mucus layer (Figure 5). Besides, *H. pylori* is able to fight the stomach acid with the enzyme

urease. Urease converts urea, of which there is an abundant supply in the stomach (from saliva and gastric juices), into bicarbonate and ammonia, which are strong bases. This creates a cloud of acid neutralizing chemicals around the bacterium, protecting it from the acid in the stomach. Thus, urease enables bacterial survival and colonization of the gastric mucus.

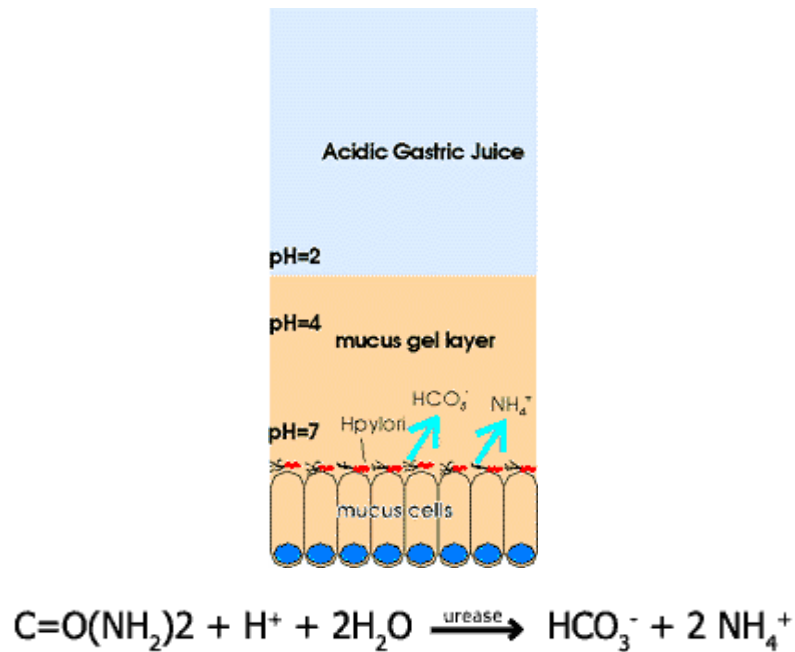


Figure 5 Urea hydrolysis: urea is broken down to ammonia and carbon dioxide

3.1.6 Motility and chemotaxis

First, for successful colonization, *H. pylori* must retain active motility in the gastric lumen until it reaches the safety of the mucus layer. Because of the pepsine and low pH of the gastric juice, bacteria have only few minutes before turning irreversibly immotile [36]. Most bacteria reside within the gastric mucus layer, but a few (2%) associate with the gastric epithelium. However, once the bacterium reached the mucus layer, it has to remain motile, as the mucus layer is a dynamic, constantly changing niche. Due to rapid mucus turn over (flow to highly acidic lumen and to the duodenum), bacteria must move against the flow of mucus towards the epithelium. Moreover, the surface neutral mucus layer becomes thinner in the infected stomach [37] making more difficult for the bacteria to survive. For movement, several unipolar flagella rotation and chemotaxis towards the

urea and sodium bicarbonate (diffusing out of epithelial cells) may play an important role (Figure 6).

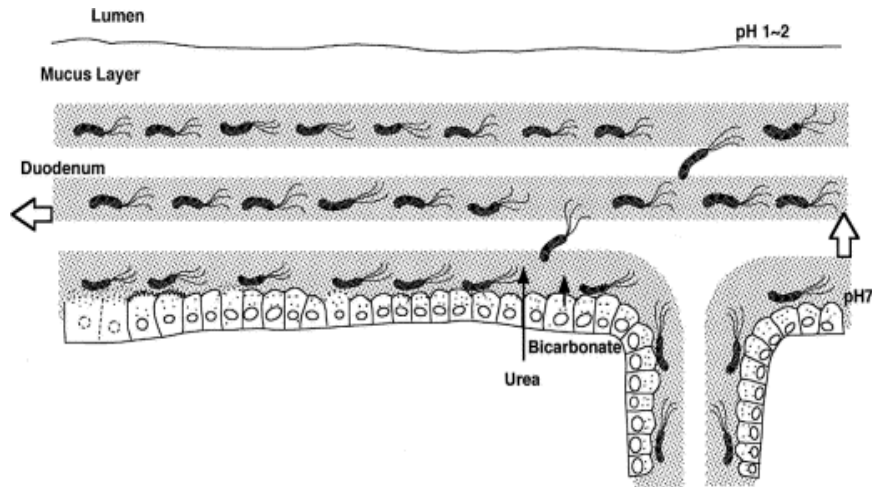


Figure 6 The chemotactic movement of *H. pylori* in the mucus layer toward urea and sodium bicarbonate.

The helical flagellar filaments rotate via the action of motor device located in the proximal portion of the flagellar structure. Bacterial flagellar motor utilize the free energy stored in the electrochemical proton gradient across the cytoplasmic membrane to do mechanical work. The stator of the motor is formed from the membrane proteins MotA and MotB, which associate in complexes that contain multiple copies of each protein. MotA interacts the motor and MotB has Asp-32 transmembrane segment (able to bind H^+), located near to the cytoplasmic end. The protons passing through the channels (from outside to inside the bacterium) induce a strong electric field in Mot molecules [38]. This field originates an impulse force to cause conformational changes and flagellar rotation. Intracellular urease give extra power for flagellar motor, as the produced NH_3 consumes free H^+ ions and so makes the cytoplasmic pH higher. The low intracellular H^+ concentration allows MotB deprotonation at Asp-32 site that speed up the proton influx and the flagellar rotation [39]. The extra power provided by intracellular urease is very important in a viscous environment but in fluid niche motility is independent from urease enzyme activity.

The spiral-shaped form, the strong ureataxis, as well as the complex motility control, should enable this bacterium to adapt to the ecological niche provided by the gastric mucus.

3.1.7 Virulence factors

H. pylori has developed a unique set of virulence factors, actively supporting its survival in the special ecological niche of the human stomach. Vacuolating cytotoxin (VacA) and cytokine-associated gen A (CagA) are the two major bacterial virulence factors involved in host cell modulation.

The VacA cytotoxin is encoded by the *vacA* gene, which is a polymorphic mosaic with two possible signal regions, s1 and s2, and two possible mid regions, m1 and m2 (Figure 7). The s1 signal region is fully active, but the s2 region encodes a protein with a different signal peptide cleavage site resulting in inhibition of vacuolating activity. The mid region encodes a cell-binding site, but the m2 type binds to fewer cell lines in vitro. Vacuolating activity is therefore higher in s1/m1 genotypes than in s1/m2 genotypes, and absent in s2/m2 genotypes.

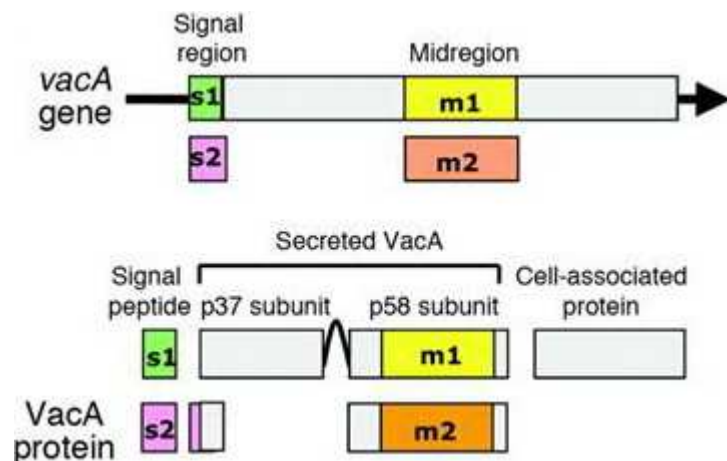


Figure 7 VacA gene polymorphism.

VacA gene is translated into a protoxin, which is subsequently processed by proteolytic cleavage into a mature protein. VacA monomers aggregate into biologically active flower shaped multimeric complex (Figure 8A). The cytotoxin causes formation of large acidic vacuoles containing markers of late endosomes and lysosomes in human epithelial cells. As to the mechanism of action, VacA has been shown to form ion-selective membrane channels both in lipid bilayers [40], [41], [42] and in the plasma membrane of epithelial cells [41], however the channels seem to be structurally different in these two situations. These pores are formed by oligomerization of membrane-bound monomers

[44] and induce a membrane depolarization necessary for vacuole formation. VacA also induces apoptosis, in part by forming pores in mitochondrial membranes, allowing cytochrome-c (Cyt-c) egress (Figure 8B).

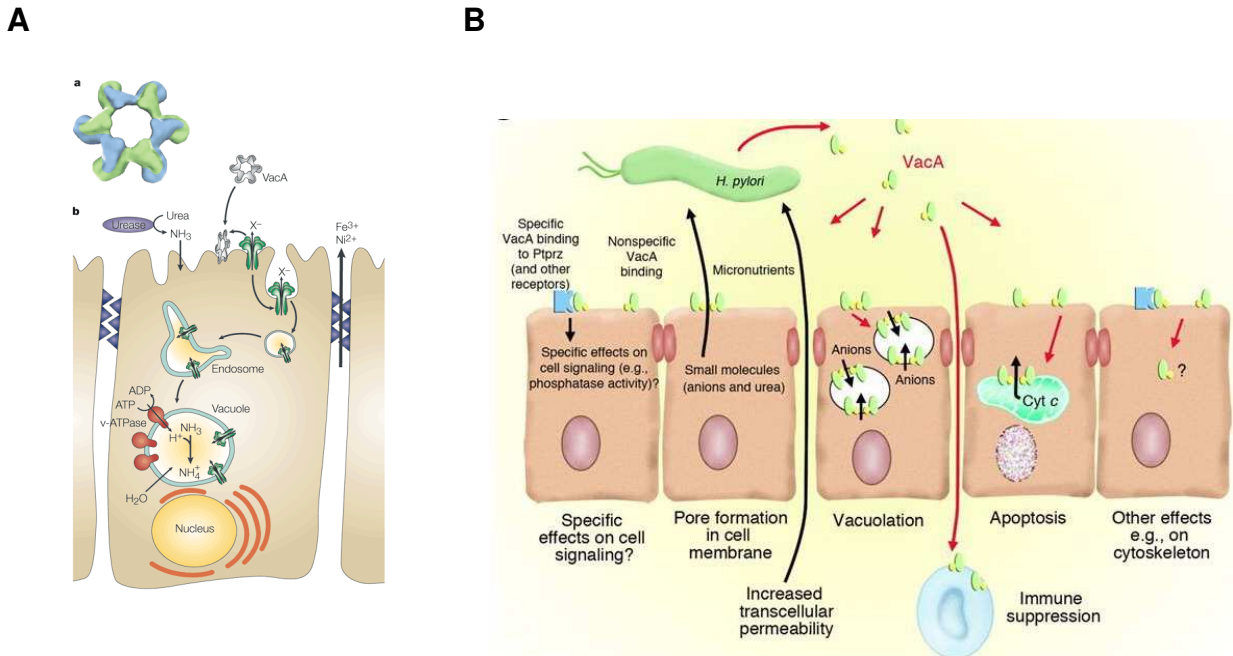


Figure 8 VacA biological active flower shaped complex (A) and induced cellular changes (A) and (B).

H. pylori may enter large cytoplasmic vacuoles, where the bacterium remains viable and motile [45]. It has been speculated, that such intracellular vacuoles may constitute a reservoir of live *H. pylori*, difficult to attack by antibiotics or phagocytes. This is supported by the finding that VacA seems to prevent phagosome trafficking and fusion of lysosomes [46]. Whether or not VacA supports survival of *H. pylori* in such vacuoles is still a point of controversy.

Cytotoxin associated gene A (*cagA*) is a part of a 40 kb DNA segment termed pathogenicity island (PAI). PAI encodes several genes (*cagB-N* and other untermmed open reading frames) upstream of *cagA*. The *CagA* is a marker for virulence. Through transformation the entire island may be restored or lost. *H. pylori* strains with partial *cag* island also have been identified, and variation in island size and genotype within individual hosts is well described. The intact *cagA* island contains genes encoding a type IV secretion system, which inject macromolecules, such as DNA and proteins into host cells [47]. One substrate for the type IV system in *H. pylori* is the *CagA* protein

(Figure 9). This protein contains tyrosine-phosphorylation sites that are recognized by the host cell Src kinase [48]. Once phosphorylated, phosphotyrosine-CagA interacts with several major signal-transduction pathways in the host cell [49] affecting phenotypes including cell morphology, proliferation, and apoptosis. *H. pylori* strain with the deleted *cag* island has remarkably little interaction with epithelial cells [50]. The injected CagA protein interacting with Grb2 activates the Ras/MEK/ERK pathway, leading to the phenotypes of cell scattering and proliferation [51]. Tyrosine-phosphorylated CagA binds and activates C-terminal Src kinase (Csk) via its SH2 domain, which in turn inactivates the Src family of protein-tyrosine kinases. Since this signaling may induce apoptosis, the Csk pathway may attenuate the other CagA interactions [52]. By inactivating Src, tyrosine-phosphorylated CagA induces dephosphorylation of cortactin, which then co-localizes with filamentous actin (F-actin), in the tip and base of hummingbird protrusions [53].

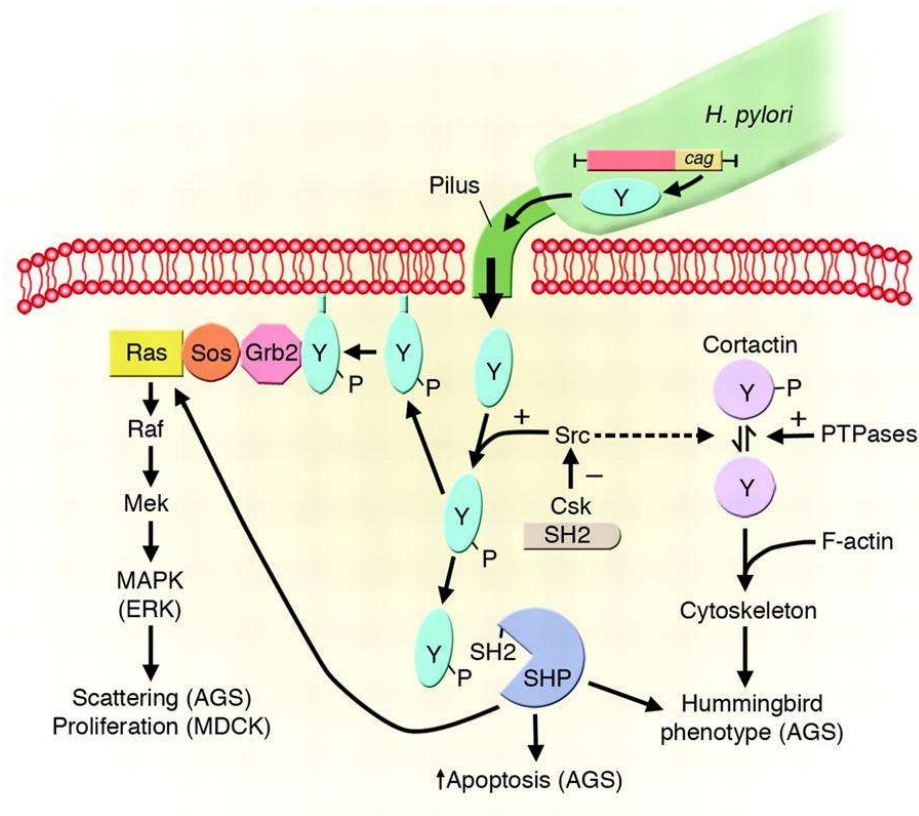


Figure 9 CagA interaction with the major signal transduction pathways in epithelial cells.

Interaction between the *vacA* and the *cagA* domains: The *vacA* and *cag* island are far apart on the *H. pylori* chromosome, yet there is a strong statistical linkage between the s1 genotype of *vacA* and the presence of the *cag* island. Similarly, the s2 genotype is associated with lack of the *cag* island [54].

According to their degree of pathogenicity, *H. pylori* strains have been divided into two groups [55]. Type I strains contain the *cag* pathogenicity island, - which is essential for IL-8 secretion by epithelial cells, and secrete a vacuolating cytotoxin, -which induce vacuolation of epithelial cells [56]. In contrast, type II strains lack the *cag* PAI and synthesize small amounts of inactive VacA. Type I strains are more prevalent in persons with ulcer disease and induce more inflammation and tissue damage than do the less virulent type II strains.

3.1.8 Adhesion to host cells

The adherence of *H. pylori* to the gastric mucosa plays a substantial role in initial colonization and long-term persistence in the human stomach. Many of the outer membrane protein family (OMP) of *H. pylori* have been proven to function as porins and adhesins. The best defined *H. pylori* adhesin-receptor interaction found to date is that between the Leb blood group antigen binding adhesin BabA, a member of a family of *H. pylori* outer membrane proteins, and the H, Lewis b (Leb), and related AB0 antigens (3–5). These fucose-containing blood group antigens are found on red blood cells and in the gastrointestinal mucosa. Persons with blood group 0 and “nonsecretor” phenotypes (lacking the AB0 blood group–antigen synthesis in secretions such as saliva and milk) are relatively common (e.g., 45% and 15%, respectively, in Europe), and each group is at increased risk for peptic ulcer disease [57]. The H1 and Leb antigens are abundant in the gastric mucosa of secretors (of blood group 0) [58], but not in nonsecretors, where instead the sLex and sLea antigens are found [59]. The blood group 0 – disease association was postulated to reflect the adherence of most *cagA*⁺ *H. pylori* strains to H1 and Leb antigens [60]. Gastric tissue inflammation and malignant transformation each promote synthesis of sialylated glycoconjugates [61], which are rare in healthy human stomachs [62]. In the endothelial lining, sialylated Lewis-glycans serve as receptors for selectin cell adhesion proteins that help guide leukocyte migration and thus regulate

strength of response to infection or injury [63]. The *H. pylori* BabA adhesin binds Leb antigen on glycoproteins [64], whereas its SabA adhesin binds sLex antigen in membrane glycolipids, which may protrude less from the cell surface (Figure 10). Thus, *H. pylori* adherence during chronic infection might involve two separate receptor-ligand interactions—one at “arm’s length” mediated by Leb, and another, more intimate, weaker, and sLex-mediated adherence. One theory is that at the site of vigorous local inflammatory response, if *H. pylori* lost Sab expression due on/off frame shift mutation, will lost sLex-binding capacity. The weakness of the sLex-mediated adherence allows *H. pylori* escape from sites where bactericidal host defense responses are most vigorous. Such adaptation of bacterial adherence properties and subsequent inflammation pressure could be major contributors to the extraordinary chronicity of *H. pylori* infection in human gastric mucosa. Additional *H. pylori* – host macromolecule interactions that do not involve Leb-type antigens have also been reported [65]. Other adhesions e.g. AlphaA and AlphaB and HopZ have been also identified [66], but the binding receptors are still unknown [67].

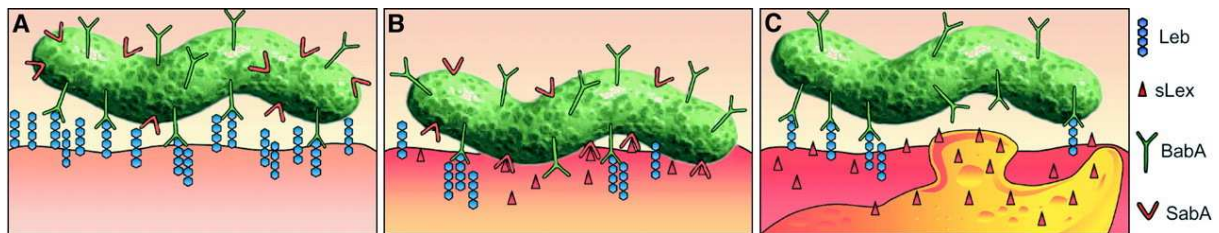


Figure 10 *H. pylori* adherence in healthy and disease. Figure illustrates the proficiency of *H. pylori* for adaptive multistep mediated attachment. (A), *H. pylori* adherence to Leb antigen (BabA and SabA binding to Leb antigen) (B), During persistent infection and chronic inflammation sLex antigens are upregulated. SabA (red Y structures) performs Selectin-mimicry by binding the sialyl-(di)-Lewis x/a glycosphingolipids, for membrane close attachment and apposition. (C), Site of vigorous local inflammation. *H. pylori* subclones that have lost sLex binding capacity due to ON/OFF frameshift mutation might have gained local advantage in the prepared escaping of intimate contact with (sialylated) lymphocytes.

3.2 Urease

In fact, this enzyme, which is in part surface associated, is produced by every strain. The amount of urease produced by the bacterium can reach 6% of total bacterial protein. The main role of urease is thought to be the neutralization of the acidic microenvironment by producing ammonia. Urease is a Ni²⁺ containing enzyme that hydrolyses urea into NH₃ and CO₂ (Figure 11). Urea is taken up by *H. pylori* through a

proton gated channel (UreI) that opens at $\text{pH} < 6.5$. Produced ammonia diffuses into the periplasm creating a neutral layer around the bacterial surface (Figure 12). Urease is essential for colonization. Isogenic urease-negative mutants were shown to be unable to colonize the gastric mucosa of mice [68] and gnotobiotic piglets even under hypochlorhydric conditions [69]. After colonization it is still synthesized in large amounts by the bacteria suggesting that neutralization of the microenvironment is not the only role of urease for colonization [70].

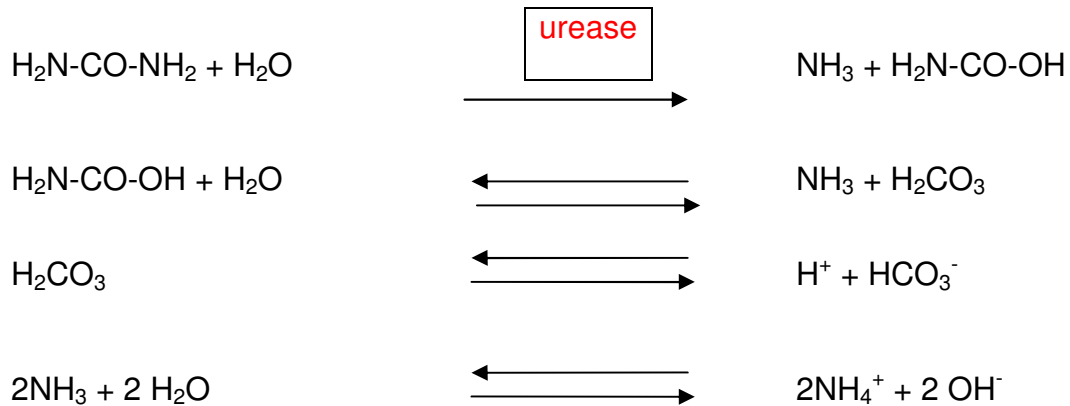


Figure 11 Urease (urea-amidohydrolase) catalyzes the hydrolysis of urea, leading to the production of carbamate and ammonia. In an aqueous environment, the carbamate rapidly and spontaneously decomposes to yield a second molecule of ammonia and one of carbon dioxide. The reaction results in a rise in pH of the local environment.

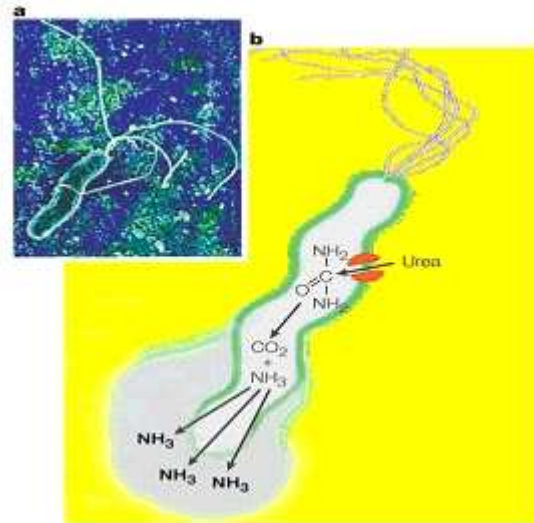


Figure 12 *Helicobacter pylori*. (a) Electron micrograph and (b) schematic representation showing shape, polar flagella, urease, H^+ -gated urea channel and the production of ammonia, which neutralizes the yellow acidic environment and the cytosol and the immediate environment around the bacterium (light blue).

Indeed several other functions for urease demonstrated *in vitro* might contribute to pathogenesis. Urease is a potent chemoattractant stimulator of mononuclear phagocyte activation and inflammatory cytokine production such as IL-6, IL-8, TNF α [71], [72]. Ammonia generated by the enzyme is detrimental to epithelial cells. Although not toxic *per se*, damage results from the hydroxide ions originating from the equilibration of ammonia with water [73], [74], [75]. Epithelial damage by ammonia would explain why patients with gastric failure – exhibiting higher urea concentrations in serum and gastric juice than normal persons – frequently have a more severe gastritis and atrophy but an equal prevalence of *H. pylori* infection [76], [77]. Moreover, ammonia potentiates vacuolization of epithelial cells caused by VacA [78], it could also play a role in circumventing killing of *H. pylori* by human neutrophils demonstrated *in vitro* [79], [80] and might be a nutrient for *H. pylori* although the bacterium is able to utilize other substrates as sources of nitrogen [81]. Urease could also give extra power for the flagellar motor in viscous environment by producing NH₃ which binds free protons and the created lower proton concentration helps deprotonation of the MotB protein and speed the conformational changes up, which in turn give more speed to the flagellar rotation.

H. pylori shows chemotaxis towards urea and sodium bicarbonate, which are both secreted through the gastric epithelium [82]. Besides permitting survival in the acid environment urease thereby helps the bacterium to penetrate the mucus more rapidly and to escape acidity. Besides these findings, urease was also discussed to play a putative role in the process of persistence and evasion of protective immune responses by inhibiting phagocytosis of the bacterium by human neutrophil granulocytes [83] and blocking opsonization by human complement [84].

3.2.1 Genetic and molecular assembly

As already mentioned, urease converts urea into NH₃ plus CO₂. Its inactivity at neutral pH prevents lethal alkalization of the cytoplasm, whereas an increase of activity is used to combat acidic environments [85]. For this pH-dependent increase of activity, *H. pylori* has developed unique pre- and post-transcriptional control mechanisms. The biosynthesis of urease is controlled by a seven-gene cluster, containing seven open

reading frames (ORFs), *ureABIEFGH* (Figure 13). While the ORFs *ureA* and *ureB* encode the two structural protein subunits *UreA* and *UreB*, the other five genes, *ureIEFGH*, encode accessory proteins.

UreA 26,5 kDa	UreB 60,3 kDa	UreI 21,7 kDa	UreE 19,5 kDa	UreF 28,6 kDa	UreG 21,7 kDa	UreH 29,6 kDa
-------------------------	-------------------------	-------------------------	-------------------------	-------------------------	-------------------------	-------------------------

Figure 13 Genetic organization of the urease gene cluster.

The regulation of *H. pylori* genes is poorly understood. The *ureIEFGH* and the read-through transcript *ureABIEFGH* are cleaved at specific sites within *ureE* and *ureF* to produce a variety of mRNAs. The whole cleavage process and further mRNA decay is pH dependent [86] (Figure 14). However, low environmental pH reduces the production of nascent urease and presumably many other proteins [87].

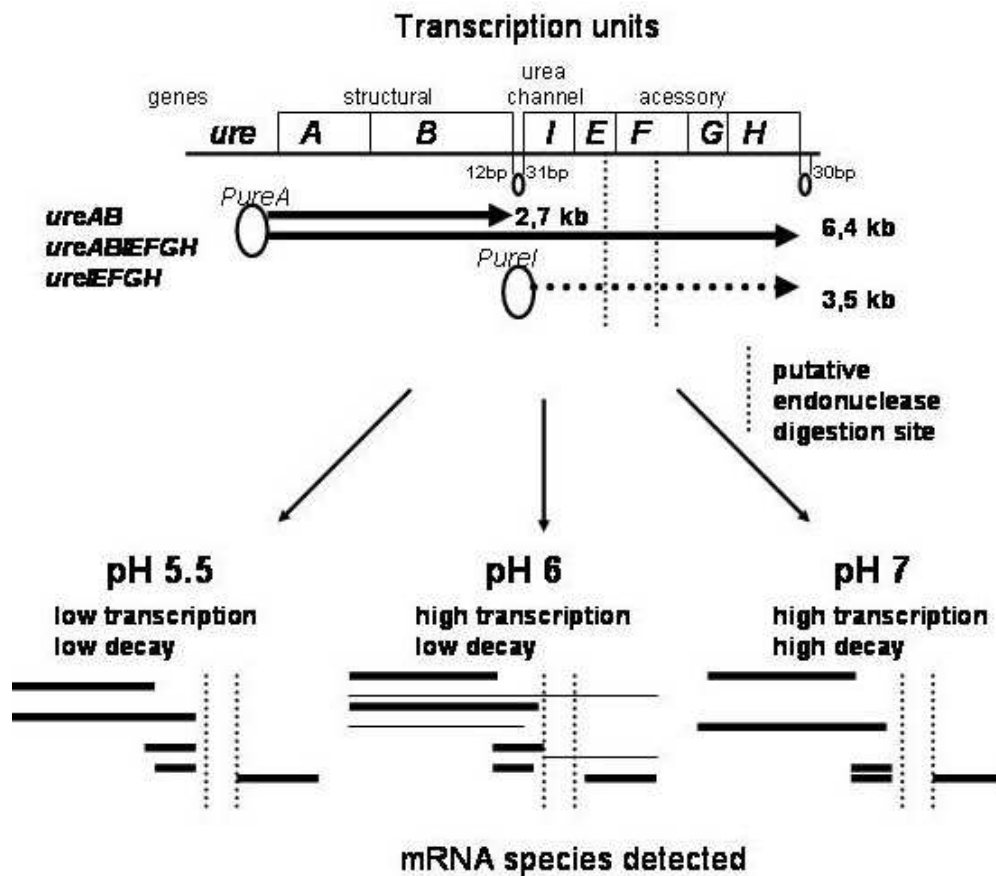


Figure 14 Transcription units of the ure operon of *H. pylori* and a proposed model of post-transcriptional processing. Depending on the pH, urease operon produce primarily three transcripts, *ureAB* (2,7 kb), *ure ABIEFGH* (6,4 kb) and *ureIEFGH* (3,5 kb). The latter two transcripts are degraded post-transcriptionally to various transcription products.

Also it has been showed, that Ni^{2+} ion concentration of the *H. pylori* medium interacts with urease expression at the translational level.

Accessory proteins play a role in the urease assembly and nickel incorporation into the metallocenter of the apoenzyme. In the biologically active urease enzyme, these accessory proteins are necessary [88]. Deletion of *ureF*, or *-G* results in complete loss of urease activity, whereas deletion of *ureE* leads to a much reduced enzyme activity. With the assistance of *nixA*, a nickel transport polypeptide (which mediates the transport of nickel across the cytoplasmic membrane), *ureE* is the natural donor in the full assembly complex at normal Ni^{2+} concentrations [89], [90], [91], [92], [93], [88]. *UreF* may influence the conformation of the apoenzyme and assist in nickel uptake of the metallocenter. *UreG* probably serves in an energy-dependent step because an ATP- or GTP-binding site was identified. *UreH* may act as chaperonin preventing nonproductive nickel ion incorporation prior to an activation step involving CO_2 (HCO_3^-). *UreH*, *-E*, *-F*, *-G* dissociate from the enzyme and are recycled for interaction with the next urease apoenzyme molecule [88].

Of the urease gene cluster, *ureI* is the only one not involved in the biogenesis of active urease [94]. The *ureI* gene sequence predicts a polytrophic integral membrane protein with homology to proteins postulated to mediate influx of amidase substrates [95]. The availability of the urease substrate is controlled by the *UreI* acid activated urea channel, which is present in the inner membrane and opens at pH less than ~6.5 increasing the access of the substrate to intrabacterial urease [96]. Hence, in acidic environment *H. pylori* produces large quantities of NH_3 that diffuses into the periplasm, and buffers this space due to the formation of NH_4^+ [97], [98], [99]. This mechanism allows for efficient utilization of urease activity for the survival of the organism at acidic pH in vitro and in the stomach of animal models [100], [101], [102], [103], [104], [105], [106].

3.2.2 Native protein structure

The reported native molecular weight of *H. pylori* urease varies from 380 to 680 kDa [107], [108], [109]. The native protein consists of 6 copies of each of the structural subunits *UreA* (30 kDa) and *UreB* (66 kDa) [107]. In *H. pylori*, two nickel ions associate with *UreB*, resulting in 12 ions per molecule [107]. On the ultrastructural level urease

forms doughnut-like structures of 13 nm diameter and 3 nm thickness, which can be visualized by electron microscopy of whole cells or of purified urease. Based on their size and the density of protein (1.5 g/cm^3) the protein content of these structures was estimated to 180-270 kDa. 2-disc and 4-disc stacks, which were also identified, could therefore correspond to 380 and 680 kDa, respectively [110]. If this is correct, disaggregated urease could consist of only 3 copies of each of the subunits. Figure 15 shows the hypothesized structural molecular assembly of the urease enzyme.

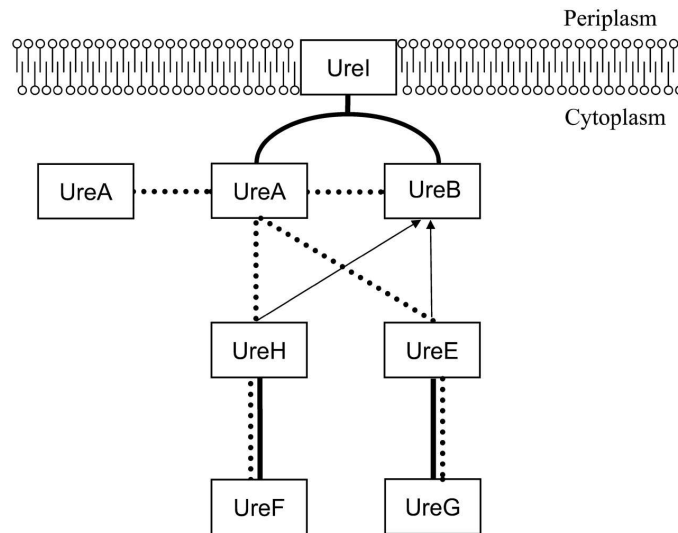


Figure 15 Model of interaction between the different urease gene cluster proteins. Lines indicate the different interactions defined by different groups. [111].

3.2.3 Localization

Urease has been shown to be located not only in the cytoplasm but also on the bacterial surface [112] and also to be secreted extracellularly [113]. It has also been assumed that only the surface-located urease is active [114], [115]. Although recognized soon after the discovery of the bacterium, the mechanism whereby urease becomes associated with the surface of *H. pylori* is still unclear because urease does not have the typical leader sequences for transfer via type II and IV pathways, it shows no motifs for membrane incorporation and no apparent secretory genes are clustered with urease encoding genes [115], [116]. In pursuance of an interesting hypothesis, termed "altruistic autolysis," urease (and other cytoplasmic proteins) is released by genetically programmed autolysis with subsequent adsorption of the released urease onto the surface of neighboring intact bacteria [118]. In fact, autolysis is known to take place in

other bacteria (e.g. *S. pneumoniae*, *N. gonorrhoeae*) [119], [120], [121]. This theory, however, was questioned by Vanet and Labigne who suggested that a specific and selective mechanism is involved in the secretion of some *H. pylori* antigens and according to their data, programmed autolysis process does not seem to play a major role [122]. Furthermore, autolysis is inconsistent with the general observation that *H. pylori* differentiates to dormant coccoid forms in late growth phases instead of lysing spontaneously [122], [124]. Whereas some authors consider that it is mainly the cytoplasmic urease that acts to reduce acidity and only a small percentage of the urease is associated with the surface [125]. Some others demonstrated that cytoplasmic urease alone is insufficient to confer resistance to acid (initial pH = 2) in the presence of urea and most probably both the cytoplasmic and the surface-associated urease are of importance [126].

3.3 Cytokines

Today the term cytokine is used as a generic name for a diverse group of soluble proteins and peptides which act as humoral regulators at nano- to picomolar concentrations and which, either under normal or pathological conditions, modulate the functional activities of individual cells and tissues. These proteins also mediate interactions between cells directly and regulate processes taking place in the extracellular environment (autocrine, paracrine, juxtacrine, retrocrine). Many growth factors and cytokines act as cellular survival factors by preventing programmed cell death.

The term Type-1 cytokines refers to cytokines produced by Th1 T-helper cells while Type-2 cytokines are those produced by Th2 T-helper cells. Type-1 cytokines include IL-2, IFN γ , IL-12 and TNF β , while Type-2 cytokines include IL-4, IL-5, IL-6, IL-10, and IL-13.

Most cytokines are generally not stored inside the cells (exception for example TGF- β). Cytokines are usually produced only by activated cells, and the expression of most cytokines is regulated at practically all levels: at transcription, translation, protein synthesis, secretion or release, and at receptor level.

Almost all cytokines are pleiotropic effectors showing multiple biological activities. In addition, multiple cytokines often have overlapping activities and a single cell frequently interacts with multiple cytokines with seemingly identical responses (cross-talk). Due to this functional overlap one or more factors may frequently functionally replace another factor or at least partially compensate for its lack. Since most cytokines have ubiquitous biological activities, their physiologic significance as normal regulators of physiology is often difficult to assess.

Many cytokines show stimulating or inhibitory activities and may synergize or antagonize also the actions of other factors. A single cytokine may elicit reactions also under certain circumstances which are the reverse of those shown under other circumstances. The type, the duration, and also the extent of cellular activities induced by a particular cytokine can be influenced considerably by the micro-environment of a cell, depending, for example, on the growth state of the cells (sparse or confluent), the type of neighboring cells, cytokine concentrations, the combination of other cytokines present at the same time, and even on the temporal sequence of several cytokines acting on the same cell. Under such circumstances combinatorial effects thus allow a single cytokine to transmit diverse signals to different subsets of cells.

Interleukins	Principal Source	Primary Activity
IL-1 α and - β	macrophages and other antigen presenting cells (APCs)	costimulation of APCs and T cells, inflammation and fever, acute phase response, hematopoiesis
IL-2	activated TH ₁ cells, NK cells	proliferation of B cells and activated T cells, NK functions
IL-4	TH ₂ and mast cells	B cell proliferation, eosinophil and mast cell growth and function, IgE and class II MHC expression on B cells, inhibition of monokine

		production
IL-5	TH ₂ and mast cells	eosinophil growth and function
IL-6	activated TH ₂ cells, APCs, other somatic cells	acute phase response, B cell proliferation, thrombopoiesis, synergistic with IL-1 and TNF on T cells
IL-7	thymic and marrow stromal cells	T and B lymphopoiesis
IL-10	activated TH ₂ cells, CD8 ⁺ T and B cells, macrophages	inhibits cytokine production, promotes B cell proliferation and antibody production, suppresses cellular immunity, mast cell growth
IL-12	B cells, macrophages	proliferation of NK cells, INF- γ production, promotes cell-mediated immune functions
IL-13	TH ₂ cells	IL-4-like activities
IL-17	T cells, epithelia cells	Stimulate IL-8 production in epithelial cells
IL-8	macrophages, other somatic cells	chemoattractant for neutrophils and T cells
INF α and - β	macrophages, neutrophils and some somatic cells	antiviral effects, induction of class I MHC on all somatic cells, activation of NK cells and macrophages

INF γ	activated TH ₁ and NK cells	induces of class I MHC on all somatic cells, induces class II MHC on APCs and somatic cells, activates macrophages, neutrophils, NK cells, promotes cell-mediated immunity, antiviral effects
Factors	Principal Source	Primary Activity
TGF- β at least 100 different family members	activated TH ₁ cells (T-helper) and natural killer (NK) cells Mucosal parietal and chief cells	anti-inflammatory (suppresses cytokine production and class II MHC expression), promotes wound healing, inhibits macrophage and lymphocyte proliferation Note: at least 100 different family members
Chemokines	Principal Source	Primary Activity
MIP-1 β	macrophages	Induce production of reactive oxygen species in neutrophils and the release of lysosomal enzymes, IL-1, IL-6, TNF α induction, chemotaxis. Activates chemokine activated killing
MCP-1	monocytes, vascular endothelial cells, smooth muscle cells, glomerular mesangial cell, osteoblastic cells, certain epithel cells	MCP-1 is chemotactic for monocytes but not neutrophils, regulates CD11 expression, induces degradation of basophiles and histamine release, activates chemokine activated killing

3.3.1 Genetic predisposition

The importance of heterogeneity in immune responses among human populations and individuals is further demonstrated by the contribution of cytokine polymorphisms to disease risk. Polymorphisms that increase the IL-8, IL-1 β response to *H. pylori* are associated with an increased risk of developing hypochlorhydria, gastric atrophy and adenocarcinoma [127], [128], [129]. Polymorphisms in TNF α and IL-10 genes have a similar, but less pronounced, association. Thus the degree of activation of the immune response, which underlies *H. pylori*-associated pathology, is dependent on both *H. pylori* strain determinants and host genetic factors.

3.4 Immune response

H. pylori infection activates immune response, which is manifested by continuous epithelial cell cytokine signaling and gastric mucosal infiltration by neutrophils, macrophages, and lymphocytes. There is a pronounced specific acquired immune response, including generation of antibodies and effector T cells.

3.4.1 The gastric mucosa as the first line of defense

The mucosal epithelium plays an important role as a first line of defense against *H. pylori* infection and also provides a barrier between the immunologically unprotected stomach lumen and the host tissue which is loaded with mononuclear cells. *H. pylori* has been shown to induce a strong cytokine response (IL-8, GM-CSF, MCP-1, IL-1 β) in both human gastric epithelial cells [130] and gastric epithelial cell lines [131], [132], [133]. This is partly due to bacterial factors e.g., urease, CagA, VacA and other antigens, which may also affect the surrounding epithelium. The mucosal cytokine response differs among patients. In addition to bacterial factors, this may also be due to environmental or host factors. As it is known, long time infection of the mucosa can lead to mucosal damage, in many cases to ulceration (gastric or duodenal ulcerations), which is characterized by the loss of epithelial cells. Healing of the mucosal injury is mediated by epithelial cell growth factors like TGF, EGF, or HB-EGF, coordinating the cell proliferation.

3.4.2 Humoral immune response

During the early phase of infection, nine highly immunoreactive *H. pylori* proteins elicit production of IgM antibodies: Alkyl hydroperoxide reductase (TsaA), Superoxide dismutase (SodB), Hydrogenase expression/formation protein (HypB), Iron(III) ABC transporter, periplasmic iron-binding protein (CeuE), EF-TU, Flagellin A, Flagellin B, Urease beta subunit (urea amidohydrolase), DnaK protein (heat shock protein 70) [134]. These proteins may be generally involved in colonization and establishment of *H. pylori* infection [135], [136].

IgM production is followed by the production of IgG and secretory IgA. However, in the gastric mucosa IgG concentration is low. This low IgG concentration together with the inhibitory effect of urease may prevent *H. pylori* opsonization [137].

3.4.3 Cellular immune response

After colonization, although *H. pylori* does not invade the gastric lamina propria it induces infiltration of lymphocytes, plasma cells, mononuclear phagocytes and polymorphonuclear neutrophils (PMNs) and stimulates the expression of proinflammatory cytokines. Previous studies have shown that *H. pylori* induce strong B-cell responses as well as activation of T cells locally in the gastric mucosa. Despite a specific humoral and cellular immune response, the infection shows lifelong persistence in the majority of cases. The inability to eliminate *H. pylori* may be due to bacterial virulence determinants and immune-evasive strategies as well as an inappropriate host immune response.

Although the immune response induced by *H. pylori* appears to be ineffective, it does have important implications for the onset of disease. The severity of gastric mucosal damage observed during chronic antral gastritis is directly correlated with the extent of phagocytic infiltration [138], [139].

In a number of studies, the local cytokine response to *H. pylori* infection was shown to be of the Th1 type, with increased IFN γ and interleukin-12 (IL-12), but not IL-4, production in the infected gastric mucosa [140], [141]. This showed to be more prominent for type I strains [142] being rather unusual for extracellular, toxin-producing bacteria,

which usually are met by B cell activation and high-level antibody production (Th2 response). However, Zabaleta et al. [143] described that the majority of gastric *H. pylori*-specific T cell clones from peptic ulcer patients express the Th1 profile and clones were shown to be specific for cytotoxin-associated protein (CagA) urease, VacA, HSP and many yet not identified epitopes. A predominant Th1 response was associated with lower *H. pylori* colonization density but also with more severe gastric inflammation and atrophic changes. On the other hand, peptic ulceration is rare during an immune suppressed Th2 predominant state (for example pregnancy or genetic predisposition).

In a recent publication, in most uncomplicated chronic gastritis patient secretion of both Th1 and Th2 cytokines (Th0 profile) was detected [144]. Thus in uncomplicated gastritis cases the immune response may be down regulated.

3.5 Dendritic cells

Dendritic cells (DCs) were first described in the mid 1970s by Ralph Steinman, who observed in the spleen a subpopulation of cells with a striking dendritic shape. DCs were described as cells that constitutively expressed both major histocompatibility complex (MHC) class I and class II antigens, spontaneously clustered T cells via antigen-independent mechanisms (later understood to represent the interplay of surface molecules on DCs that were mutually complementary to surface molecules on T cells), and most importantly, stimulated naive CD4⁺ and CD8⁺ T cells to respond to nominal and alloantigens more effectively than any other previously described antigen presenting cell (APC).

DCs are a heterogeneous group of cells that display differences in anatomic localization, cell surface phenotype, and function. However, DCs have several features in common [145], [146]. First, originating from CD34 bone marrow stem cells, precursor DCs are seeded via the bloodstream to the tissues where they give rise to immature DCs that include Langerhans cells (LCs) and interstitial DCs (also called dermal DCs). Second, immature DCs have the ability to take up antigen, via both receptor- and non-receptor-mediated mechanisms, and readily degrade antigens in endocytic vesicles to produce antigenic peptides capable of binding to MHC class II. Third, in response to danger signals, i.e. tissue damage, pathogen-derived products, or inflammatory cytokines, DCs

mature and migrate to lymphoid organs where they interact with antigen-specific CD4⁺ T cells to initiate immune responses [147], [148], [149], [150], [151], [152], [153]. Fourth, distinct chemokine receptors occur on immature DCs, compared with mature DCs, which regulate their traffic into tissue sites in response to inflammatory chemokines [154], [155], [156], [157]. Fifth, as DCs mature, they express a high density of MHC class II molecules complexed with antigen for recognition by the T cell receptor (TCR) expressed on CD4⁺ T cells and costimulatory molecules to stimulate CD4⁺ T cell proliferation. Finally, other factors in the microenvironment at the time of DC maturation have been shown to dictate whether DCs will produce IL-12 and initiate Th1 responses or have their IL-12-producing capacity suppressed and initiate Th2 responses [153].

DCs can induce CD8⁺ T cell immune response through antigen presentation via MHC class I molecule.

Dendritic cell subsets

DCs can also be propagated from bone marrow and blood using various combinations of growth factors (Figure 16), such as granulocyte macrophage-colony stimulating factor (GM-CSF), tumor necrosis factor- α (TNF α), interleukin (IL)-4, stem cell factor (SCF), transforming growth factor- β (TGF- β), IL-3, and Flt3 ligand (Flt3L) [158], [159], [160], [161], [162], [156], [163], [164]. GM-CSF in combination with IL-4 or TNF α and other cytokines provides important growth factors for interstitial DCs and LCs. In addition, LCs also requires TGF- β for their differentiation [165], [163]. IL-3 is a cytokine required by plasmacytoid DCs, a noninterstitial, non-LC DC subtype, that express CD123 (IL-3 R α) and are found in lymphoid tissue [166]. Flt3L is used to stimulate the proliferation of stem cells and progenitor cells in vitro and expand and mobilize all DCs and their progenitors in vivo [160], [167], [168], [161].

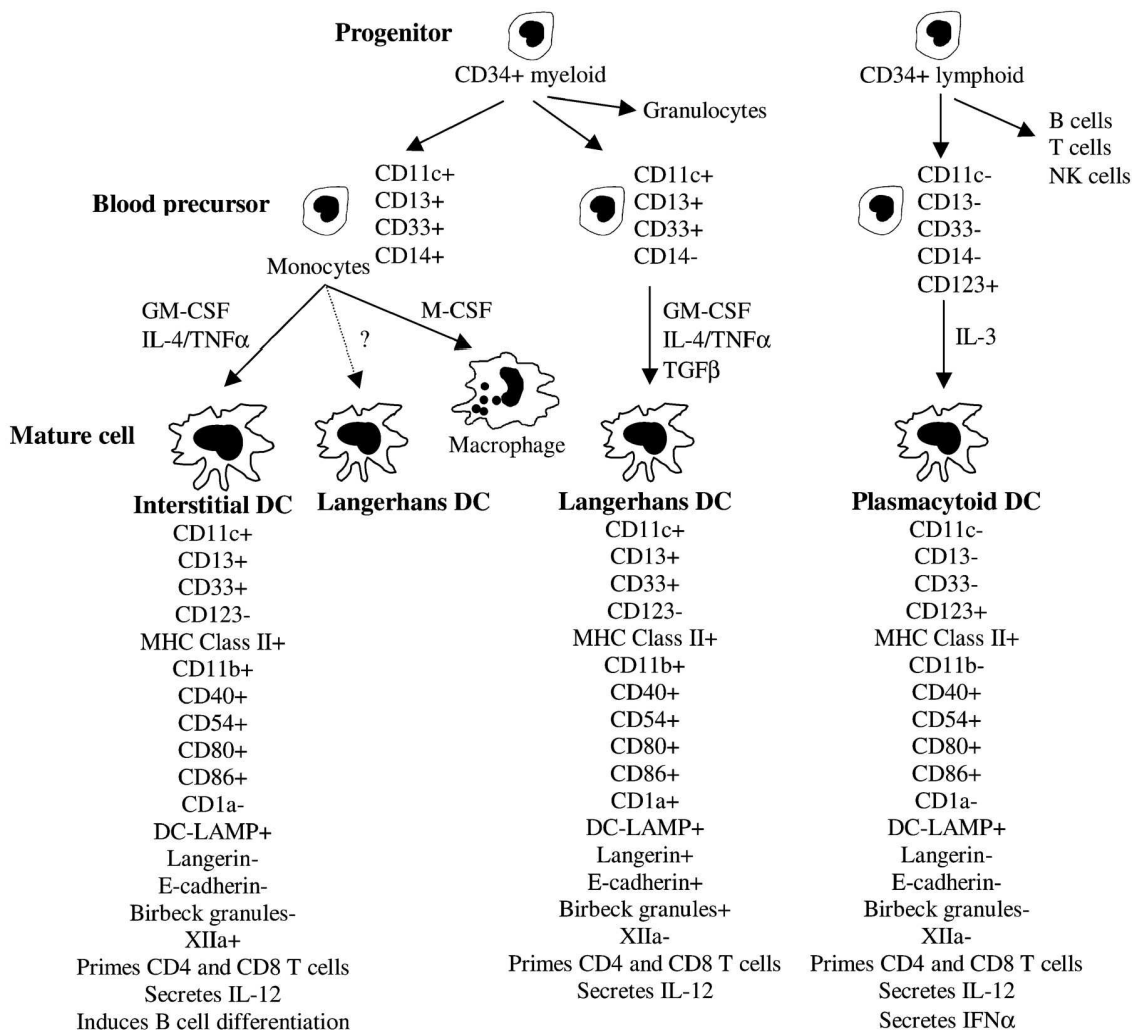


Figure 16 Schema for derivation of human dendritic cell (DC) subsets from CD34+ myeloid and lymphoid progenitors. In humans, DCs are found as precursor populations in bone marrow and blood and as more mature forms in lymphoid and nonlymphoid tissues (top). Both myeloid and lymphoid lineage DCs can be propagated from bone marrow progenitors and blood precursors using various combinations of growth factors, such as granulocyte macrophage-colony stimulating factor (GM-CSF), tumor necrosis factor- alpha (TNF- α), interleukin (IL)-4, transforming growth factor- beta (TGF- β), and IL-3. Interstitial DCs and Langerhans DCs subsets (middle) are found at sites that interface with the external environment. Plasmacytoid DCs are found in the T cell zones of lymphoid organs and in the thymus and blood.

DCs are migratory cells that traffic from one site to the next, performing specific functions at each site [169], [170], [171], [157]. Bone marrow-derived DCs circulate as precursors in blood before entering tissue where they become resident immature DCs that monitor their environment (Figure 17.). Interstitial DCs and LCs are found at sites that interface with the external environment, i.e. mucosal surfaces and in the skin. In peripheral tissues, immature DCs have the ability to migrate toward inflammatory foci where they take up and process available antigens and then migrate through the

lymphatics to draining lymph nodes. There they home to T cell-rich areas and interact with T cells to initiate an immune response.

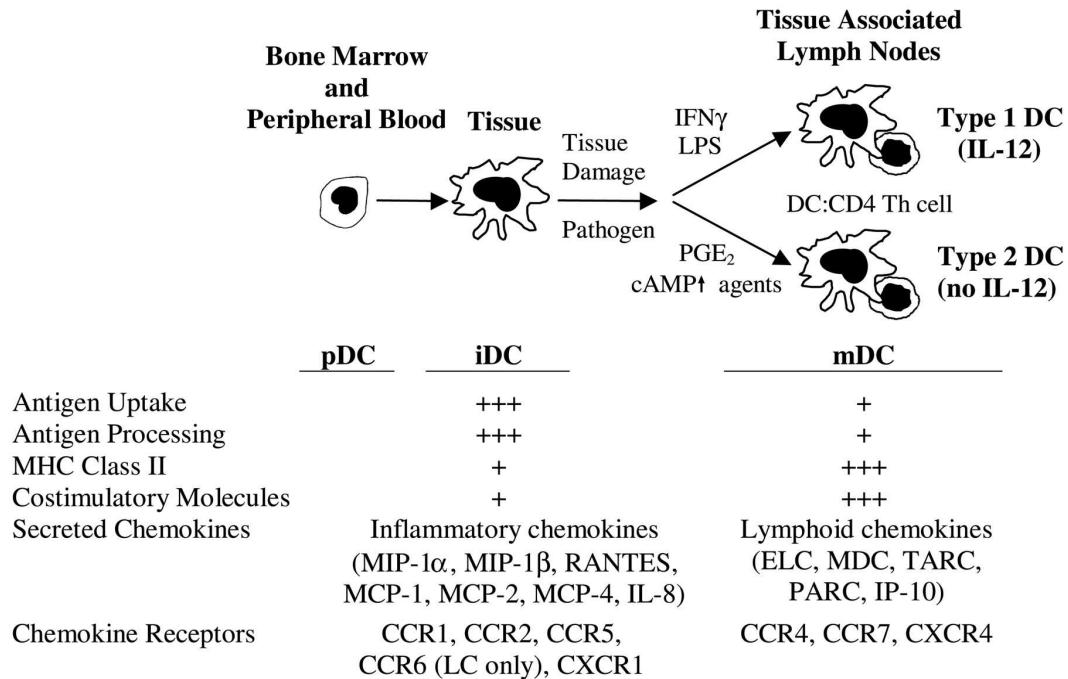


Figure 17 The migratory and maturation pathways of DCs. DCs are migratory cells that traffic from one site to the next, acquiring specific abilities at each site and performing specific functions in a stepwise fashion. pDC, precursor DC; iDC, immature DC; mDC, mature DC.

3.5.1 DC-T cell Interaction

During the development of an adaptive immune response, the phenotype and function of DCs play an important role in initiating tolerance, memory, and polarized Th1 and Th2 differentiation. As discussed, DC subsets have been proposed as playing differing roles in defining the outcome of an immune response, although clearly some plasticity within defined subsets is possible so that each subset can exert tolerizing and polarizing influences on responding T cells [172]. Important factors other than signals delivered by DCs that drive primary immune responses are concentration of antigen in the microenvironment, concentration of cytokines and other soluble factors present in the fluid phase in the vicinity of the APC-T cell interface and, of course, the genetics of the host that may limit how the interacting cells may respond.

CD4⁺ and CD8⁺ T cells respond to peptide antigen displayed on MHC class II and MHC class I molecules, respectively.

Figure 18 shows a model of DC-T cell interaction. MHC I and II (referred to as *signal 1*). These accessory molecules on DCs are required to ensure that T cells will divide and differentiate into effector cells (*signal 2*). In the absence of sufficient costimulation, T cells exhibit anergy or undergo apoptosis. Secretion or lack of secretion of factors by DCs, particularly IL-12, are instrumental in the final differentiation of T cells into type 1 or type 2 effector T cells, respectively (*signal 3*). As a negative-feedback signal at the end of the immune response, cytotoxic T lymphocyte antigen (CTLA)-4 molecules appear on the T cell surface and binds to CD80 and CD86 molecule and block T cell activation. The model is the simplest one to explain the development of a productive immune response by CD4⁺ T cells, but the list of membrane and secreted molecules that play roles in regulating the interaction of DCs and T cells is growing.

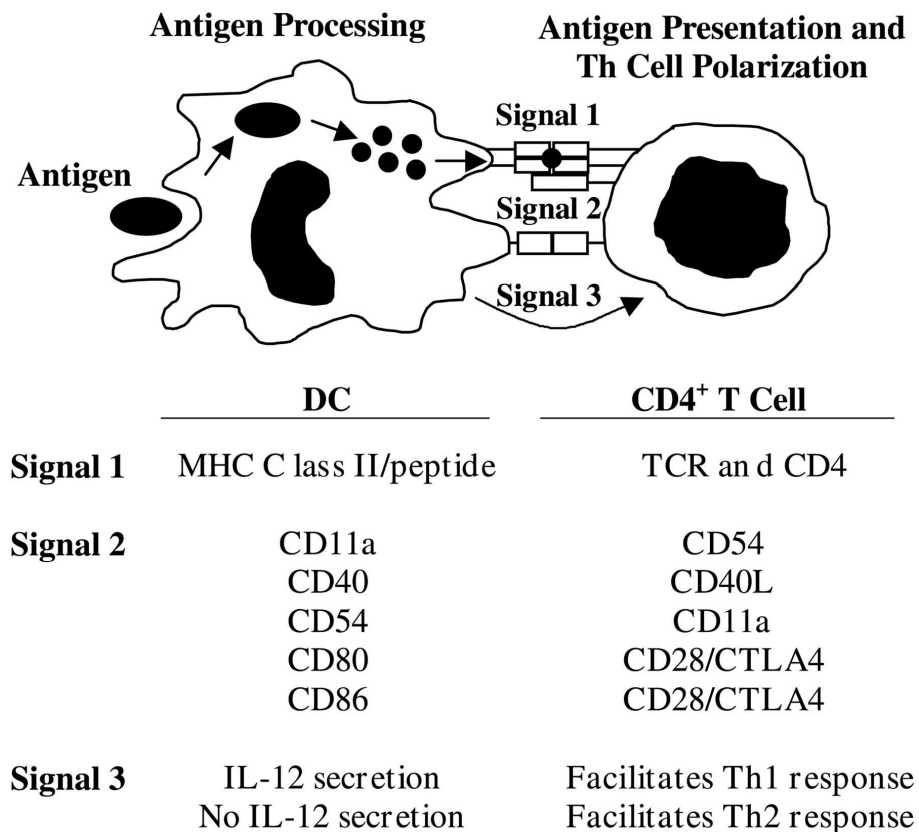


Figure 18 Model for DC-CD4⁺ T cell interaction. DCs provide three signals to antigen-specific CD4⁺ T cells to initiate T cell proliferation and differentiation. DCs take up antigen and readily degrade antigens to produce antigenic peptides capable of binding to MHC class II. DCs express a high density of MHC class II/peptide complexes on their cell surface for recognition by the T cell receptor (TCR) expressed on CD4⁺ T cells (signal 1) and costimulatory molecules (signal 2) to stimulate CD4⁺ T cell proliferation. Secretion or lack of secretion of interleukin-12 (IL-12) by DCs (signal 3) is important in the final differentiation of CD4⁺ T cells into type 1 or type 2 effector T cells, respectively. All accessory molecules are not included. See text for additional details.

3.5.2 Antigen uptake

DCs take up and present peptides from complex antigens, immature DCs are avidity endocytic, whereas mature DCs have downregulated this activity [173]. DCs degrade antigens within a MHC class II-rich endosomal compartment (MIIC) yet preserve sufficient peptide structure to be expressed on their cell surface bound to MHC class II molecules. DCs take up antigens by phagocytosis, utilizing membrane receptors to trigger uptake, by receptor-mediated pinocytosis in clathrin-coated pits and by fluid-phase pinocytosis. DCs can take up whole cells, including necrotic and apoptotic cells. They can also acquire antigens from live cells for presentation to cytolytic T cells [174]. Receptors available to some or all DC subsets for antigen uptake include Toll-like receptors (TLR2, TLR4), the Fc γ Rs CD32 and CD64, the high- and low-affinity IgE receptors Fc ϵ RI and Fc ϵ RII (CD23), respectively; the complement receptors CD11b and CD11c; a C lectin type of mannan binding receptor, DEC205 (CD205), and the scavenger receptor pair for apoptotic cells $\alpha_v\beta_5$ and CD36 [146], [175]. More recently, immature human interstitial DCs were shown to express the Fc α R CD89 [176]. Furthermore, TLR2 and TLR4 were shown to be expressed inside the DCs, and induce full cytokine production only after antigen phagocytosis and intracellular receptor interaction. During maturation, as endocytosis decreases, these receptors are usually downregulated whereas MHC I-II, costimulatory molecules such as CD80, CD83, DC86 and adhesion molecules such as CD54 are upregulated [177], [178].

3.5.3 *Helicobacter pylori* and Dendritic cell interaction

One of the main attributes of dendritic cells in *H. pylori* defense compared to monocytes is that dendritic cells are resistant to *H. pylori*-induced apoptosis [179]. Thus, DC activation by *H. pylori* is crucial for the development of an immune response. The ability of DCs to open up tight junctions, together with their ubiquitous distribution in the human body, including gastrointestinal mucosa, increases the probability of a direct contact of bacteria and DCs. Very recently, studies have demonstrated activation and maturation of human DCs by *H. pylori*. Also DCs pulsed with *H. pylori* were shown to induce NK cell activation as well as Th1 effector responses [180].

3.5.4 Role in peripheral tolerance mechanisms

Peripheral tolerance mechanisms include T cell death, T cell anergy, and active suppression by regulatory T (Tr) cells. Once in the periphery, as described above, productive immune response will be established when DCs, which have taken up antigen, are activated and present optimal levels of MHC/peptide complexes in the context of accessory molecules. In the normal host if self-antigens are presented, no T cells should be available to respond, because of central tolerance induction. However, if T cells recognize only low levels of MHC/peptide, have a low affinity for their cognate ligand, or receive no costimulation from DCs, they become anergic or undergo apoptosis. Two main subsets of CD4⁺ T cells with regulatory activity have been described: type 1 (Tr1) and CD4⁺CD25⁺ Tr cells.

If a naive T cell encounters its antigen on immature DCs (iDCs), it may differentiate into regulatory T cells (Tr) rather than T-effector cell. The resultant Tr cells are phenotypically and functionally identical to Tr1 cells because their generation requires production of IL-10 by iDCs, and they suppress T-cell responses through an interleukin-10 (IL-10), - and a transforming growth factor beta (TGF- β)-dependent mechanism. Tr1 cells do not express high constitutive levels of CD25 or the transcription factor FoxP3.

In contrast, CD4⁺CD25⁺ Tr cells can either arise directly in the thymus or be induced by antigen in the periphery. Little is known about the molecules that control the development and function of CD4⁺CD25⁺ Tr cells. The transcription factor FOXP3 is recently entered the spotlight as a critical component of CD4⁺CD25⁺ Tr cell development and function, but the mechanism of FOXP3-mediated transcriptional repression and the affected target genes are still largely unknown [181]. Role of other factors in addition to FOXP3 are also suggested during the process of activation and/or differentiation for the development of CD4⁺CD25⁺ Tr cells [182]. In contrast to Tr1 cells, the naturally occurring CD4⁺CD25⁺ Tr cells appear to be cell-contact-dependent. CD4⁺CD25⁺ T cell populations are heterogeneous and only a subset of clones continues to express high levels of CD25 and is suppressive. The intensity of CD25, cytotoxic T lymphocyte antigen (CTLA)-4, and glucocorticoid-induced tumor necrosis factor (TNF) receptor expression correlates with the suppressive capacity of these Tr cell clones. None of the

CD4⁺CD25⁺ T cell clones with suppressive function produce IL-10, but all produce TGF- β . Suppression mediated by CD4⁺CD25⁺ T cell clones is partially dependent on TGF- β , but not on constitutive high expression of CD25 [183]. The main role of CD4⁺CD25⁺ Tr cells is to suppress autoimmunity.

3.6 Persistence of infection

If a microbe is to persist in a host, it has to avoid clearance by the immune system. The lifelong colonization by *H. pylori* demonstrates the effectiveness of the *H. pylori*'s strategies to evade host immunity. The first important step is to survive without tissue invasion and remain in the apical mucus layer which is not protected by the immune system. However, even in this niche, approximately 2% of the bacteria have direct epithelial cell contact and some *H. pylori* proteins cross the epithelial barrier and both innate and acquired immune systems are activated. To reduce the direct contact with the immune cells, although it is not able to completely avoid immune activation, *H. pylori* has evolved mechanisms to reduce recognition by immune sensors, downregulate activation of immune cells and escape immune effectors. The innate immune system recognition of microorganisms involves Toll-like receptors (TLRs) that discriminate pathogen associated molecular patterns. *H. pylori* has evolved to minimize such stimulation. TLR4 recognize bacterial LPS, but because of lipid A core modifications, *H. pylori* LPS has low biological activity as compared to LPS from other species [184], [185] [186]. TLR5 usually recognizes bacterial flagella but not *H. pylori* flagellar protein FlaA [187]. TLR9 recognizes the largely unmethylated DNA of most bacteria, but the highly methylated *H. pylori* DNA likely minimizes recognition [188].

H. pylori infection also activates the acquired immune system, although it has evolved mechanisms to downregulate and to avoid acquired immune system effectors. Recognition by the acquired immune system requires antigen presentation. Although somatostatin inhibits dendritic cell activation [189], *H. pylori* can also directly interfere with both uptake and processing of antigens, partially through a VacA effect. VacA blocks phagosome maturation in macrophages, selectively inhibits antigen presentation in T cells [190], blocks T cell proliferation and activation by interacting with calcineurin to block signaling. This results in a failure of the activated T cell to produce IL-2 and IL2R α ,

but also a number of chemokines such as macrophage inflammatory protein (MIP)-1 α , and MIP-1 β - that might be essential for a concerned immune response [191], [192] and induces selective cell apoptosis [193], [191], [194]. Furthermore, Lee-Ann et al. showed that phagocytosis of type I *H. pylori* strains (but not type II organisms) exhibits two unusual features [195]. First, actin polymerization and phagosome formation are delayed until several minutes after bacterial attachment to macrophages. Second, *H. pylori* phagosomes undergo extensive clustering and fusion during the first few hours after bacterial ingestion. Organisms inside these "megosomes" remained viable for at least 24 h. [196], [197], [198]. Also, intracellular killing was shown to be impaired by *H. pylori*.

Furthermore, a yet unknown secreted protein, which is between 30-60 kDa, was shown to induce T cell-cycle arrest of the G1 phase of T cells by suppressing a cyclin-dependent kinase activity [199]. *H. pylori* evades host adaptive responses also by mimicry of the gastric epithelial fucosylated (Lewis) antigens. Urease also seems to be protective for the bacterium by preventing the bacterial – host interaction [200], [201]. The urease significantly inhibits *H. pylori* adherence to Kato III cells by a mechanism largely independent of enzymatic activity [202]. It is thinkable that *H. pylori* urease masks bacterial outer membrane components that are involved in adherence and thus impedes the interaction of bacterial adhesins with host cell receptors. This effect, which has been attributed to the capsule antigen of several bacterial species [203], [204], also could be one of the properties of *H. pylori* urease, which, although not a capsule, may act as such with respect to the inhibition of adherence. This also is consistent with previous findings demonstrating that urease inhibits phagocytosis by granulocytes and monocytes and opsonization by human complement by a mechanism which is largely independent from ammonia production [205], [206], [207], [208].

In addition *H. pylori* is able to activate local regulatory T cells and directly downregulate the local immune response. In a very recent study, authors reported the presence of CD4⁺CD25⁺ Tr cells in *H. pylori* infected (symptomatic and asymptomatic) patients in the stomach and duodenal mucosa in contrast to uninfected mucosa. These specific regulatory T cells were able to suppress memory T cell responses to *H. pylori* in infected individuals. Additionally, higher levels of mucosal cytotoxic T lymphocyte-associated

antigen 4 (CTLA-4) protein and higher level of FOXP3 mRNA in infected persons [209] were also observed.

In spite of the mentioned mechanisms, the fact that *H. pylori* induces HB-EGF expression by gastric epithelial cells may also contribute to the persistent nature of the infection, in terms of re-epithelialization, ulcer healing, and thus reduction of the direct contact between bacterium and the immune system [210].

The relative contributions of the different host manipulation and evasion strategies to *H. pylori* persistence are not established, possibly differing in individual hosts, but the existence of these varied mechanisms implies that immune surveillance of the gastric lumen is powerful, and the bacterial survival requires its subversion.

4 Aim of the study

The aim of the present in-vitro study was to further investigate the contribution of *H. pylori* urease in the persistent nature of the infection. For this purpose, isogenic live bacteria (a parental strain, mutants lacking urease or producing an enzymatically inactive apoprotein, and complemented clones), the respective bacterial lysates, purified surface-associated urease or the recombinant structural subunits were used to stimulate appropriate cell cultures.

First, the effect of urease on the expression of HB-EGF, which is of importance in ulcer healing and may therefore prevent the interaction between *H. pylori* and the immune system, was examined at the transcriptional, secretional and functional level using the human gastric epithelial cell line Kato III.

Furthermore, the possible influence of *H. pylori* urease on the type of immune response (Th1/Th2) was investigated by stimulation of PBMCs and determination of CD4⁺ T cell activation and intracellular and extracellular cytokine production (IL-10, IFN γ , IL-4).

Finally, the effect of urease on maturation of monocyte derived dendritic cells and cytokine secretion by these cells was also investigated, since cytokines released by dendritic cells may also influence the type of immune response. Release of TGF- β 1, which like HB-EGF may contribute to ulcer healing and, furthermore may play a role in the induction of immune tolerance, was also assessed.

5 Materials and Methods

5.1 *Bacteria and culture conditions*

E. coli strains DH5 α and SG19003 were grown on Luria-Bertoni (LB) medium where appropriate kanamycin (20 μ g/ml), chloramphenicol (30 μ g/ml) and/or ampicillin (100 μ g/ml) were added. *E. coli* strains were cultured at 37°C under aerobic conditions. *H. pylori* wild-type N6, isogenic mutants and complemented clones were used. Isogenic mutants N6*ureB*::TnKm and N6*ureG*::TnKm were obtained from wild-type N6 by shuttle mutagenesis with the transposon mini-Tn3 as described by Ferrero et al [211] and Cussac et al [212] and are kanamycin resistant. N6*ureB*::TnKm is lacking urease while N6*ureG*::TnKm lacks the urease accessory protein *UreG*, and produces an enzymatically inactive apoenzyme. Parental and mutant strains were kindly provided by A. Labigne (Unité de Pathogénie Bactérienne des Muqueuses, Institut Pasteur, Paris).

Complemented clones of N6*ureB*::TnKm were designed by stable transformation with the vector pHel2 containing the cloned genes *ureA* and *ureB* and their specific promoter sequence. The orientation of the cloned insert was found to be crucial for urease expression. The K2-type of complemented clones functionally expressed urease at higher levels than did N6 and the K8-type clones exhibited similar urease activity compared to that of the wild-type N6. This is also supported by the data of SDS-PAGE analysis, which indicate considerably higher urease subunit contents in K2-type clones than in wild-type N6 or K8-type clones. *H. pylori* culture was done with Brucella (BD Biosciences, NJ, USA) agar or broth supplemented with 5% FCS (Life Technologies Gibco-BRL / Invitrogen GmbH, Paisley, UK), where appropriate kanamycin (20 μ g/ml) and chloramphenicol (5 μ g/ml) were added to the culture medium. Cultures were incubated at 37°C under microaerobic conditions (85% N₂, 10% CO₂, 5% O₂). For stimulation of human cells, bacteria grown on Brucella agar (Merck, Darmstadt, Germany) for 72 h were used to inoculate 10 ml of Brucella broth (Merck) to an initial optical density at 560 nm (OD₅₆₀) of 0.2. On the next day, a 2-5 ml aliquote of this preculture was added to 50 ml Brucella broth and incubated for additional two days.

5.2 Genetic complementation of mutant N6ureB::TnKm

The genetic complementation of the urease lacking mutant was based on a protocol described previously. Briefly, using upstream primer ure1 (36-mer; 5'-GAG AGG AAG ATC TTC GCT GAT GTC ATG ATA GAT GTG-3') and downstream primer ure2 (37-mer; 5'-GAG AGG AAG ATC TCC TAG AAA ATG CTA AAG AGT TGC G-3'), the ureAB and promoter region elongated on both sides by a sequence including a *Bgl*II restriction site (AGATCT) was amplified by PCR. The amplicon was digested and ligated into the digested and dephosphorylated pHel2 vector (Figure 19). The recombinant plasmid was transformed into calcium-competent *E. coli* DH5 α and chloramphenicol-resistant clones were selected. For the present study, recombinant *E. coli* clones stored in liquid nitrogen were used.

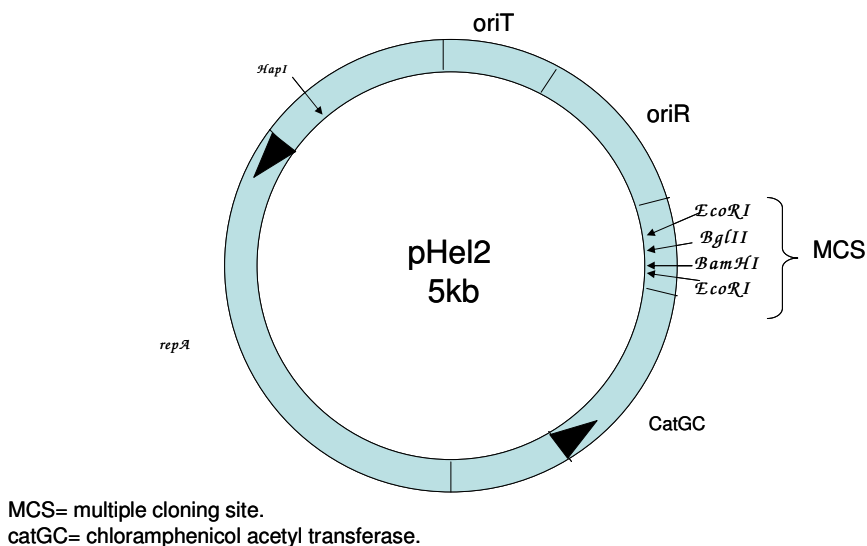


Figure 19 Cloning vector pHel2.

The insert orientation was assessed by gelelectrophoresis (1% agarose, 1 \times TAE) after digestion of reisolated plasmids (1 μ g) with *Bam*HI (2.5 U/ μ g DNA, 37°C 2 h; New England Biolabs GmbH, Frankfurt, Germany). Restriction digestion analysis by *Bgl*II (2.5 U/ μ g) and *Hpa*I (2.5 U/ μ g) was also performed. All reactions were carried out in a volume of 20 μ l and in the presence of the appropriate buffer (1 \times *Bam*HI-buffer, 1 \times NEB-buffer #3, 1 \times NEB-buffer #4; respectively). 10 μ l GLS were added prior to gel loading. A 1-10 kb molecular weight marker was used. Purified pHel2 vector DNA was used as control.

5.2.1.1 Electroporation

Recombinant plasmids from 8 *E. coli* clones (or pHel2 alone as a control) were electroporated into *H. pylori* N6ureB::TnKm. A protocol from Segal et al [242] with minor modifications was utilized. *H. pylori* N6ureB::TnKm was grown in 50 ml Brucella-broth supplemented with 5% FCS and kanamycin in a tissue culture flask for 2-3 days under microaerobic conditions at 37°C. The bacteria were harvested by centrifugation (2400 × g, 10 min, 4°C), washed with cold electroporation buffer and resuspended to a final concentration of 4-8 × 10¹⁰/ml. 40 µl of this suspension were placed in prechilled 0.2 cm electroporation cuvettes, 6 µg column-purified plasmid dissolved in water (5-10 µl; desalted by ultrafiltration using Microcon-100, Amicon) were added and the electric pulse was delivered (2500 V, 25 µF capacitor, 200 Ω; BioRad Gene-Pulser II, Hercules, CA, USA). Subsequently, the bacteria were plated on Brucella-agar supplemented with 5% FCS and kanamycin and incubated under microaerobic conditions at 37°C over night. On the next day, the bacteria were suspended in sterile 0.9% NaCl directly on the plate, aliquoted on 2-3 new Brucella-agar plates supplemented with 5% FCS, kanamycin and chloramphenicol and incubated further up to 10 days. Several double-resistant (Chlo^R, Kana^R) *H. pylori* single colonies were expanded, subjected to a urease activity test and stored at -70°C.

5.2.1.2 Characterization of complemented clones

To screen clones for urease activity, 20 µl of a bacterial suspension in PBS (OD₅₉₀ 0.5) were mixed with 300 µl of urease activity testing buffer in a 96-well flat bottom microtiter plate and handled as mentioned in 5.5.1. For a more precise characterization of the urease activity of a number of selected clones the Berthelot and Lowry method was used. These clones were further analyzed for the amount of UreAB production in comparison to wild-type N6 by SDS-PAGE and Western blotting.

Plasmid DNA of 42 urease positive or negative *H. pylori* double resistant clones (10 ml culture in Brucella broth supplemented with 5% FCS, kanamycin and chloramphenicol; 3 days, 37°C, microaerobic) was column-purified (QIAGEN-mini kit, Quiagen Vertiebs GmbH, Wien, Austria) 0.6 µg of plasmid DNA was subjected to restriction enzyme

digestion with *Bgl*II and *Bam*HI (5 U/μg DNA, 37°C 2 h) GLS was added prior to loading a 1% agarose gel (1× TAE). A 1-10 kb DNA weight marker was used.

5.3 *SDS-PAGE and Western blotting to detect *H. pylori* urease*

300 μl of a bacterial culture (OD₅₆₀ 0.2) were centrifuged (10 min, 3,600 x g). The pellet was washed twice with PBS and denaturation of proteins was done by resuspending bacteria in 200 μl sample buffer and heating the mixture to 75°C for 20 min. 2 μg protein (approximately 5-10 μl) were loaded on a mini-gel (mini-PROTEAN II cell; BioRad Laboratories, Ca, USA). Standard proteins served as markers for molecular weight protein ladder 10-200 kDa (MBI Fermentas, USA). After electrophoresis (150 V, 45 min), gels were fixed in fixing solution for 10 min and stained using Coomassie staining solution for 30 min. Gels were destained in 10% acetic acid over night or for 2 h with continuous change of the destaining solution. Then, gels were washed in water, scanned into a jpeg file, and gels were stored between 2 sealed plastic layers by 4°C.

For Western blot analysis, SDS-PAGE gels were not stained but piled carefully on point marked nitrocellulose membrane (Hybond-C 0.45 μm, Amersham Pharmacia Biosciences, Little Chalfont, UK). This was placed between up and down 3 x ice cold transfer-buffer soaked paper sheet. Proteins were electroblotted (0.8 mA/cm², 1 h) with transfer buffer onto nitrocellulose membrane employing a Multiphor II NovaBlot semidry-unit. The protein transfer was verified by staining the gel with Coomassie Brilliant Blue and the membrane by Ponceau S until the colour change was visualised (max 5 min). After destaining in distilled water, membrane was washed twice with TBS buffer for 10 min. The membrane was blocked by an over night shacked incubation in 20 ml BLOTTO at 4°C. Membrane was washed twice with TBS-Tween/Triton for 10 min following 10 min with TBS buffer. Polyclonal rabbit antibodies against recombinant UreA and UreB provided by Dr. H. DeReuse (Pasteur Institute, Paris, France) were used to detect *H. pylori* urease subunits. The membrane was incubated with an antibody dilution in BLOTTO (anti-UreA 1:100,000 and anti-UreB 1:10,000, respectively) for 2 h at room temperature with constant agitation and washed 3 times in TBS-Tween/Triton buffer following 10 min with TBS. Primary antibodies were detected by incubating the membrane in horse radish peroxidase (HRP) conjugated goat anti-rabbit-IgG (A545;

Sigma-Aldrich Corp, MO, USA) dilution (1:10,000 in TBS) for 45 min at room temperature with constant agitation. After 4 washing steps with TBS-Tween/Triton the wet membrane was absorbed with paper and soaked with 2 ml ECL-Western blotting detection reagents ECL-1 and ECL-2, according to the manufacturer's specification (Amersham Pharmacia Biotech, Buckinghamshire, UK). The membrane was exposed on Kodak X-omat film (Eastman Kodak, Pochester, N.Y.) immediately and the film was developed.

5.4 Modified Lowry Protein Assay

For protein determination Modified Lowry Protein Assay kit (Sigma, Deisenhofen, Germany) was used. 200 µl of protein solution were first reacted with 1 ml reagent containing alkaline cupric sulphate in the presence of tartarate. After mixing well, sample was incubated exactly 10 min at room temperature. This was followed by addition of 100 µl 1 N Folin-Ciocalteu Phenol reagent. Incubation lasted additional 30 min. The absorbance of the blue-coloured product was read at A_{750} in a spectrophotometer (Hitachi U-2000). Empty buffer served as blank. Standard curve was generated with 1-1500 µg/ml BSA in buffer (Figure 20).

A_{750}	Protein µg/ml
2,112	1500
1,761	1000
1,44	750
1,102	500
0,648	250
0,373	125
0,08	25
0,013	5
0	1

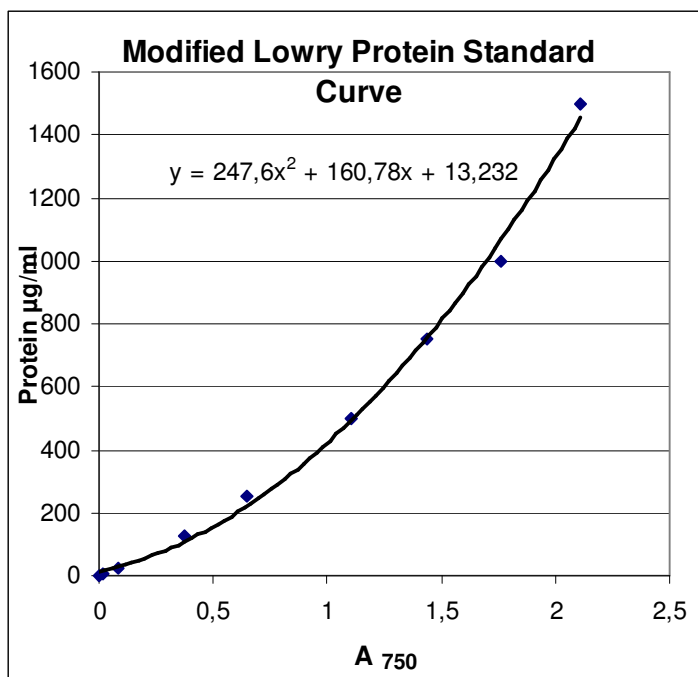


Figure 20 Modified Lowry Protein standard

5.5 Urease activity

5.5.1 Semiquantitative urease test

The test was usually performed as follows: 10 ml of the bacterial culture were centrifuged for 10 min at 4,000 x g, washed with phosphate-salin buffer (PBS) and the optical density (OD₅₆₀) was set to 0.7. 50 µl of the suspension were mixed with 250 µl urease activity testing puffer (37°C) in a 96-well flat bottom microtiter plate. For more than 1 sample a multichannel pipette to minimize handling delay was used. Blank wells received 50 µl PBS. The plate was immediately measured in an ELISA-reader (Dynatech MR 7000) at several time points for up to 40 min (every 5 min). In the presence of urease the colour changed from yellow to pink, which was measured at 570 nm Absorbance was plotted against time.

5.5.2 Urease specific activity using the Berthelot and Lowry method

To quantify urease activity more precisely, the Berthelot method, [213], [214] was used which allows for the quantitation of NH₄ production. Briefly, bacterial cultures on Brucella agar (72 h) or in Brucella broth (48 h optical density OD₅₆₀ 0.1-0.3) were used. Bacteria were washed in PBS and resuspended in 50 mM HEPES (pH 7.5) and OD₅₆₀ was set at 0.7. 1:20 to 1:1,000 dilutions were performed and 5 µl of each dilution were added into 1 ml fresh made 50 mM HEPES containing 25 mM urea. The dilutions were chosen to ensure that urease activity would be linear for at least 20 min. A sample was incubated at 37°C for 20 min in a thermomixer. Then, 200 µl were pipetted into a new tube and 400 µl of a phenol-nitroprusside solution and 400 µl of a hypochlorite solution were added in sequence. The reactions were mixed and incubated for 30 min at 37°C. Then, the absorption at 625 nm was determined. NH₄⁺ production was quantified using a standard curve (Figure 21). Urease specific activity was expressed as mmol of ammonia produced per mg of bacterial protein per min. Bacterial protein concentration was determined by the modified Lowry method using a commercially available kit (Sigma-Aldrich Corporation, MO, USA). The urease specific activity of an isolate was based on the average of 5-8 separate assays performed with different bacterial preparations on different days.

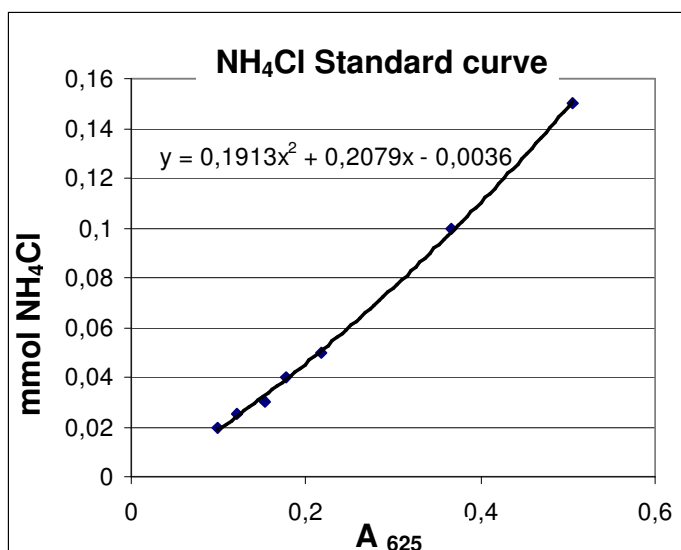


Figure 21 NH₄⁺ Cl standard curve.

5.6 Purification of surface associated *H. pylori* urease

5.6.1 Preparation of water extract of *H. pylori*

Cultures of wild-type N6 in Brucella broth were incubated under microaerobic conditions for 2 days. Bacteria were then centrifuged (10 min, 4,000 × g), washed with sterile 0.9% NaCl and collected in SA-600 sorvall centrifuge tubes. 8-15 ml iced distilled water were added and immediately tubes were vortexed vigorously for 1 min. After centrifugation at 16,500 × g (10 min 4°C) the supernatant was filtered through a 0.22 μm syringe filter. The protein content was quantified by modified Lowry Protein Assay and the preparation was tested for endotoxin content by the *Limulus* amoebocyte lysate assay according to the manufacturer's protocol (QCL-1000; BioWhittaker, Walkersville, MD). Urease activity was tested by the semiquantitative method.

5.6.2 Column chromatography

Water extract was mixed with $\frac{1}{10}$ volume of 10 × gel filtration buffer, filtered through a 0.22 μm syringe filter unit and concentrated to approximately 4 ml in a stirred ultrafiltration cell.

Chromatographic instrument: An FPLC system model ÄKTA purifier (Pharmacia Biotech, Uppsala, Sweden) with UV-, conductivity-, and pH sensors as well as automatic valves

was employed. The pump unit is equipped with two pump modules capable of producing up to 25 MPa of pressure. The whole system was placed in a cold lab and all separations were carried out at 16°C. Proteins were detected by absorbance at 280 nm. Temperature and pressure were recorded routinely. System controlling and surveillance was done with the software UNICORN 2.3 installed on a personal computer. Samples were injected using prefilled wire-loops or a 10 ml super-loop. Fractions were collected automatically either continuously or according to UV-peaks (software option “peak fractionation”).

Column chromatography: Three subsequent chromatographic separations were established. Initially, the concentrated water extract was subjected to a Sephacryl S-300 HR 26/60 column (60 × 2.6 cm I.D., Pharmacia) equilibrated with gel filtration buffer. The flow rate was 1 ml/min and 4 ml fractions were collected continuously after V_0 was reached. After screening the fractions for urease, the contents of positive tubes corresponding to a single peak were pooled, dialyzed against ion-exchange loading buffer and concentrated to approximately 3 ml. In the next step anion-exchange chromatography was performed using a Mono Q HR 5/5 column (5 × 0.5 cm I.D., Pharmacia) equilibrated with the same buffer. The flow rate was 1 ml/min and UV-peaks were collected during elution with a linear NaCl-gradient (0-500 mM, 18 ml). After screening the fractions for urease, the contents of positive tubes corresponding to a single peak were pooled, dialyzed against gel filtration buffer and concentrated to 0.5 ml. Subsequently, the material was loaded onto a Superdex 200 HR 10/30 column (30 × 1 cm I.D., Pharmacia) equilibrated with gel filtration buffer. The flow rate was 0.5 ml/min and UV-peaks were collected. Finally, urease-positive fractions were concentrated to approximately 1 ml.

Dialysis and concentration: A 10 ml stirred ultrafiltration cell model 8010 (Amicon, Beverly, MA, USA) containing a YM membrane with M_r 30000 cut off was employed. The cell was connected to a N_2 -gas supply and a pressure-resistant reservoir filled with the appropriate buffer for dialysis. Concentration- or dialysis-mode could be changed instantly by switching a valve. Dialysis was considered 99% complete when 5-times the volume of the sample had passed through the membrane [243]. To concentrate small

samples simultaneously disposable filter units Centricon-10 (Amicon) were also used. The purity of the urease was controlled by using SDS-PAGE and Western blot analysis.

5.7 Purification of recombinant urease

Recombinant *E. coli* SG19003 strains carrying the pQE-Tri plasmids with either UreA or UreB were kindly provided by C. Prince (Munich, Germany). The cloning sites of pQE-Tri expression plasmid are shown in Figure 22. The promoter and primer sequence regions are shown in Figure 23.

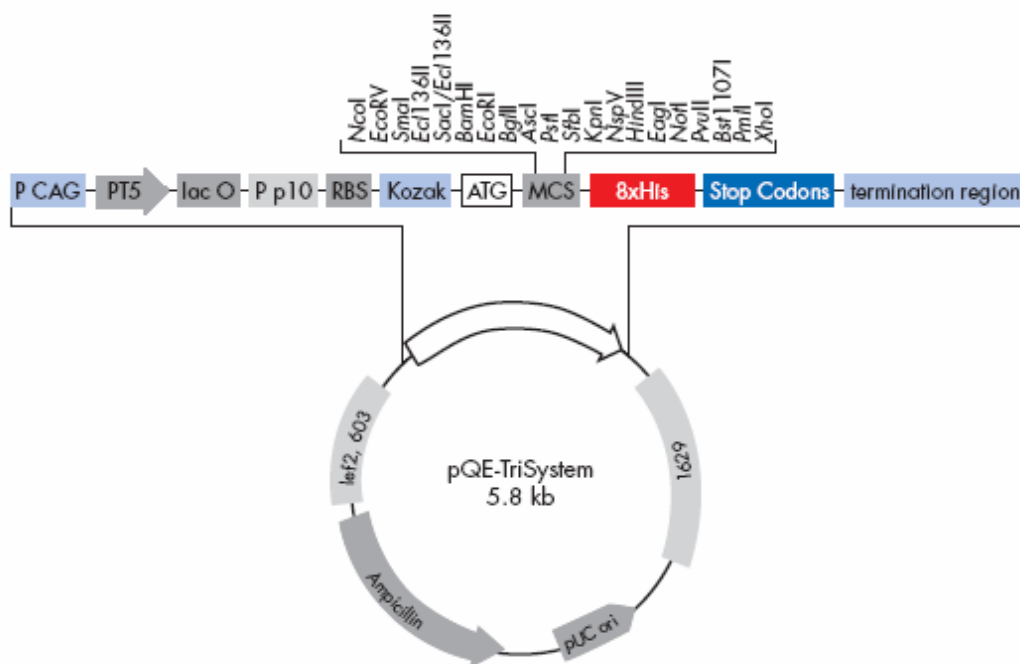


Figure 22 pQE-TriSystem vector for parallel protein expression using a single construct in *E. coli*, insect, and mammalian cells. PT5: T5 promoter, lac O: lac operator, RBS: ribosome binding site, ATG: start codon, 8xHis: His tag sequence, MCS: multiple cloning site, Stop Codons: stop codons in all three reading frames, Ampicillin: ampicillin resistance gene, P CAG: CMV/actin/globin promoter, P p10: p10 promoter, Kozak: Kozak consensus sequence, termination region: transcription terminator region, lef2, 603/1629: flanking baculovirus sequences to permit generation of recombinant baculoviruses, pUC ori: pUC origin of replication.



Figure 23 Overview of the pQE-TriSystem promoter region and sequencing primer annealing positions

5.7.1 Culture media and overexpression conditions

For the synthesis of the 8 x His tagged UreA or 8x His-tagged UreB the following procedure was applied: A single colony of *E. coli* SG13009 harboring plasmid pQE-Tri with the appropriate insert was used to inoculate 40 ml of LB medium supplemented with ampicillin and kanamycin. After over night incubation at 37°C with shaking at 250 rpm, cells were harvested, resuspended in fresh LB medium and used to inoculate 1 liter of LB supplemented with ampicillin and kanamycin in a 5 liter Erlenmeyer flask. Bacteria were allowed to grow at 37°C with shaking at 180 rpm. At OD₆₀₀ of 0.6 to 0.8, isopropyl- β -thiogalactopyranoside was added to a final concentration of 0.5 mM. Further incubation of the culture continued at 24°C with shaking at 180 rpm. To determine optimal induction time, aliquots were taken after 1, 5 and 12 h and protein expression was visualized on SDS-PAGE stained with Coomassie Blue. After a 12 h incubation period bacteria were harvested and stored at -20°C until use.

5.7.2 Purification of the His-tagged proteins

Purification of the recombinant proteins was performed under denaturing conditions with Ni-Sepharose according to the manufacturer's protocol (Amersham Pharmacia Biotech; Figure 24).

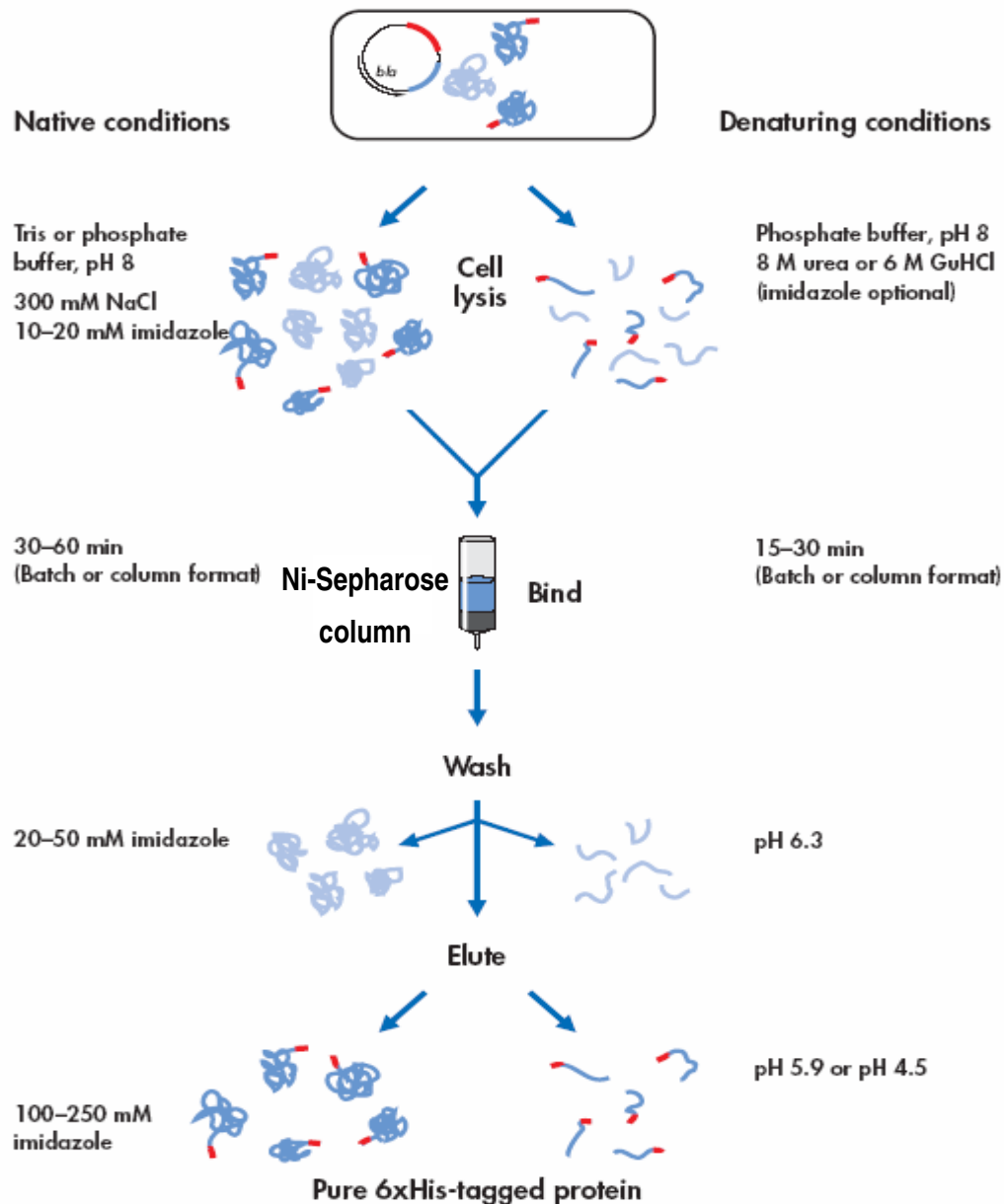


Figure 24 Purification of the His-tagged proteins.

Briefly, the bacterial pellet of 1 liter over night culture was resuspended in 25 ml His-Tag Lysis buffer. After a 3 times freeze in liquid N₂/thaw in 37°C water bath procedure, the lysed bacterial suspension was centrifuged (60 min, 20,000 rpm, 4°C). The supernatant was collected and immediately filtered through a cellulose membrane device with 0.22 µm pore size. Purification was carried out under denaturing condition in the presence of 8 M urea. After the Ni-Sepharose Column (HisTrap FF, Amersham Pharmacia Biotech) was washed with binding buffer the filtered supernatant (containing highly expressed His tagged fusion proteins) was applied to the column with a flow rate at 1 ml/min. Then, the column was washed with wash buffer and this tagged fusion proteins were eluted with elution buffer. Recombinant UreA was dialysed against PBS in order to remove imidazole. Since recombinant UreB precipitated, the eluate was dialyzed over night against L-arginine, glutamithion and 100 mM Tris-HCL (pH 7.8) and than twice for 4 h each against 10 mM Tris-HCl and 100 mM NaCl (pH 7.8). For endotoxin removal, Detoxi-Gel AffinityPack Pre – packed Columns (Pierce Biotechnology, Rockford, USA) were used. Columns were regenerated with 1% sodium deoxycholate followed by 5 column volumes of pyrogen-free water to remove detergent. Gel was equilibrated with 5 column volumes of pyrogen-free PBS before applying sample to the column. After sample has entered the gel bed - for greater efficiency - bottom and top caps were replaced to keep sample inside the gel bed for 1 h of incubation time at room temperature. After this time period, pyrogen-free PBS was added and sample was collected. The endotoxin content was examined by LAL-assay according to the manufacturer's protocol (QCL-1000, Bio Whittaker and Walkersville, MD, USA) Purified recombinant UreA and UreB were separated by 12% SDS-PAGE and detected either by Coomassie blue staining or by Western blot analysis as described previously in 5.3. Protein concentration was determined according to the modified Lowry Protein assay method. For further concentration (if needed), a Centricon YM-10 device was used. Aliquots were lyophilized and/ or stored at -80°C prior to use.

5.8 HB-EGF expression by Kato III cells

5.8.1 Tissue culture cell line Kato III

The semiadherent human gastric epithelial cell line Kato III (ATCC HTB-103) was maintained in RPMI 1640 (Biochrom, Berlin, Germany) containing 10% FCS at 37°C in a humid atmosphere with 5% CO₂. Before use, cells were washed two times with RPMI 1640 containing 10% FCS. Cell viability was examined by trypan blue staining, and cells were adjusted to a final concentration of 2 x 10⁶ cells/ml with RPMI 1640 containing 10% FCS in a 12-well tissue plate.

5.8.1.1 Stimulation of Kato III cells

H. pylori strains were harvested from the liquid culture medium, washed twice with PBS (Life Technologies Gibco-BRL) and adjusted to an OD₆₀₀ of 1 (approximately 1 x10⁹ cfu/ml) with RPMI 1640 containing 10% FCS. Kato III cells were stimulated with bacteria (2 x 10⁸ cfu/ml), purified surface associated urease (10 µg/ml), or HB-EGF (10 µg/ml; R&D Systems, Mannheim, Germany), over a time period of 24 h at 37°C in a humid atmosphere with 5% CO₂. In some test series, Kato III cells were pretreated for 30 min with either the specific MEK1 and MEK1/2 inhibitors PD98059 (100 µM; Promega, Madison, Wis.) and U0126 (20 µM; Promega) – both inhibiting activation of p44/p42 MAP kinases - or the specific p38 MAP kinase inhibitor SB203580 (10 µM; Promega) [215]. At defined time points cells were harvested and total RNA was extracted.

5.8.2 RNA isolation

Total RNA was extracted using NucleoSpin RNA II (Macherey & Nagel, Düren, Germany). Harvested cells were mixed with 400 µl RA1 buffer and 4 µl β-mercaptoethanol and the suspension was applied to NucleoSpin Filter units and centrifuged for 30 min (11,000 x g). After addition of 300 µl 100% ethanol, the mixture was loaded onto a NucleoSpin RNA column, blistered together with a 2 ml centrifuge tube and centrifuged for 30 sec at 8,500 x g. For DNase digest, 95 µl of the DNase reaction mixture (10 µl DNase I and 90 µl DNase reaction buffer) were applied directly onto the centre of the membrane of the column and incubated for 15 min at room

temperature. After two washing steps with 600 μ l RA3 buffer (30 sec, 8,500 x g), and 250 μ l RA3 buffer (2 min at 11,000 x g), total RNA was eluted with 100 μ l RNase-free water by centrifugation 11,000 x g for 1 min. The quality of RNA was determined by agarose gel electrophoresis. 1 μ l of total RNA was mixed with the equal volume of RNA gel loading buffer, denatured for 5 min at 65°C, loaded on the gel and separated for 45 min at 60 volts. The 18S and 28S RNA bands were visualised under UV light after staining the gel with ethidium bromide. The amount of total RNA was assessed at OD₂₆₀ using an UV spectrophotometer (Pharmacia).

5.8.3 cDNA synthesis

cDNA synthesis was done using the TaqMan reverse transcription kit (PE Applied Biosystems, Foster City, Ca, USA) according to the manufacturer's description. The reverse transcription reaction mix was prepared in a final volume of 100 μ l containing 1 x RT buffer, 5.5 mM MgCl₂, 500 μ M of each deoxynucleotide triphosphate, 2.5 μ M random hexamers, 0.4 U/ μ l RNase inhibitor, 1.25 U/ μ l Multiscribe reverse transcriptase and 1 μ g total RNA. Samples were incubated for 10 min at 25°C, then for 30 min at 48°C, and finally for 5 min at 95°C to inactivate reverse transcriptase.

5.8.4 Quantitative Real-time RT-PCR

5.8.4.1 Theoretical basis

Reactions are characterised by the point during cycling when amplification of the PCR product is first detected, rather than the amount of PCR product accumulated after a fixed number of cycles. The larger the starting quantity of the target molecule, the earlier a significant increase in fluorescence is observed, whereas lower starting copy number results in higher C_t values. The parameter C_t (threshold cycle) is defined as the fractional cycle number at which the fluorescence generated by cleavage of the probe passes a fixed threshold above baseline. Figure 25 shows the different features of a real time PCR amplification and Figure 26 explains the definition of the threshold cycles.

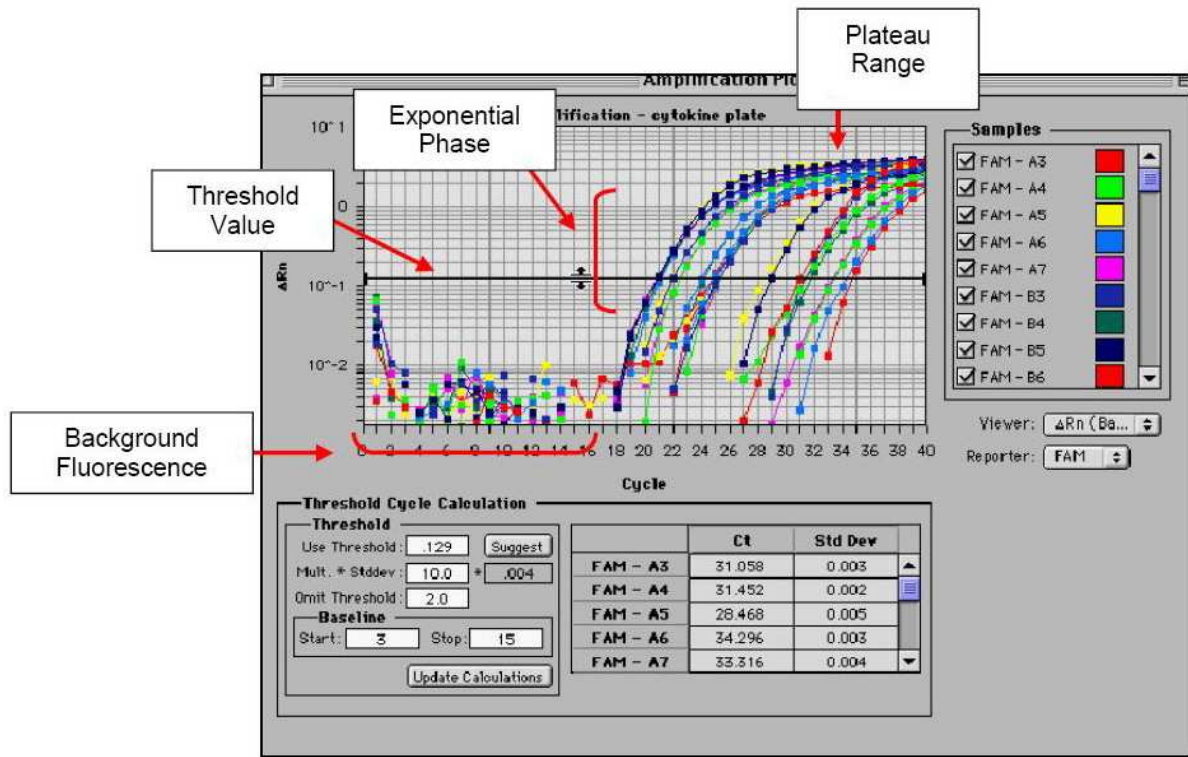


Figure 25 The different features of a real-time PCR amplification.

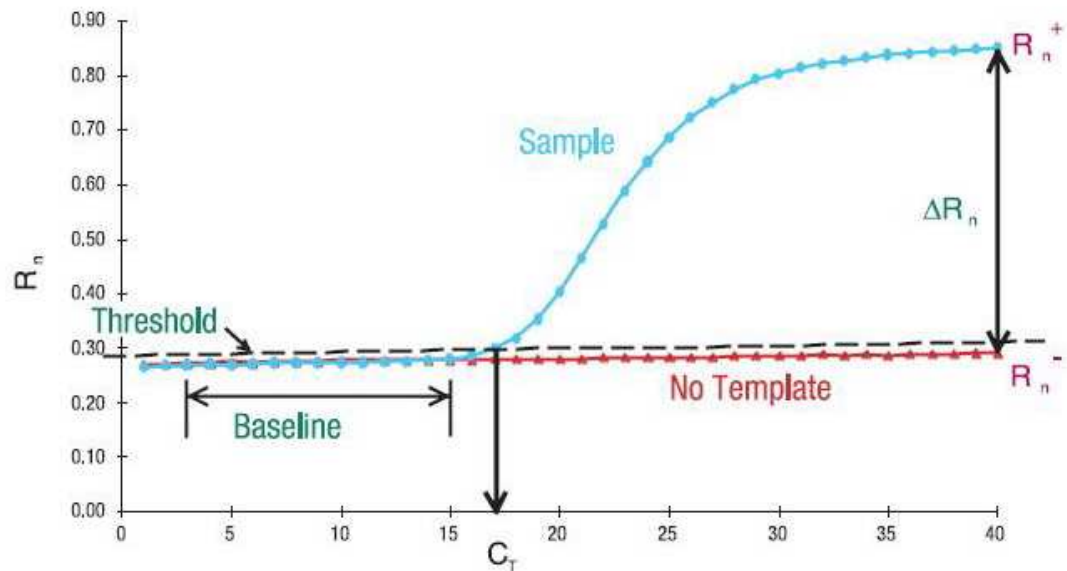


Figure 26 Definition of the threshold cycle: The threshold cycle occurs when the sequence detection application begins to detect the increase in signal associated with an exponential growth of PCR product.

The exact amount of total RNA and its quality (level of degradation) must be determined for each sample. Therefore, transcripts of the β -actin housekeeping gene were quantitated as the endogenous control (reference), with each unknown sample normalized to β -actin content. The relative target gene expression level was also normalized to a calibrator, a sample that contained the lowest amount of the target polyA⁺-RNA.

5.8.4.2 Primers and TaqMan probes for real-time RT-PCR

The PCR-primers and the TaqMan probe to amplify and detect the heparin-binding EGF-like growth factor (HB-EGF) was designed using the Primer Express software version 1.0 (PE Applied Biosystems, Foster City, MA, USA). The forward and reverse primers were designed to lie in adjacent exons (separated by a long intron) to prevent amplification of genomic DNA that may be contained in samples. The TaqMan probe was labelled with 6-carboxyl fluorescein (FAM) as the reporter dye at the 5' end and 6-carboxyl tetramethyl-rhodamine (TAMRA) as the quencher fluorescent at the 3' end. The fluorochrome VIC was used as reporter dye at the 5' end of the β -actin probe. BLASTN searches against dbEST and nr (nonredundant set of GenBank, EMBL, DDBJ database sequences) were conducted to confirm the total gene specificity of the nucleotide sequences chosen for the primers and probes and the absence of DNA polymorphisms. For sequences see Table 1.

Primer and Probes	Sequence (5'→3')	Location	PCR product
HB-EGF forward	AGAATGCAAATATGTGAAGGAGCTC	609-633	80bp
HB-EGF reverse	GCCCATGACACCTCTCTCCAT	688-669	
HB-EGF probe	CTCCTGCATCTGCCACCCGGG	642-662	

Table 1 Primers and probe used in real time RT-PCR to quantify gene expression

5.8.4.3 PCR conditions

Real-time RT-PCR was performed on an ABI PRISM 7700 Sequence Detector, using the ABI PRISM 7700 Sequence Detector Software 1.6 (PE Applied Biosystems). The amplification reaction was performed in a total volume of 25 μ l containing 1 x universal master mix (PE Applied Biosystems), 600 nM forward primer, 600 nM reverse primer, 200 nM TaqMan probe and 1 ng cDNA. For the endogenous control 1 x each pre-

developed TaqMan assay human β -actin (PDAR hu β -actin; PE Applied Biosystems) and universal master mix and 1 ng cDNA (5 μ l) were used. The reaction was performed in MicroAmp optical 96-well plate (PE Applied Biosystems) with thermal cycling conditions including 2 min at 50°C, proceeded with 40 cycles of 95°C for 15 sec and 60°C for 1 min. Each sample was analyzed in triplicate, and the ΔR_n and C_t values were averaged from the values obtained in each reaction.

5.8.4.4 Normalization

The comparative C_t method was used for quantitation of HB-EGF polyA⁺-RNA levels. This method eliminated the need for standard curves, using arithmetic formulas to achieve the same result for relative quantitation. The amount of target normalized to an endogenous control and relative to a calibrator is given by $2^{-\Delta\Delta C_t}$.

The ΔC_t value is determined by subtracting the average β -actin C_t value from the average HB-EGF C_t value. The calculation of $\Delta\Delta C_t$ involves subtraction of the ΔC_t calibrator value.

5.8.5 Detection of soluble HB-EGF protein by Western blot analysis

2×10^6 Kato III cells were cocultured in serum free RPMI 1640 with *H. pylori* wild-type and mutant strains (MOI 100 or purified surface associated urease 10 μ g/ml) at 37°C in a CO₂ incubator. At different time points, the supernatant was centrifuged (20 min, 4,000 x g, 4°C) and concentrated to a volume of 80 μ l using Centricon-YM3 microconcentrators (Amicon, Bedford, MA, USA). The protein content was quantified by the modified Lowry protein reaction. Of each sample, 20 μ g protein were mixed with 2 x SDS-gel sample buffer 1:1 (in an endvolume of 20 μ l), denatured for 20 min at 75°C and 5 μ l of samples were loaded onto the 12% mini SDS-PAGE gel and electrophoresed for 90 min at 120 V. After electrophoresis, proteins were transferred onto a polyvinylidene difluoride membrane (PVDF; Pierce) by electroblotting. Unspecific binding sites were blocked with PBS-Tween 20 (0.1%) plus 1 % bovine serum albumin (BSA; Sigma-Aldrich Corp, Deisenhofen, Germany) for 1 h at room temperature. The membrane was incubated with goat-anti HB-EGF polyclonal antibody (1:300 dilution; Santa Cruz Biotechnology, Santa Cruz, CA) for 2 h at room temperature with constant agitation.

After 3 washing steps in TBS-Triton/Tween, bound antibodies were detected with donkey anti-goat IgG (1:10,000 dilutions; Santa Cruz Biotechnology) conjugated to HRP, in TBS-Triton/Tween for 45 min at room temperature. Subsequently, membrane was washed 4 times with TBS-Triton/Tween, immersed in 2 ml ECL Western blotting detection reagents 1 and 2 (Amersham Pharmacia Biotech) for 1 min, exposed on Kodak X-omat film for 20 min and the film was developed. Relative density of HB-EGF protein bands was calculated by densitometric analysis of Western blot patterns using TotalLab v1.10 alpha software (Phoretix, Newcastle upon Tyne, UK). On each blot, HB-EGF production was set by 100% for the sample stimulated with N6. The Experiment was repeated 3 times.

5.8.6 Detection of mitogen activated protein-kinases (MAPKs) by Western blot analysis

For detection of p44/p42 (ERK1/2), p38 and p54/p46 (JNK) mitogen activated protein kinases, 2×10^6 Kato III cells were seeded in serum-free RPMI 1640 and incubated overnight at 37°C before challenge. Then, cells were fed with fresh serum free medium and subsequently stimulated with *H. pylori* strains or purified urease. At defined time points, cells were washed 3 times with PBS. The protein content was determined by modified Lowry protein assay. Of each sample, 20 µg were mixed with 2 x SDS sample buffer, denatured for 20 min at 75°C, and separated on a 12% SDS-PAGE gel. After electrophoresis proteins were transferred onto polyvinylidene difluoride membrane (PVDF; Pierce, Rockford, ILL, USA) by electroblotting. Non specific binding sites were blocked with PBS-Tween 20 (0.1%) plus 1% bovine serum albumin for 1 h at room temperature.

For investigation of activated mitogen-activated protein kinases (MAPKs) phospho-specific antibodies for each MAP kinase were used. Phospho-specific polyclonal p44/p42 MAP kinase antibody was used to detect catalytically active, at Thr²⁰² phosphorylated p44 and at Thr²⁰⁴ phosphorylated p42. Phospho-specific polyclonal p38 MAP kinase antibody was used to detect p38 activated by phosphorylation at Thr¹⁸⁰ and Thr¹⁸². Phospho-specific polyclonal p54/46 MAP kinase antibody was used to detect JNK but only when they are phosphorylated at Thr¹⁸³ and Thr¹⁸⁵. All three antibodies

were purchased from New England Biolabs (Beverly, MA, USA). Non-phospho-specific polyclonal antibodies to p44/p42, p38 and p54/p46 MAPKs (Santa Cruz Biotechnology) were used as controls. Membranes were either incubated with rabbit-anti p44/p42 (1:1,000) antibody, or rabbit-anti p38 (1:1,000) antibody or rabbit-anti p54/46 (1:1,000) antibody at 4°C over night with gentle agitation. After 3 washing steps in TBS-Triton/Tween, bound antibodies were detected with goat anti-rabbit IgG horseradish peroxidase conjugate (1:5,000 dilution; Santa Cruz Biotechnology) conjugated to HRP in TBS-Triton/Tween for 45 min at room temperature. After 4 washing steps with TBS-Triton/Tween, detection and analysis were performed as described in 5.3.

5.8.7 Cell proliferation assay

For determination of cell proliferation, Quick cell proliferation assay (BioVision, Mountain View, CA, USA) was used. The measurement of cell proliferation by WST-1 is based on the ability of viable cells to cleave tetrazolium salts by mitochondrial dehydrogenase. Augmentation in the amount of developed colour directly correlates with the number of metabolically active cells. The assay was performed according to manufacturer's recommendation. 5×10^4 cells/well were seeded in a 96-well microtiter plate in a final volume of 100 μ l/well in serum-free RPMI 1640 in the presence of the bacteria (5×10^6 cfu/ well), purified urease (10 μ g/ml) or HB-EGF (10 μ g/ml) and incubated at 37°C in CO₂ atmosphere. At defined time points, 10 μ l WST-1/ECS solution were added per well and samples were incubated for additional 60 min. Test series were also performed with cells pretreated with either PD98059 or U0126 (specific p44/p42 MAPK inhibitors) or SB203580 (specific p38 inhibitor). The absorbency of samples was determined using an ELISA-reader at 450 nm against the reference wavelength of 600 nm. Samples were run in triplicate and 3 independent experiments were performed.

Since the Quick cell proliferation assay was based on assessing the metabolic activity of viable cells and did not directly measure changes in actual cell counts, viable cells were counted, namely those excluding the dye trypan blue, using microscopy. Cell viability was shown to be reduced from 95% to 75% during 48 h incubation period. However, at none of the time points any differences with respect to cell viability could be observed between cells stimulated with different *H. pylori* strains, urease, HB-EGF, and untreated

controls. Also the presences of MAP kinase inhibitors were not found to affect cell viability.

5.9 Stimulation of PBMCs

5.9.1 Isolation of PBMCs from peripheral blood

Peripheral blood mononuclear cells were prepared from maximum 500 ml whole blood from healthy *H. pylori* seronegative and seropositive voluntary colleagues. *H. pylori* carriers were identified by serological screening using ELISA for detecting *H. pylori* specific antibodies (*H. pylori* test IgG; Eurospital, Trieste, Italy). Neither the *H. pylori*-infected nor the noninfected volunteers had any previous history of gastrointestinal symptoms or illness. None of the donors was on any medication the last 3 weeks before entering the study. Blood was diluted with PBS (Life Technologies, Gibco-BRL) in 1:1 ratio, 25 ml was carefully sealed on 20 ml Ficoll-Plaque (Pharmacia Biotech, Uppsala, Sweden) followed by density centrifugation for 45 min by 400 x g at room temperature; PBMC layer was separated and washed twice in PBS to remove Ficoll (Figure 27). To remove platelets, cell suspension was centrifuged twice (200 x g, 10 min) and supernatant was carefully removed. Cells were counted using Bürker-Türk chamber (Figure 28) and resuspended in the appropriate medium (RPMI 1640, UC-medium, ex-vivo 15 medium, dependent on the experiment) supplemented with FCS (1-10%) to a final concentration of 10^6 cells/ml.

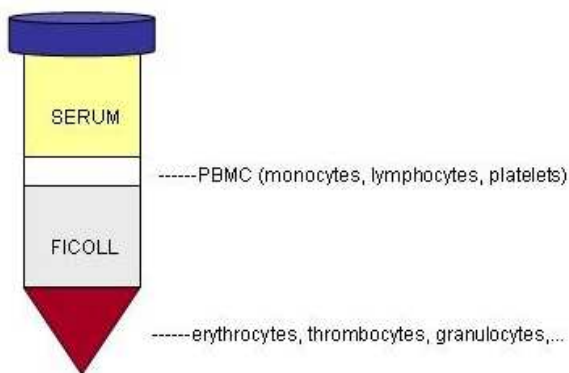


Figure 27 PBMC separation after Ficoll-Plaque density centrifugation.

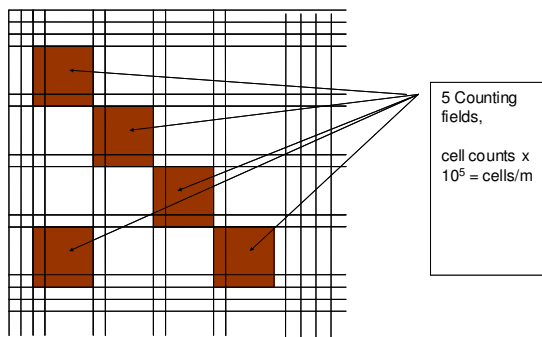


Figure 28 Cell counting using Bürker-Türk chamber.

5.9.2 Cytokine secretion assay and flow cytometry

In parallel samples, PBMCs (3×10^6 Cells) were stimulated in 3 ml RPMI 1640 supplemented with 10% FCS with either viable bacteria or (MOI 20); N6, N6*ureB*::TnKm, N6*ureG*::TnKm, K8, bacterial lysates (50 $\mu\text{g/ml}$ total protein from each isogenic strain) or purified surface-associated urease (10 $\mu\text{g/ml}$) for up to 96 h. At defined time points (6, 12, 24, 48, 72 and 96 h; for each time point and stimulus a sample was available), samples were divided into 3 tubes each, which were then used to determine secretion of either IL-10, IL-4 or IFN γ using the respective MACS cytokine catching reagent kit (Milteny Biotech GmbH, Bergish Gladbach, Germany) according to the instructions of the manufacturer. Briefly, after washing steps, cells (10^6) were labelled in cold buffer with the specific catching reagent capable of binding 1 of the cytokines secreted during the following incubation at 37°C for 45 min. Then, cells were washed and labelled with anti-cytokine PE-conjugated antibody, anti-CD69-PC5 and anti-CD-4-FITC (Table 2). Activated, cytokine producing CD4⁺ T cells were detected by flow cytometry. If needed, cytokine-secreting cells were enriched by anti-PE magnetic Microbeads prior to flow cytometry (Figure 29).

MABs	Labelled with fluorochrome	Clone	Firma	Dilution
Anti-human CD69	PC5		Immunotech	10 μ l/10 ⁶ cells
Anti-human CD4	FITC		Immunotech	10 μ l/10 ⁶ cells
Anti-human IL-10	PE	JES3-19F1	BD	1:50
Anti-human IL-4	PE	8D4-8	BD	1:100
Anti-human IFNg	PE	4S.B3	BD	1:1000

Table 2 The origin and concentration of used fluorochrome labelled antibodies.

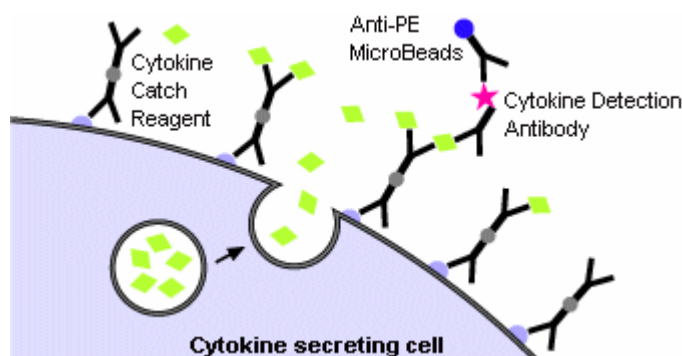


Figure 29 Principle of cytokine secretion assay. Cell surface is labelled by cytokine catch reagent, which is also able to bind to the cell surface. The produced cytokine (green) binds immediately after secretion to the catching reagent. Caught cytokine is detected with specific anti-cytokine-PE labelled antibody. For magnetic enrichment, second antibody conjugated with microbeads was used.

5.9.3 Intracellular cytokine detection by flow cytometry

PBMCs (5×10^5 cells/ml) in Ultra Culture medium (Bio Whittacker, Walkersville, MD) supplemented with 10% FCS, 2 mM L- Glutamin (Sigma) and 3.5 μ l/l 2- β -mercaptoethanol were stimulated with the same stimuli as under 5.9.2 in the presence of 10 μ l/ml Phytohemagglutinin (PHA; Life Technologies, Inc, Grand Islandm NY). On day 3, the supernatant was removed and fresh medium was added containing 20 U/ml IL-2 (Boehringer, Mannheim, Germany). On day 7, cells were restimulated with the same stimulus as on day 0 for 12 h. During the last 6 h, 10 μ g/ml Brefeldin A (Sigma,

Deisenhofen, Germany) was added and cells were further stimulated in the presence or absence of PMA (1 µg/ml; Sigma) / Ionomycin (1.25 µM; Sigma). In parallel samples, cells were incubated for longer periods (14 or even 21 days) prior to restimulation. By longer incubation periods the medium was replaced by fresh medium on days 7 and 14; fresh medium was added on days 10 and 19 (1:1), see Figure 30. Samples were run without the addition of Brefeldin A also. In this case, on days 7, 14 and 21 (after restimulation), the supernatants were collected and stored at -80°C prior to the assessment of the cytokine content by Bio-Plex assay (BioRad Laboratories GmbH, Munich, Germany). Cells treated with 1.6 µg/ml anti-CD3 (Immunotech, Hamburg, Germany) and 3.3 µg/ml anti-CD28 (Immunotech) were used as positive control. In a test series, all samples were treated with anti-CD28 (3.3 µg/ml).

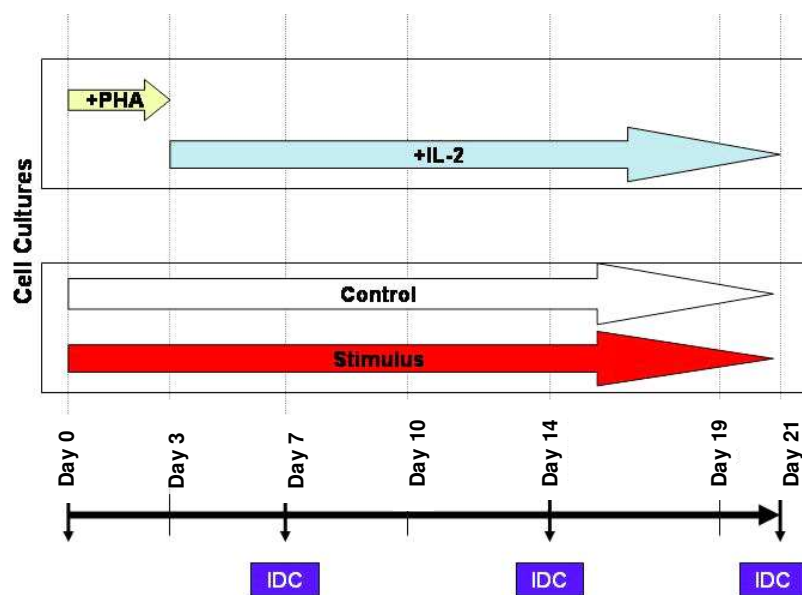


Figure 30 Graphical presentation of the experiment shows treatment of PBMCs before intracellular cytokine detection. IDC= restimulation and intracellular Detection of Cytokines, PHA= Phytohemagglutinin.

Intacellular cytokine staining:

Each sample was divided into 3 micronic tubes ($0.2-0.5 \times 10^6$ cells/ tube). Cells were washed and resuspended in 750 µl PBS. 1 ml fresh diluted 4% formaldehyde was added followed by a 20 min incubation in the dark at room temperature. Cells were washed 2 x with 500 µl PBS, the supernatant was carefully removed, and cell membrane was permeabilised by resuspending the pellet in 700 µl 0.1% fresh diluted saponin (Sigma)

buffer for 5 min. Cells were washed with 500 μ l 0.1% saponin buffer and 50 μ l of each antibody dilution (anti-CD3- FITC, anti-CD69-PC5, anti-cytokine-PE), in 0.1% saponin buffer were added to the pellet and incubated in the dark at room temperature for 25 min. Surface-antigen marker antibodies anti-CD3-FITC and anti-CD69-PC5 were added after permeabilization together with the anti-cytokine PE-stained antibodies, because during incubation CD3 and CD4 may become internalised. After the last incubation period, 1 ml 0.1% saponin buffer was added, centrifuged for 5 min and supernatant was aspirated. Cell pellet was resuspended in 250 μ l isoton II dilutions (Instrumental Laboratories, Beckman, Coulter Inc., Germany) and samples were analyzed by flow cytometry.

5.10 Stimulation of monocyte derived dendritic cells

5.10.1 Monocyte isolation from PBMCs

For isolation of monocytes from peripheral blood, two different methods were used. The first method uses the capability of monocytes to adhere; the second method uses anti-CD14 MicroBeads, MACS (Milteny Biotech GmbH).

5.10.1.1 Monocyte isolation using gelatin coated culture dishes and stimulation of DCs

Preparation of gelatine coated dishes: 2 g gelatin (Merck, Darmstadt, Germany) was diluted in a microwave in 100 ml aqua bidest, sterile filtered, and 5-7 ml were poured in to each culture dish. After 1 h incubation at 37°C, excessive gelatine was removed, and plates were let to dry for 20-30 min in a laminar air flow and then for 5 days at 37°C (in an incubator in the absence of humidity). Before use, the gelatine layer has been washed with PBS.

PBMCs were isolated from 450-500 ml peripheral blood, and cells were resuspended in 50 ml RPMI 1640 supplemented with 10% FCS (HyClone, Logan UT, USA). Then cells were plated on 5 gelatine coated 100 mm x 20 mm cell culture dishes (approximately 6×10^7 cells/dish in 10 ml volume). After 45 min of incubation at 37°C in a CO₂ atmosphere, adherence was controlled by microscopy. The nonadherent lymphocytes were removed

and adherent monocytes (approximately 2×10^6 cells/dish) were incubated for additional 10 min in RPMI supplemented with 5 mM EDTA. Monocytes were then easily collected and after 2 washing steps in PBS, cells were counted in a Bürker-Türk chamber and the cell concentration was adjusted to 1×10^6 cells/ml in RPMI 1640 supplemented with 10% FCS (HyClone), 2mM L-Glutamin (Sigma) and 1% Gentamicin (Sigma). During a 5 day incubation in the presence of GM-CSF (1600 U/ml, Leucomax, Aesca Pharmacia) and IL-4 (1500 U/ml in the first 2 days and then 1000 U/ml, Promokine). Monocytes differentiated into immature DCs. Then, cells were washed gently and stimulated in fresh RPMI 1640 containing 10% FCS, GM-CSF (1,600 U/ml) and IL-4 (1,000 U/ml) for up to 48 h with one of the following stimuli: 100 ng/ml *E. coli* LPS as positive control (Sigma), viable bacteria (MOI 50) and bacterial lysates (50 µg/ml) as described in 5.9.2, recombinant UreA (2.5 µg/ml) and recombinant UreB (2.5 µg/ml). Experimental approach is shown in Figure 32. At defined time points (6, 24 and 48 h) the supernatants were collected and stored at -80°C prior to quantitation of the cytokine content by 17-Plex (BioRad). TGF-β1 was analyzed by ELISA (Promega GmbH, Mannheim Germany). In each sample, the maturation state of DCs was assessed by flow cytometry on the basis of the expression of the following markers: CD83, CD86, mannose receptor.

5.10.1.2 Monocyte isolation using anti-CD14 MicroBeads

CD14⁺ cells were isolated from PBMCs using anti-CD14 MicroBeads, MACS (Milteny Biotech GmbH) according to the instructions of the manufacturer (Figure 31). Briefly, PBMCs were incubated with anti-CD14 MicroBeads (10 µl/10⁷ cells) for 20 minutes at 4°C, washed and resuspended in a buffer solution. Then, cell suspension was loaded on a column (prerinsed with buffer), which was placed in the magnetic field of a MACS separator. The magnetically labelled CD14⁺ cells were retained on the column. After 3 washing steps, the column was removed from the magnetic field, and CD14⁺ cells were eluted.

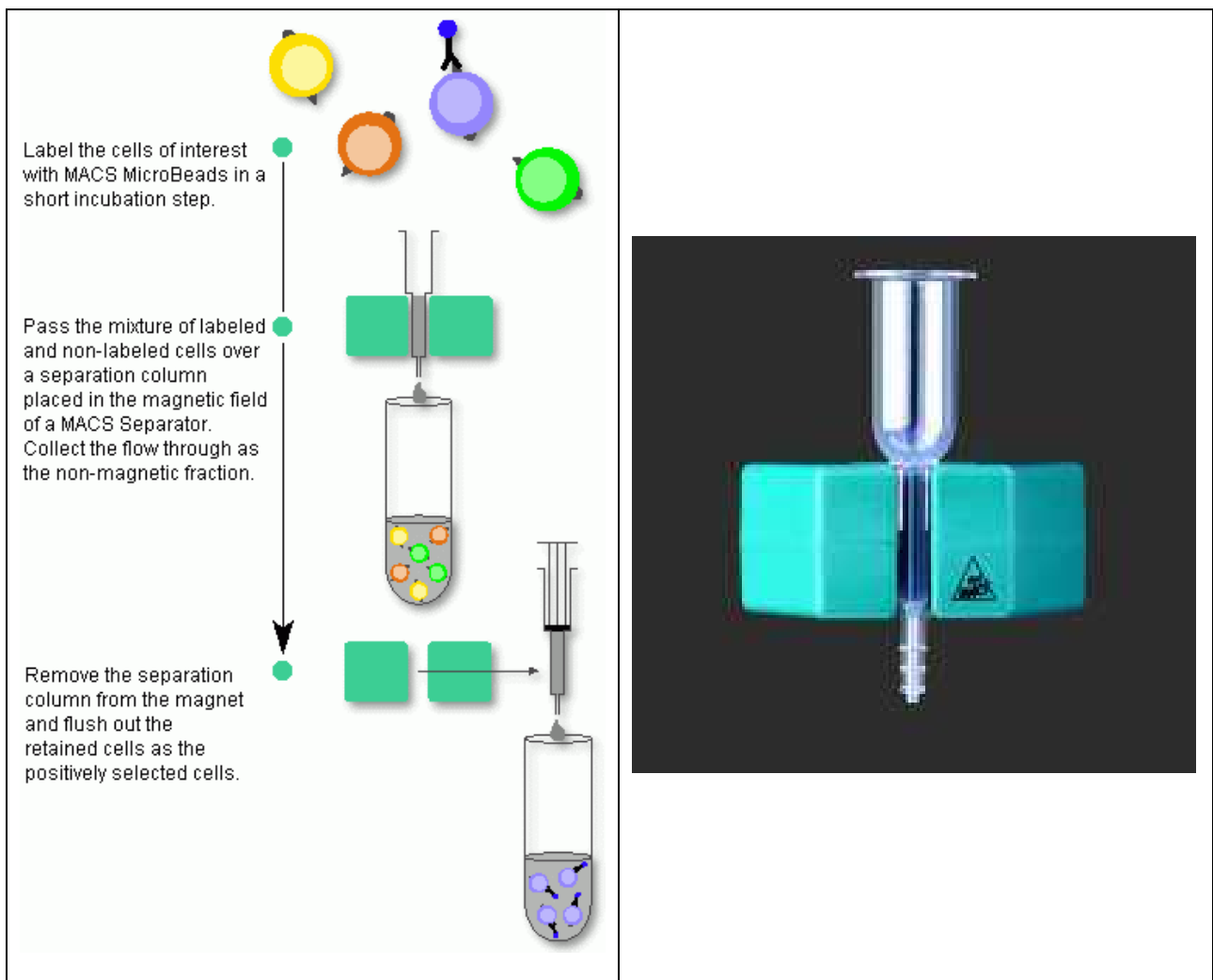


Figure 31 Isolation of CD14⁺ cells using anti-CD14 MicroBeads

With this method $3-5 \times 10^7$ monocytes could be purified from 100 ml whole blood. As shown by flow cytometry using anti-CD14-FITC, the purity of the CD14⁺ cell fraction was 95%. The monocyte concentration was adjusted to 1×10^6 cells/ml in ex-vivo15 (Bio Whittacker) supplemented with 5% FCS (HyClone), GM-CSF and IL-4 and cells were preceded as described in 5.10.1.1 (Figure 32).

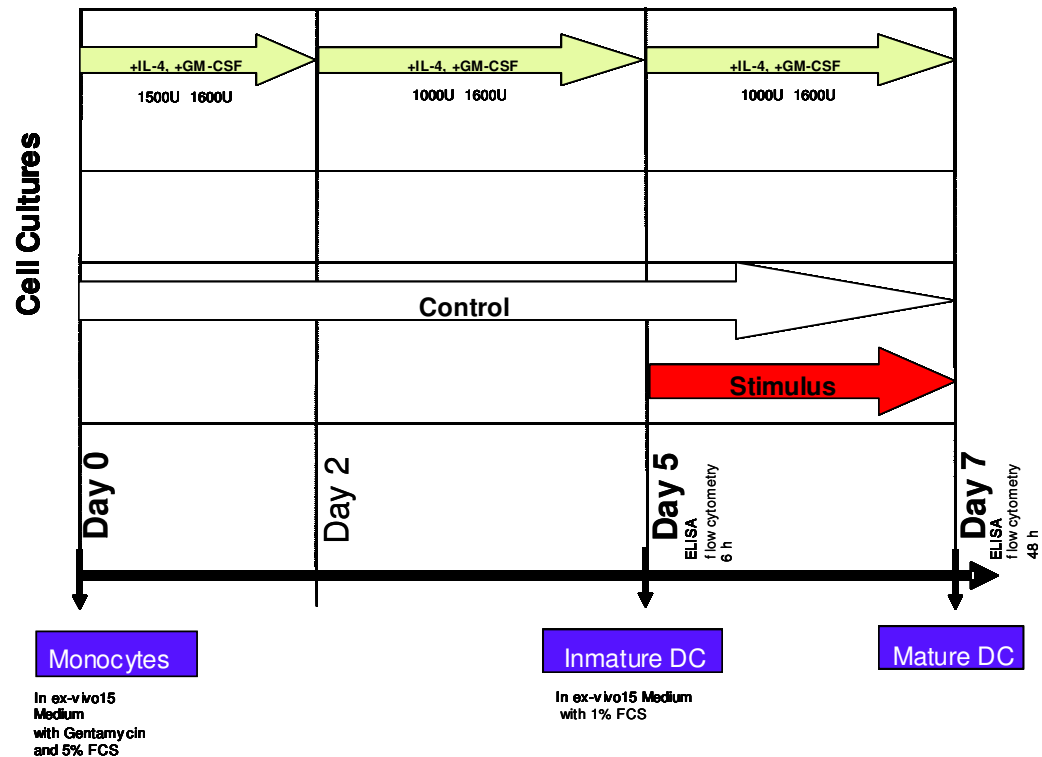


Figure 32 Overview of the experiment. During the 5 day incubation in the presence of GM-CSF and IL-4 monocytes differentiated into immature DCs. On day 5, cells were washed and stimulated for up to 48 h. Dendritic cell maturation was monitored by flow cytometry and supernatants were collected.

5.10.2 Analysis of the maturation state of DCs by flow cytometry

DCs were transferred to micronic tubes, washed and resuspended in PBS containing 1% human serum. Then, cells were incubated with in the presence of fluorochrome-labelled MAbs (Table 3) for 30 min at 4 °C in a volume of 100 μ l.

MAbs	Labelled with Fluorochrome	Clone	Firma	Dilution
Anti-human CD83	FITC	HB15e Mouse IgG1, k	BD Pharmingen, (San Diego, Ca)	1: 10; 10 μ l/10 ⁶ cells
Anti-human CD86	Cy-Chrome	IT2.2 Mouse IgG2b, k	BD Pharmingen	1: 10; 10 μ l/10 ⁶ cells
Anti-human Mannose-receptor	PE	3.29B1.10 IgG1	Immunotech	1: 10; 10 μ l/10 ⁶ cells

Table 3 Origin and concentration of the fluorochrome-labelled antibodies used by monitoring DC maturation by flow cytometry.

After a washing step, cells were resuspended in 350 μ l Isoton II dilution (Instrumentation Laboratories, Beckman Coulter Inc, Germany) and were analysed by flow cytometry.

5.10.3 Quantitation of cytokines in cell culture supernatants

Cytokines in cell culture supernatants were measured by Bio-Plex (BioRad) with the exception of TGF- β 1, which was measured by ELISA. Bio-Plex cytokine assay employs a liquid suspension array for quantitation of cytokines in supernatants. Using 96-well microtiter plate formatted assay, the level of multiple cytokines in a single well can be quantified (Figure 33). The principle of the Bio-Plex cytokine assay is similar to a capture sandwich immunoassay. An antibody directed against each desired cytokine is covalently coupled to a different color-coded polystyrene bead. The conjugated beads are allowed to react with sample containing a known (standard) or unknown amount of cytokines. After inbound cytokines are removed, biotinylated detection antibodies directed against a different epitope on each cytokine are added to the reaction. The result is the formation of a sandwich of antibodies around each cytokine. The complexes are detected by the addition of streptavidin-phycoerythrin (streptavidin-PE), which has fluorescence characteristics distinct from the beads. A specialized microtiter plate reader carries out quantification (Figure 34). Assay was prepared according to the instruction of the manufacturer. Briefly, special 96 well microtiter plates with membrane bottom were used, to prevent beads lost during the washing steps. 50 μ l cytokine specific bead mixture were added to each prerinsed well, and then buffer was vacuum pumped using a special pump. 50 μ l of supernatants were added to the wells containing the beads and plates were shaken vigorously in the dark for 30 min. After 3 washing steps, 50 μ l detection antibody mixtures were added to each well and incubated with shaking, in the dark for 30 min. After 3 washing steps, 25 μ l of streptavidin solution was added to each well and further incubated with shaking in the dark for 10 min, then after the 3 washing steps, 175 μ l of assay buffer was added and plates were measured by the specialized 96-well plate reader.

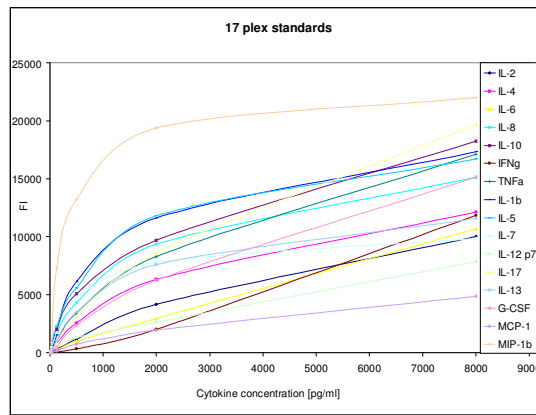


Figure 33 Standard curves of detected 17 cytokines in 1 sample using 17-Plex

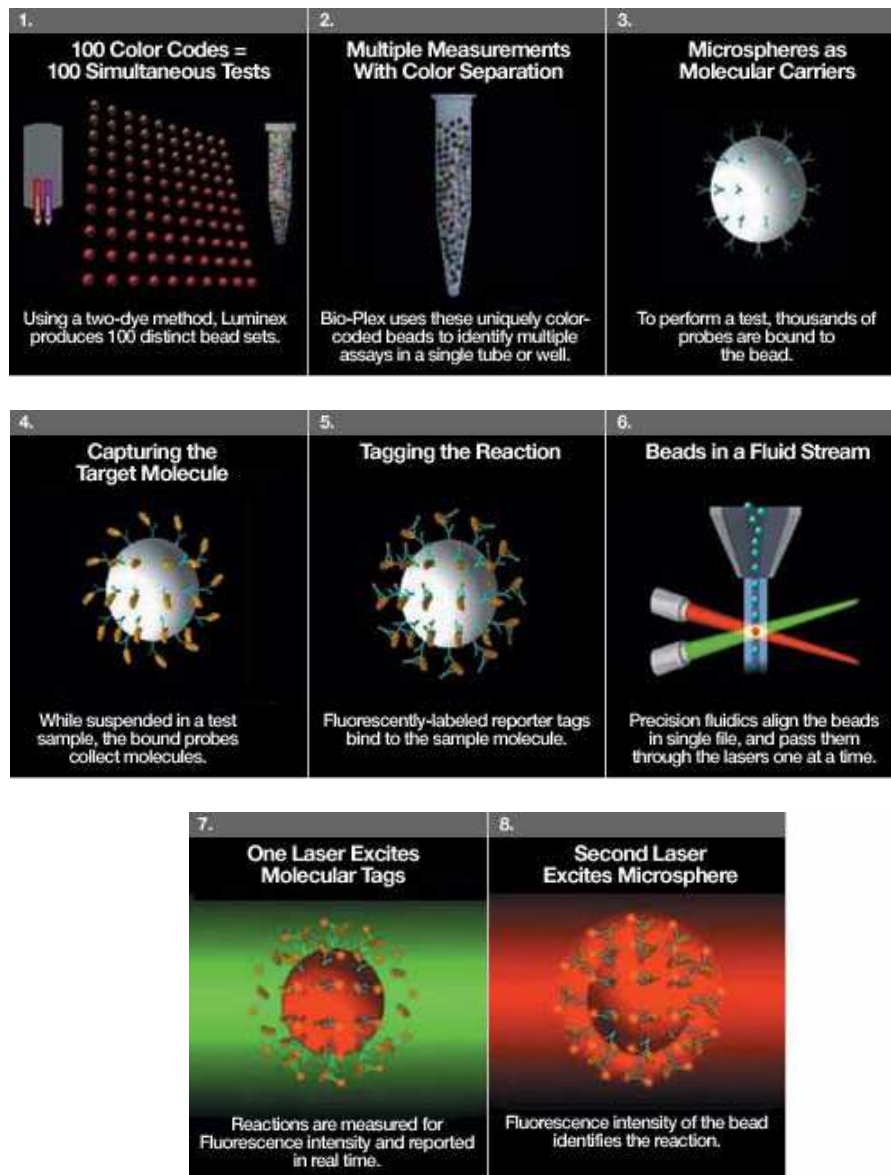


Figure 34 Principle of Bio-Plex cytokine detection assay.

Samples were measured and diluted to 1:10 and 1:50. For low cytokine detection level between 3200 pg/ml-0.8 pg/ml, high sensitive standard was used for quantitation. Normal standard was used for cytokines between 32000 pg/ml-80 pg/ml.

Bioactive TGF- β 1 was quantified after acid treatment by conventional ELISA (Promega) according to the instructions of the manufacturer. Briefly, 30 μ l supernatant were diluted with 120 μ l DPBS, and were acid treated for 15 min by adding 3 μ l 1N HCl. Samples were then neutralized by adding 3 μ l 1N NaOH. 100 μ l of the acid activated samples were analysed on coated ELISA plates.

5.10.4 Flow cytometry

All measurements were done on an EPICS XL-MCL flow cytometer (Instrumental Laboratories Beckman Coulter Inc., Germany) equipped with an argon laser operating at an excitation wavelength of 488 nm. FITC fluorescence emission was monitored by use of the FL1 channel, PC5 and Cy-Chrome were monitored by use of the FL2 channel, and PE was monitored by use of the FL3 channel. Stability of the optical and fluid system was controlled by DNA-check beads (Coulter). Data analysis was performed with ESPO 32 software.

Statistical analysis

Differences of means were tested for statistical significance by the nonparametric Kruskal-Wallis-test using SPSS software (SPSS 10.0; SPSS Science). Multiple pair wise comparisons of means were done by the Wilcoxon-Mann-Whitney U-Test, corrected with Shaffer-Procedure. P values <0.05 were considered as significant.

5.11 Buffers

Not commercially available media, solutions and buffers in alphabetical order:

Ampicillin stock	100 mg/ml in H ₂ O, sterile filter, store in aliquots at -20 °C
APS	10% APS, sterilfiltered, store at -20 °C in aliquotes
Binding buffer (His-tagged proteins)	(20 mM NaHPO ₄), 300mM NaCl, 10mM Imidazole, pH 8)+ 8 M Urea
Blocking buffer	3% BSA (Sigma) in TBS buffer
BLOTTO	TBS-T + 5% nonfat dry milk, 10 mM Na-azide
Brucella agar / broth	Dissolve powder from Merck in water, autoclave
Chloramphenicol stock	10 mg/ml in ethanol, store at -20 °C in aliquotes
CIAP	Calf intestinal alkaline phosphatase, Promega
Coomassie stain	10% acetic acid, 25% isopropanol, 0.5 g/l Coomassie Brilliant Blue G-250
Denaturing solution	0.5 M NaOH, 1.5 M NaCl
Destaining solution	10% acetic acid
Electroporation buffer	272 mM sucrose, 15% glycerol, 2.43 mM K ₂ HPO ₄ , 0.57 mM KH ₂ PO ₄ ; pH 7.4, sterilfilter, store at 4 °C
Elutions buffer (His-tagged proteins)	(20 mM NaHPO ₄), 300 mM NaCl, 200 mM Imidazole, pH 8) 10% glycerol+ 8 M Urea
Gel filtration buffer	50 mM NaH ₂ PO ₄ , 150 mM NaCl, 1mM EDTA; pH 7.0
GLS	40% sucrose, 100 mM EDTA, 0.5% SDS, 0.05% bromphenol blue, sterile filtered, store at 4 °C
GM-CSF stock	400 µg/ml stock diluted to 7,5µg/ml with medium,

	aliquotes -70°C add 10 µg/ml
Hypochlorite solution	0.25% Sodiumhydroxid (NaOH) with 0.21% Sodium hypochlorid (NaClO)
IL-2 stock	25 µg (50,000 U) in 5 ml PBS, aliquots, store at -20°C
IL-4 stock	1 µg/ml stock (2:3 H ₂ O:Medium), aliquots, store at -20°C add 20 µg/ml
Ion-exchange buffer	20 mM Bis-Tris propane; pH 6.9
Ionomycin stock	5 mg in 6.7 ml DMSO, sterile, aliquots -20°C
IPTG (1M)	238 mg/ml in H ₂ O, sterile filter, store in aliquots at -20°C
Kanamycin stock	25 mg/ml in H ₂ O, sterile filter, store in aliquots at -20°C
LB agar	10 g/liter tryptone, 5 g/liter yeast extract, 10 g/liter NaCl
LB medium	10 g/l tryptone, 5 g/l yeast extract, 10 g/l NaCl; pH 7.0, autoclave
Lysis buffer	(20 mM NaHPO ₄), 300 mM NaCl, 10 mM Imidazole, pH 8) with 25 µl Lysosime (50 mg/ml Stock)+ 8 M Urea
MACS cold buffer	PBS (Gibco), 2 mM EDTA and 0.5% FCS (HyClone), sterile
PBS	1.9 mM NaH ₂ PO ₄ , 8.1 mM Na ₂ HPO ₄ , 154 mM NaCl, adjust to pH 7.2 autoclave
PHA stock	Powder in 20 ml H ₂ O, aliquotes -20°C

Phenol-nitroprusside solution	0,0025% Nitroprusside Natrium Dihidrate Na ₂ [Fe(CN) ₅ NO] 2H ₂ O+ 1ml phenol
PMA stock	100 µg/ml in UC-Medium, aliquots, store at -20 °C
Ponceau S stain	0.2 % Ponceau S, 3% trichloroacetic acid, 3% sulfosalicylic acid
RNA agarose gel	0.6 g agarose, 28 ml DEPC treated water, 9 ml 5 x MOPS and 8 ml formaldehyde
RNA gel loading buffer	400 µl 5 x MOPS, 700 µl formaldehyde, 400 µl formamine, 400 µl 50% glycerol-bromphenol blue
RNA gel running buffer	180 ml 5 x MOPS, 720 ml DEPC treated water
Saponin-buffer	10 g saponin and 23.8 g HEPES in 100 ml PBS, sterile filtered, store at 4 °C
SDS-PAGE running buffer	25 mM Tris·Cl (pH 8.3), 200 mM glycine, 3.5 mM SDS
SDS-PAGE sample buffer	2x: 100 mM Tris·Cl (pH 6.8), 4% SDS, 20% glycerol, 0.2% bromphenol blue; add 2% 2-mercaptoethanol before use
SDS-PAGE separation gel buffer	1 M Tris·Cl (pH 9.1)
SDS solution	10% (w/v) sodium dodecyl sulfate
SDS-PAGE stacking gel buffer	1 M Tris·Cl (pH6.8)
TAE	50x: 2 M Tris, 5.7% glacial acetic acid, 50 mM EDTA
TBS buffer	20 mM Tris·Cl, pH 7.5; 500 mM NaCl; 0.05% Tween 20 (Sigma, P1379)

TBS-Tween/Triton buffer	20 mM Tris·Cl, pH 7.5; 500 mM NaCl; 0.05% Tween 20 (Sigma, P1379); 0.2% Triton X-100 (Sigma, X-100)
TE	10 mM Tris·Cl (pH 7.4, 7.6 or 8.0), 1 mM EDTA
Transfer buffer (Western blot)	5×: 130 mM Tris·Cl (pH 8.3), 960 mM glycine; dilute and add 20% methanol before use
Urease activity buffer	3 mM NaH ₂ PO ₄ , 110 mM urea, 7 µg/ml phenol red; pH 6.8, sterilfilter, store at 4 °C
Wash buffer (His-tagged protein)	(20 mM NaHPO ₄), 300 mM NaCl, 20 mM Imidazole, pH 8) 10% glycerol+ 8M Urea

6 Results

6.1 Characterization of complemented clones

6.1.1 Insert orientation

From transformed *E. coli* Dh5 α clones, recombinant plasmids were isolated and subjected to restriction enzyme digestion at 37°C for 2 h. Digestion with *Bam*HI revealed 2 different types of clones (Figure 35), the K2-type (bands of 7.2 and 0.8 kb) and the K8-type (bands of 5.7 and 2.3 kb), which was due to the different gene orientation of *ureAB* and the chloramphenicol-resistance marker (*cat*_{GC}) to each other K8 type→→, K2 type→←).

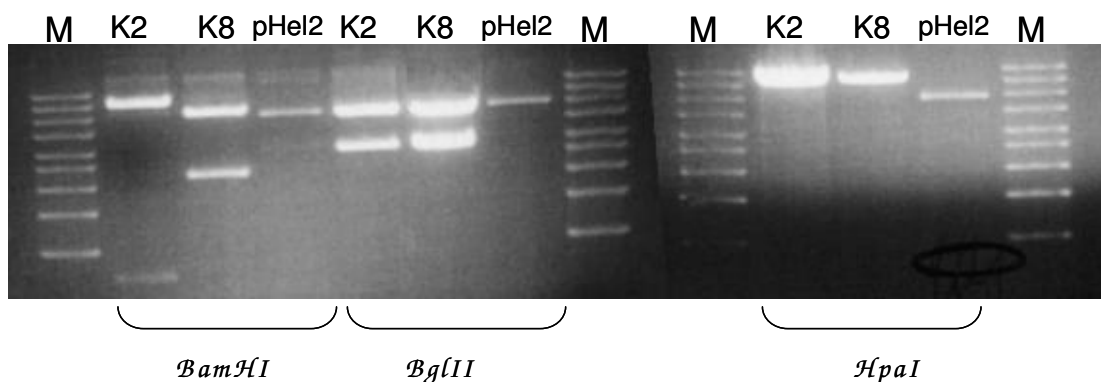


Figure 35 Restriction digestion patterns of recombinant pHel2 plasmids of the K2- and the K8-type reisolated from *E. coli* Dh5 α .

6.1.2 Protein Expression

SDS-PAGE and Western blot analysis of the urease expression of *H. pylori* clones selected after complementation of N6*ureB*::TnKm with recombinant plasmids of different types are shown in Figure 36. *H. pylori* clones produce larger amounts of urease than N6 whereas K8 clones produce similar urease amounts as the parental strain.

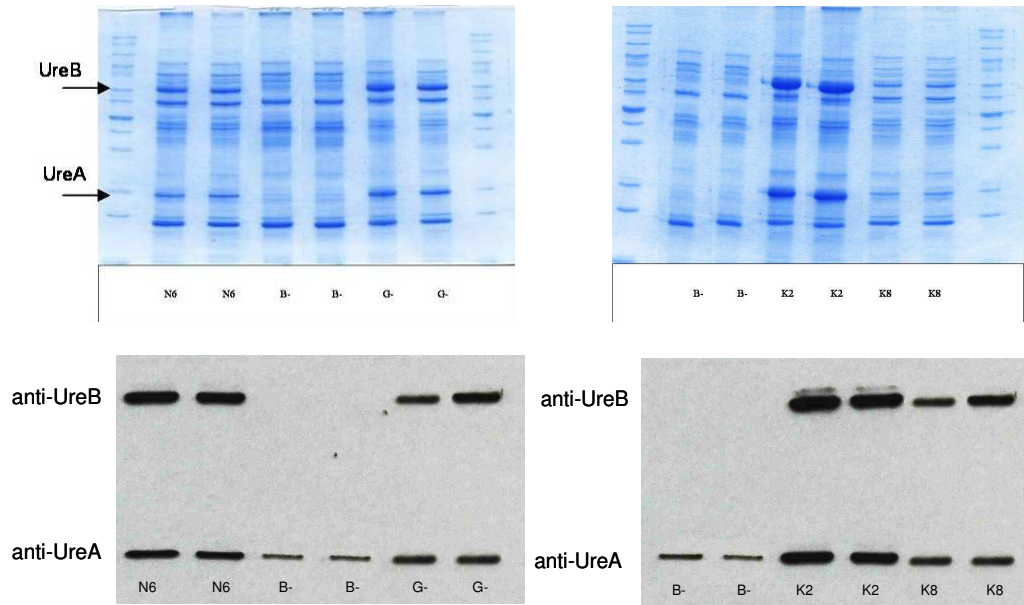


Figure 36 SDS-PAGE and Western blot characterization of the urease production of K2 and K8 *H. pylori* clones in comparison to the isogenic mutants *N6ureB::TnKm* (B-) and *N6ureG::TnKm* (G-) and the parental strain N6. UreB: 67 kDa, UreA: 23 kDa. SDS-PAGE: 12%, 10-200 kDa protein marker. Western blot: polyclonal rabbit anti-UreA 1:100,000 and anti-UreB 1:10,000; HRP-conjugated goat anti-rabbit-IgG.

6.2 Urease activity

6.2.1 Semiquantitative test

Isogenic mutants *N6ureB::TnKm* and *N6ureG::TnKm* showed no urease activity. The K8-type isogenic clone showed similar urease activity as the wild-type N6 whereas the K2-type clone showed urease activity higher than that of N6 (Figure 37).

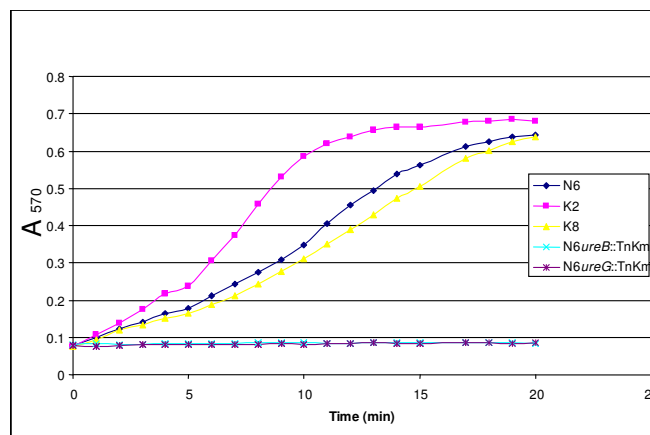


Figure 37 Urease semiquantitative test. *H. pylori* urease converts urea into NH_3 and changes the pH of the buffer. Colour change from yellow to pink was monitored in ELISA plate reader. Absorbance at 570 nm was measured for up to 40 min every 5 min.

6.2.2 Urease specific activity using the Berthelot and Lowry method

Urease specific activity of K2- and K8-type clones in comparison to N6 (Table 4).

Bacterial strain	mM ammonia / mg protein / minute (\pm SD)
N6 wild-type	26(\pm 5)
K8 clone	34(\pm 3)
K2 clone	83(\pm 14)

Table 4 Urease specific activity using the Berthelot reaction and the Lowry protein assay. Values represent the average \pm standard deviation of five to eight separate measurements performed with different bacterial preparations on different days.

6.3 Purification of surface associated *H. pylori* urease

As primary column a size-exclusion resin (SEX, Sephacryl S-300 HR 26/60) was employed. After sample load, up to 95% of the contaminating proteins were discarded in the first run without losing a lot of urease (Figure 38).

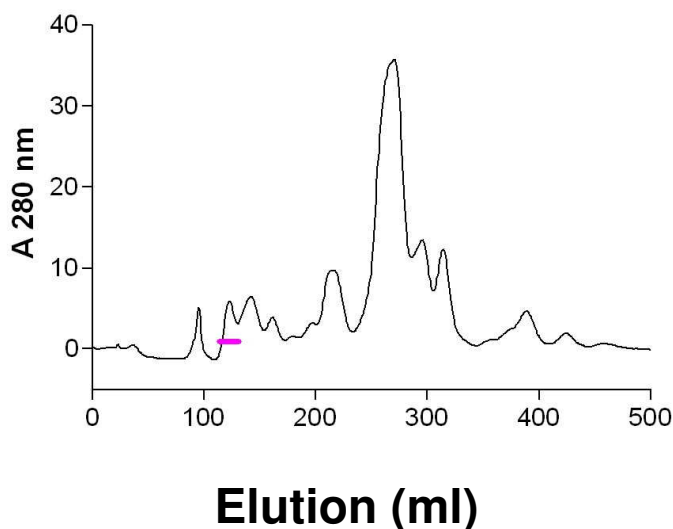


Figure 38 *H. pylori* was grown in broth, centrifuged and extracted with water (1min). After adjusting the salt concentration of the supernatant to 50 mM NaPO₄-buffer pH 7.0 and 150 mM NaCl, 2.8 ml were sterile filtered and subjected to SEX (Sephacryl S-300 HR 26/60) at 1 ml/min. Urease-positive fractions are marked by the pink bar.

In a second purification step the anion-exchange column Mono Q HR 5/5 was used. The determination of the optimal pH of 6.9 for purification was facilitated by using the “bufferprep” option of the instrument and the on-line pH measurement. Since the isoelectric point (pI) of urease is 5.9 it should be expected that the enzyme is negatively charged at a near neutral pH. High purity (~92%) could already be reached after step 2

and was further increased by a third purification step again using size-exclusion chromatography (Superdex 200 HR 10/30) to approximately 96%.

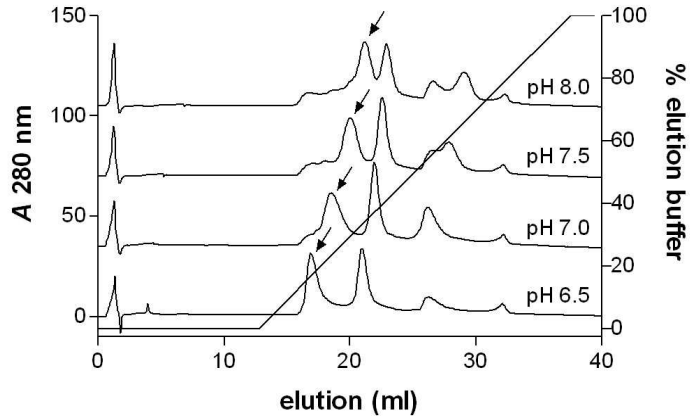


Figure 39 After initial fraction by SEX, urease-positive fractions were pooled, dialyzed against anion-exchange (AIX) buffer (35 mM Bis-Tris, 25mM Tris) and subjected to AIX (Mono Q HR 5/5) at 1ml/min. The column was equilibrated and run at the indicated pH (adjusted by HCL). Elution was achieved by a linear NaCl-gradient up to 1 M. Arrows indicate the peak with urease activity.

6.3.1 Protein analysis of samples after each purification step

Throughout the chromatographic procedure samples were taken, denatured in sample buffer and subjected to SDS-PAGE as well as Western blotting. The gradual enrichment of both urease subunits is especially well documented by the Western blot (Figure 40).

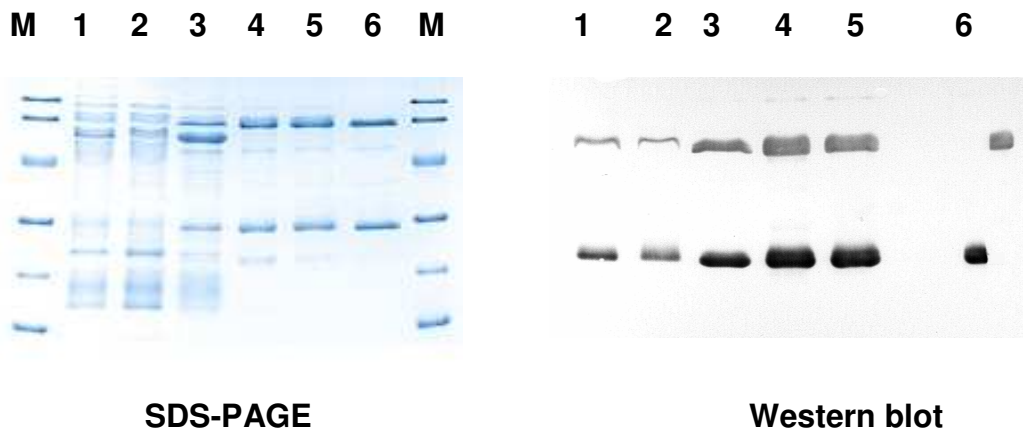


Figure 40 Purification monitoring by electrophoresis. *H. pylori* was harvested (1) and a water-extract was prepared (2). The supernatant was passed sequentially over Sephacryl S-300 HR 26/60 (3), Mono Q HR 5/5 (4, 6) and Superdex 200 HR 10/30 (5) as described in 5.6.2. After each step, aliquots were taken, denatured in sample buffer and subjected to SDS-PAGE (12% separation gel, 200 V) and Coomassie-staining. Lane 6 contains material from another experiment done with a lower initial amount of protein. M = LMW-marker. After electrophoresis using a 12% gel, the proteins were electrotransferred onto nitrocellulose and a Western blot was performed with UreA- and UreB-specific antibodies. Lane 6 was cut apart and probed with each antibody separately to show specificity.

6.4 Purification of recombinant urease subunits

E. coli SG13009 carrying either UreA or UreB recombinant proteins were grown in LB medium, in the presence of IPTG (0.5 mM). Incubation at room temperature, 37°C and 4°C was performed for different time periods. A 12 h incubation period at room temperature was shown to be most appropriate for rUreA and rUreB protein expression (Figure 41). Under these conditions, however, expression of recombinant UreB was lower than that of rUreA.

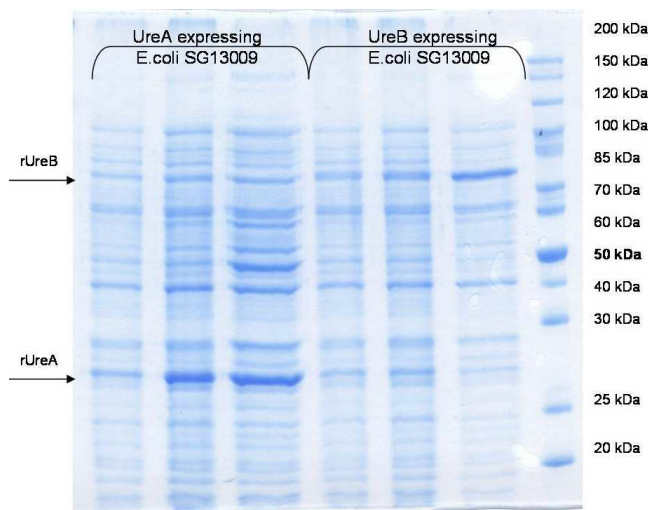


Figure 41 Small amounts of *E. coli* SG13009 were taken after 1 h, 5 h and 12 h induction with IPTG, and protein expression was visualized on SDS-PAGE stained with Coomassie Blue. Line 1-3 rUreA expressing *E. coli* SG13009, 1h, 5h and 12h after, Line4-6 rUreB expressing *E. coli* SG13009 after 1 h, 5 h, 12 h. Line 7: Protein marker.

Both native and denaturing conditions were used during preliminary experiments and denaturing conditions resulted in higher amounts of purified proteins. Thus, denaturing conditions were used.

Also, elution buffers with different imidazole concentration (20, 40, 100, 125, 150, 200 and 250 mM) were tested. Finally, for protein purification an elution buffer containing 200 mM imidazole was used. For column wash, a buffer with lower (100 mM) imidazole concentration was used as it allowed elution of contaminating proteins and resulted only in a minor loss of the recombinant His-tagged proteins.

Purity of the rUreA and rUreB proteins was verified by SDS-PAGE and Western blot analysis (Figure 42).

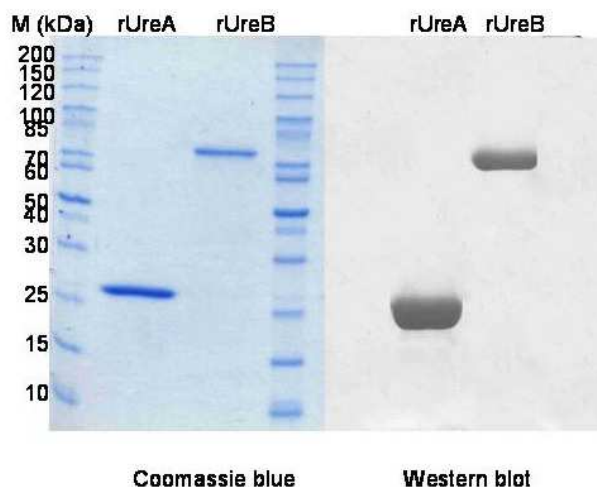


Figure 42 SDS-PAGE (left) of purified rUreA and rUreB proteins. Western blot analysis (right) of the recombinant proteins were detected with anti-His antibody (1:1,000).

After endotoxin contamination was removed using Detoxi-Gel AffinityPack (Pierce). The endotoxin content as described by LAL assay was 0.95 and 1.16 EU/ml stock solution for rUreA and rUreB, respectively.

6.5 Expression of the HB-EGF by Kato III cells after *H. pylori* infection

6.5.1 Quantitation of HB-EGF polyA⁺-RNA

Real time PCR was used to determine the content of HB-EGF polyA⁺-RNA at defined time points. The amount of target polyA⁺-RNA for each sample at each time point was normalized to the housekeeping gene β -actin and finally to the calibrator (untreated control at 8 h). No amplification occurred when total RNA or human genomic DNA was used as template. In preliminary experiments, Kato III cells were stimulated with different concentrations of the wild-type strain N6 for 1 h at a ratio of bacteria to cells of 100:1, 10:1, and 1:1. The expression of HB-EGF showed to be dependent on the concentration of N6. The highest expression was observed at a ratio of 100:1 (data not shown), which was then used for further experiments. Time course monitoring of HB-EGF polyA⁺-RNA transcripts showed the maximum of gene expression after 1 h of infection (Figure 43). A statistically significantly ($P < 0.05$) higher expression of HB-EGF could be observed after 1 h and 2 h of stimulation with wild-type N6 or N6ureG::TnKm compared to

N6ureB::TnKm or untreated cells. Values obtained with N6ureG::TnKm did not differ considerable from those obtained with N6. Interestingly, values obtained with the urease-lacking N6ureB::TnKm were similar to those of untreated cells.

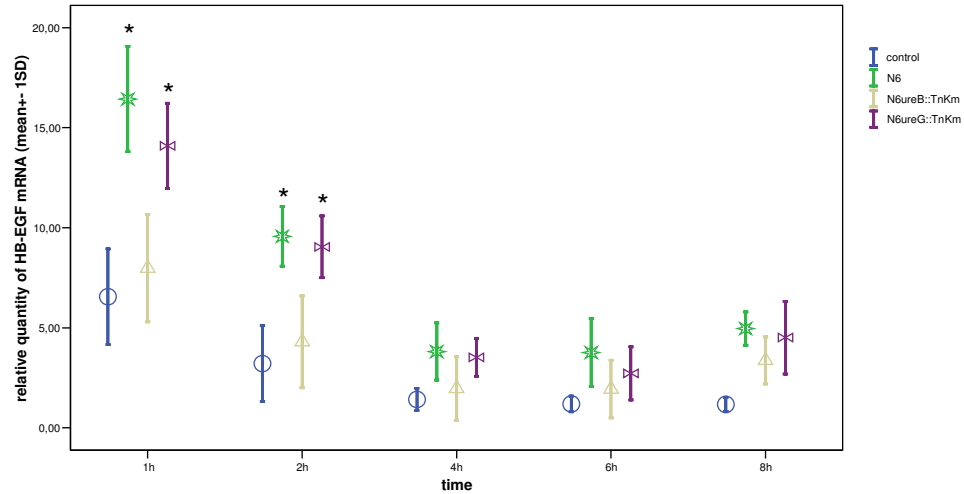


Figure 43 Relative quantities of HB-EGF polyA+-RNA (mRNA) in Kato III cells untreated or following stimulation with isogenic strains N6, N6ureB::TnKm or N6ureG::TnKm. The quantity of HB-EGF mRNA for each sample was normalized to endogenous reference β -actin and reported to untreated control mRNA level at 8 h as a calibrator. Data show mean \pm standard deviation of the mean. * $P < 0.05$ N6 or N6ureG::TnKm versus N6ureB::TnKm or untreated control $n = 4$.

To evaluate whether urease protein itself may also trigger selective HB-EGF gene expression, 10 μ g/ml purified urease was used to stimulate 10^6 Kato III cells for 1 h, resulting in a more than 2-fold ($P < 0.05$) higher amount of HB-EGF polyA+-RNA than in untreated cells (Figure 44).

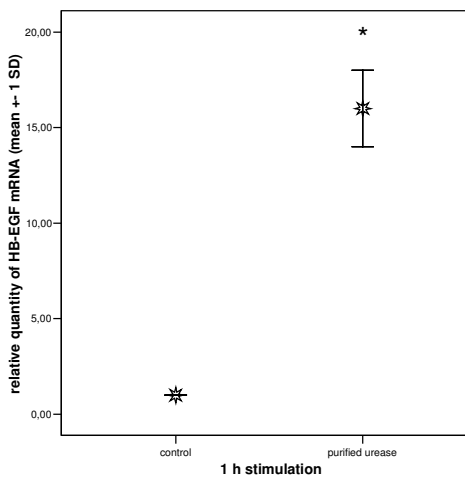


Figure 44 Relative quantity of HB-EGF mRNA after 1 h stimulation of Kato III cells with purified *H. pylori* urease compared to untreated control. The quantity of HB-EGF mRNA for each sample was normalized to endogenous reference β -actin and reported to untreated control mRNA level at as a calibrator. Data show mean \pm standard deviation of the mean. ($n = 3$), * $P < 0.05$.

6.5.2 Detection of soluble HB-EGF protein release by Western blot analysis

To determine whether HB-EGF protein production correlates with polyA⁺-RNA expression, supernatants of *H. pylori* treated and untreated (control) Kato III cells were analyzed by Western blots, supported by TotalLab v1.10 Alpha 1 software analysis, after different stimulation periods (4 h and 24 h). The ~19 kDa HB-EGF protein was secreted in the medium of *H. pylori* treated Kato III cells and could already be detected after 2 h of stimulation, though only in supernatants of cells infected with either N6 or N6ureG::TnKm but not in those of cells infected with N6ureB::TnKm (data not shown). As shown in Figure 45, 4 h incubation resulted in 3.5-fold and 2.5-fold higher HB-EGF release in supernatants of cells stimulated with N6 or N6ureG::TnKm, respectively, than in those of cells infected with N6ureB::TnKm. After an over night stimulation, no considerable differences between isogenic strains could be observed.

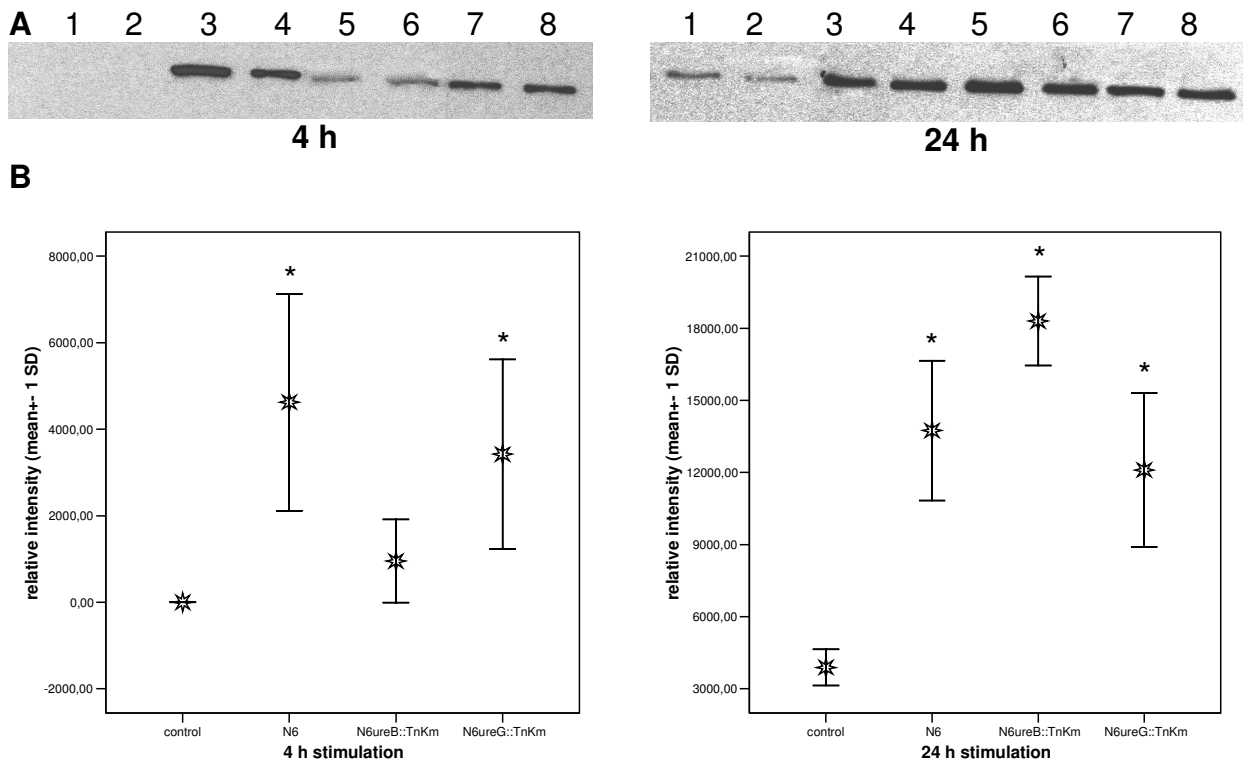


Figure 45 (A) Western blot analysis of HB-EGF protein release in supernatants of Kato III cells stimulated for 4 and 24 h with N6 (3,4), N6ureB::TnKm (5,6), N6ureG::TnKm (7,8) or untreated controls (1,2). For detection polyclonal goat anti-HB-EGF antibody (1:300; Santa Cruz Biotechnology) and HRP-conjugated anti-goat donkey-IgG (1:10,000, Santa Cruz Biotechnology) were used. Figure shows one representative blot. (B) Analysis of relative intensities using TotalLab v1.10 Alpha 1 software. Data show mean ± standard deviation of the mean. Experiment was repeated 3 times (n = 3), *P < 0.05.

Western blot analysis, supported by TotalLab v1.10 Alpha 1 software analysis, was also performed after 4 h stimulation of cells with purified urease. Results are shown in Figure 46.

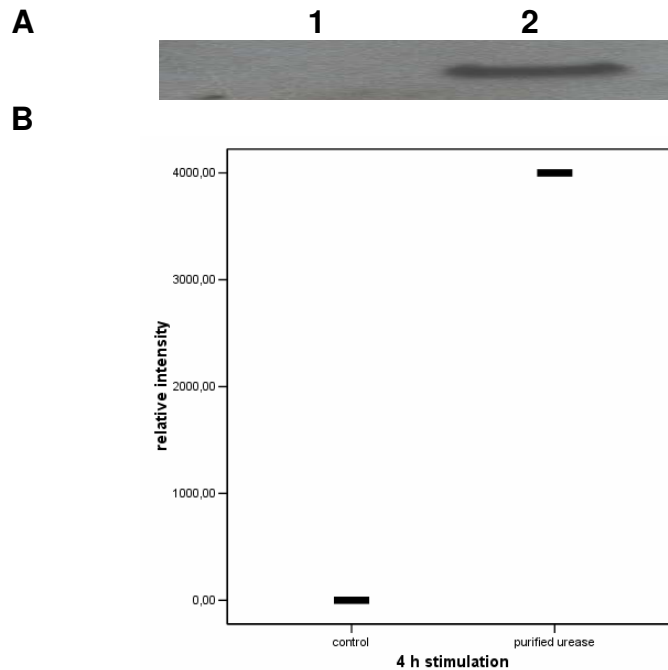


Figure 46 (A), In contrast to untreated cells (1), HB-EGF protein was detected in the supernatants of Kato III cells stimulated for 4 h with 10 $\mu\text{g/ml}$ purified urease (2). For detection polyclonal goat anti-HB-EGF antibody (1:300; Santa Cruz Biotechnology) and HRP-conjugated anti-goat donkey-IgG (1:10,000, Santa Cruz Biotechnology) was used. (B), Analysis of relative intensities using TotalLab v1.10 Alpha 1 software.

6.5.3 Effect of MAPK inhibitors on HB-EGF gene expression

Pretreatment of Kato III cells with PD98059 or U0126, both inhibiting activation of p44/p42 MAP kinases, resulted in low HB-EGF polyA⁺-RNA levels – similar to those of untreated controls – irrespective of the stimulus used to stimulate cells (Figure 47). In contrast, pretreatment of cells with the specific p38 MAP kinase inhibitor SB203580 did not alter the differences observed between the different stimuli with respect to HB-EGF gene expression.

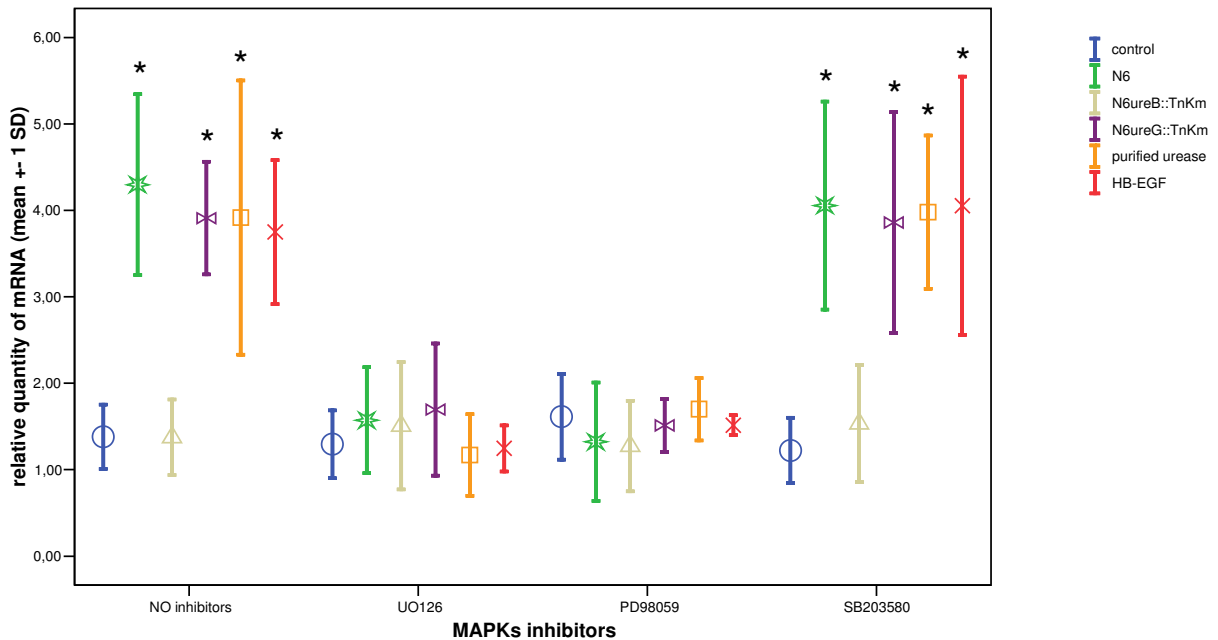


Figure 47 Influence of MAPK inhibitors on the relative quantity of HB-EGF mRNA after treatment of Kato III cells with N6, N6ureB::TnKm, N6ureG::TnKm, purified urease, and HB-EGF for 1 h. Each sample was normalized to β -actin and finally to the calibrator (sample with the lowest HB-EGF mRNA content in each of the experiments). Data show mean \pm standard deviation of the mean. (n = 3), *P < 0.05.

6.5.4 Effect of *H. pylori* urease on MAP kinases activation

After 30 min, 1, 2, 4 and 6 h of incubation of Kato III cells with bacteria or purified urease, Western blot analysis of cell lysates using phosphor-specific antibodies to p44/p42, p38 or p54/46 was performed. As shown in Figure 48 B, after 1h of incubation a statistically significantly higher phosphorylation of both p44 and p42 was observed in cells stimulated with N6 or N6ureG::TnKm, than in those stimulated with N6ureB::TnKm (P < 0.05). A Western blot performed using non-phospho-specific control antibodies that recognize p44/p42 regardless of their phosphorylation state is also shown (Figure 48 A). In cells stimulated with purified urease, after 1 h of incubation, activation of p44 and p42 was significantly higher than that in untreated controls (P < 0.05). P38 and p64/p56 showed only minor levels of activation, and no differences could be observed with respect to the *H. pylori* strain used to stimulate cells or between urease treated cells and untreated controls (data not shown).

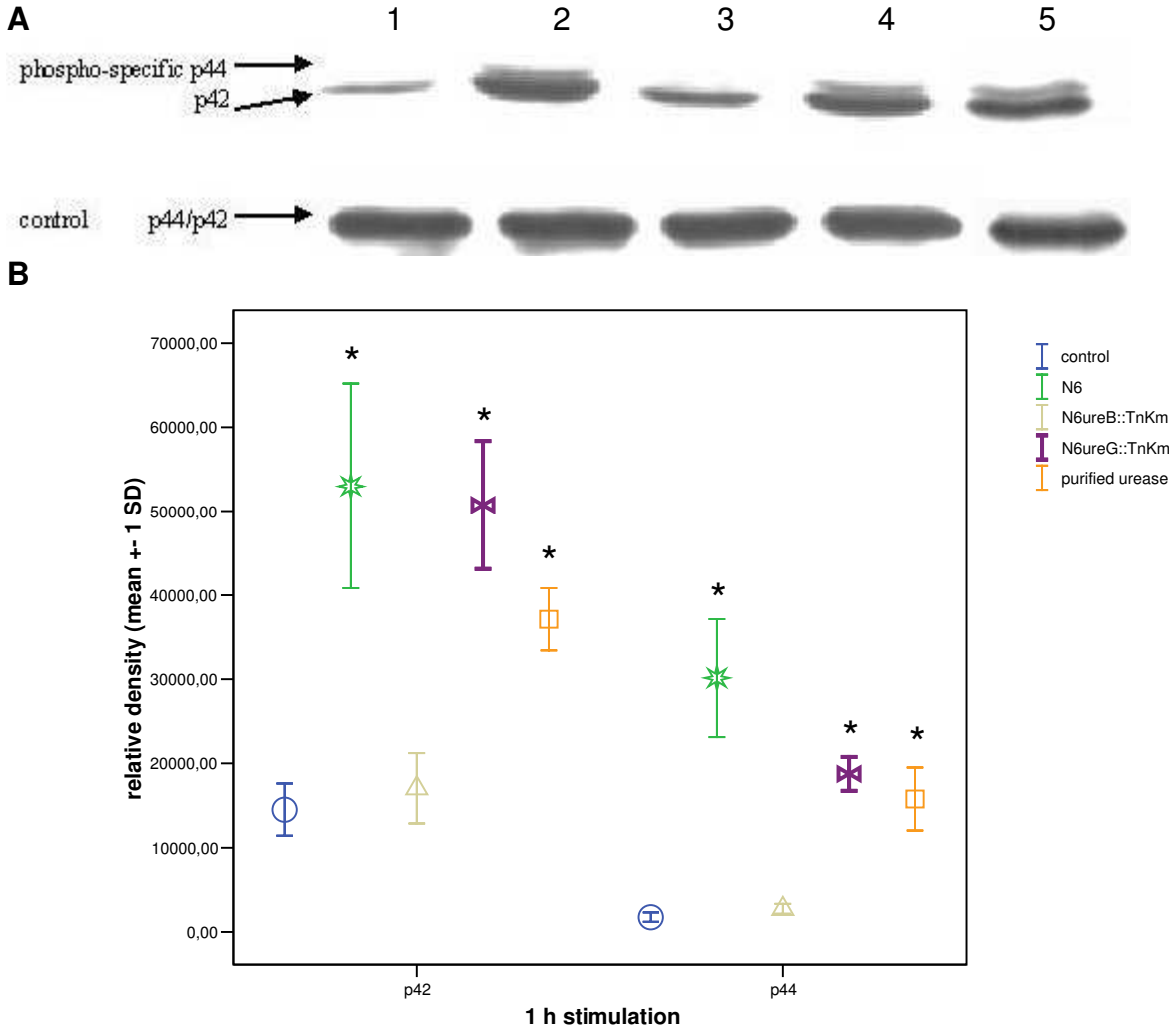


Figure 48 (A), Western blot analysis of p44/p42 MAP kinases activation after 1 h of incubation in untreated Kato III cells (1) and in those stimulated with N6 (2), N6ureB::TnKm (3), N6ureG::TnKm (4) and purified urease (5) using phospho-specific antibodies in comparison to controls using non-phospho-specific antibodies (figure shows one representative blot). (B), Analysis of relative intensities using TotalLab v1.10 Alpha software and SPSS v10. Data show mean \pm standard deviation of the mean. (n = 3) *P < 0.05.

6.5.5 Cell proliferation assay

Cell proliferation of Kato III cells stimulated with the different *H. pylori* isogenic strains, purified urease or HB-EGF (positive control) was examined at different time points. In samples obtained after 6 h, of stimulation, higher levels of proliferation (P < 0.05, n = 3) were observed in stimulated cells than in untreated control cells (Figure 49). After 24 h of stimulation, a statistically significantly higher proliferation was observed (P < 0.05, n = 3) in cells stimulated with N6 or N6ureG::TnKm than in those stimulated with

N6ureB::TnKm, the latter showing similar levels of proliferation as untreated controls (Figure 49). Proliferation of cells treated with purified urease or HB-EGF was statistically significantly higher ($P < 0.05$, $n = 3$) than that of untreated controls. Pretreatment of cells with SB203580 did not affect cell proliferation characteristics (data not shown), while PD 98059 or U0126 each caused a considerable reduction of cell proliferation and differences between samples with respect to cell proliferation were also abolished (data not shown). Cell viability was examined using trypan blue stain and was shown to be reduced from 95 to 75% during the 24 h incubation period. No differences with respect to cell viability could be observed between samples at any of the time points (data not shown). Also the presence of MAPK inhibitors was not found to affect cell viability (data not shown).

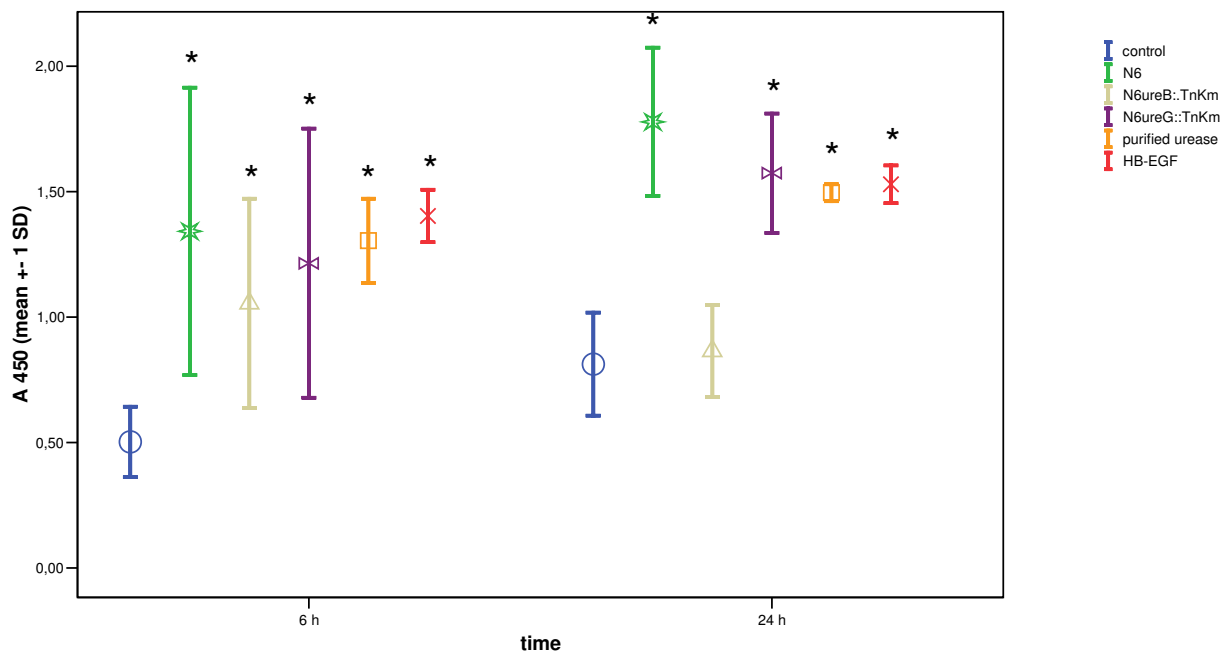


Figure 49 Proliferation of Kato III cells after 6 h and 24 h in response to isogenic *H. pylori* wild-type and mutant strains, purified urease and HB-EGF. Data show mean \pm standard deviation of the mean. ($n = 3$), * $P < 0.05$.

6.6 Stimulation of PBMCs

6.6.1 Extracellular cytokine measurement - cytokine secretion assay

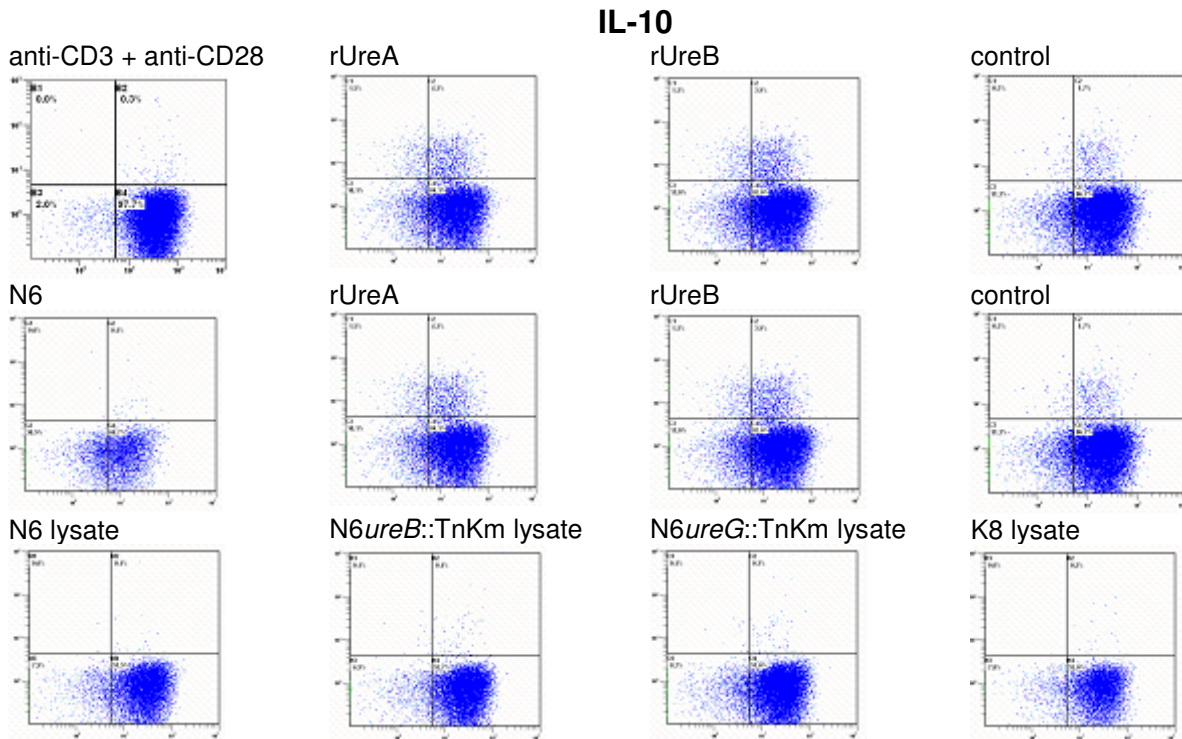
Stimulation of PBMCs for different time points resulted in low $CD4^+$ T cell activation and no detectable amount of IL-10, IFN γ and IL-4. Under these experimental conditions the

cytokine producing CD69⁺CD4⁺ T cell number was under the system's detection level, even after magnetic enrichment of the cytokine producing cells.

6.6.2 Intracellular cytokine detection

Intracellular cytokine (IL-10, IFN γ and IL-4) production of CD69⁺CD4⁺ T cells stimulated in the presence of anti-CD28 costimulator molecule with the different *H. pylori* isogenic strains, bacterial lysates, or rUreA or rUreB was examined after 7, 14, 21 days of stimulation. Experiments using no restimulation or using original stimuli for restimulation on the day of cytokine measurement failed to detect the production of IL-4, IL-10 and IFN γ by using intracellular staining. Intracellular production of cytokines by CD69⁺CD4⁺ T cells could only be detected in experiments, where PMA/Ionomycin was used for additional stimulation for 6 h before intracellular staining. Detection was performed using flow cytometry and row data of one representative experiment after 7 days of stimulation are shown in Figure 50.

A



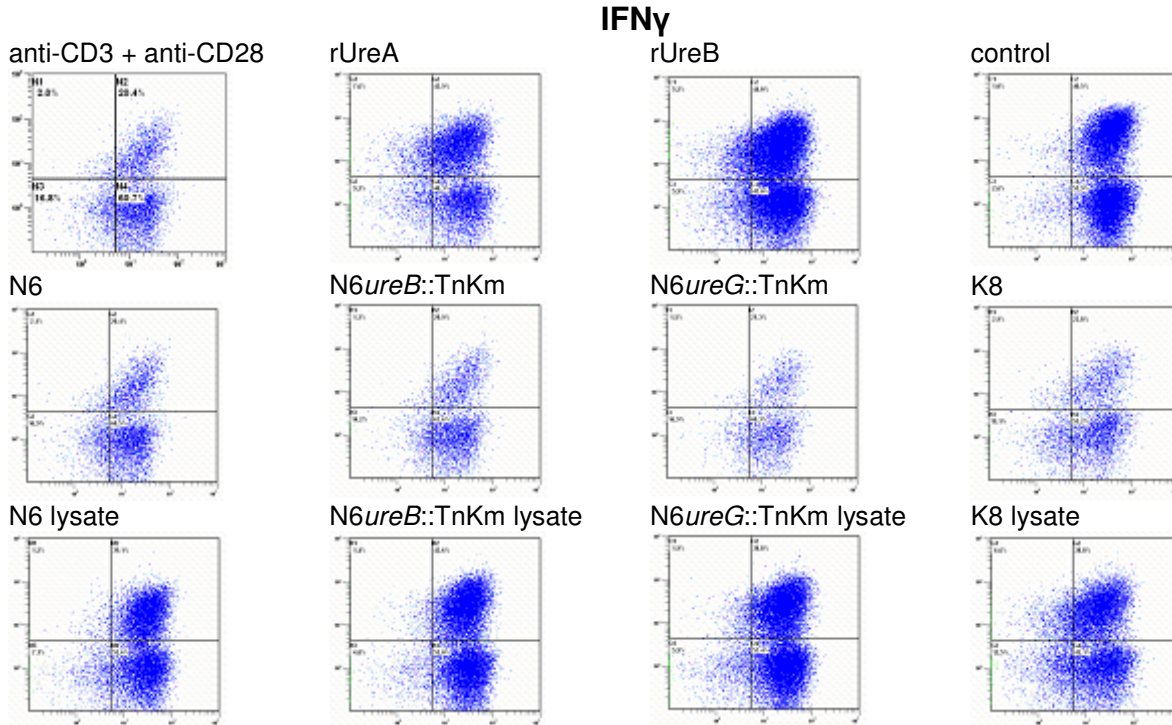
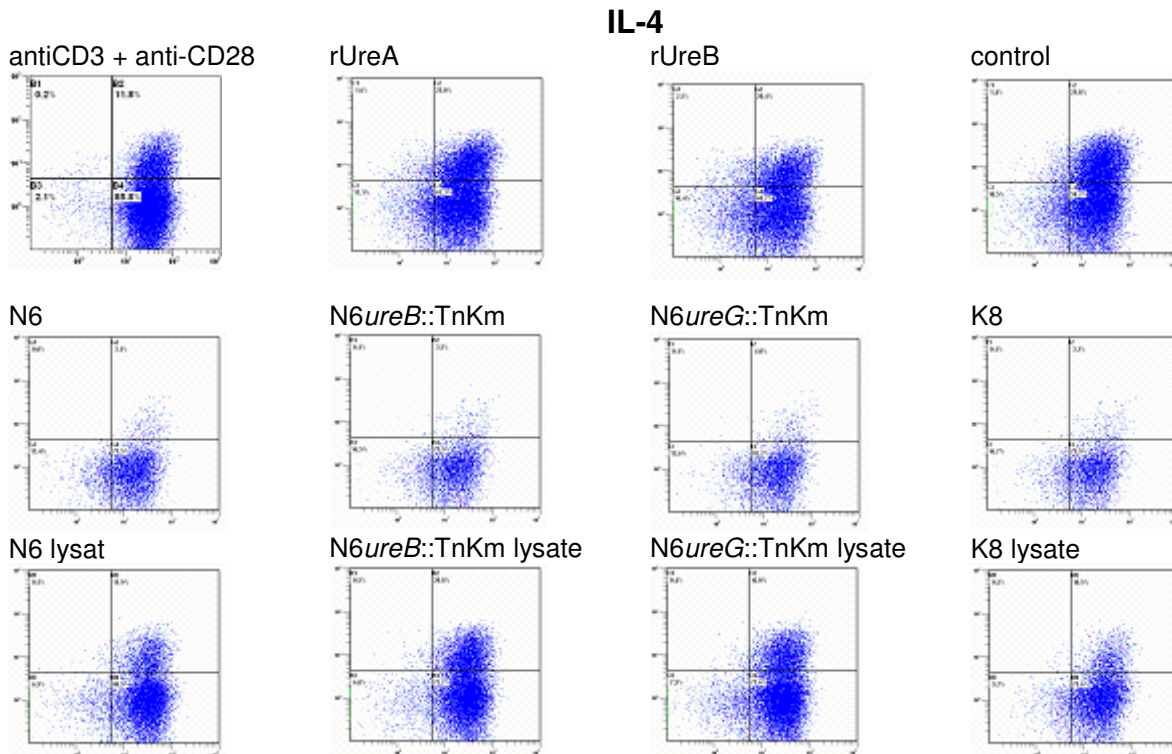
B**C**

Figure 50 Plots of cytokine producing CD69⁺CD4⁺ T cells (upper right square in each histogram) following 7 days stimulation with rUreA, rUreB, N6, N6*ureB*::TnKm, N6*ureG*::TnKm, K8 or lysates in the presence of anti-CD28 as costimulator.

Statistical analysis was calculated using the SPSS v12.0 software (Figure 51).

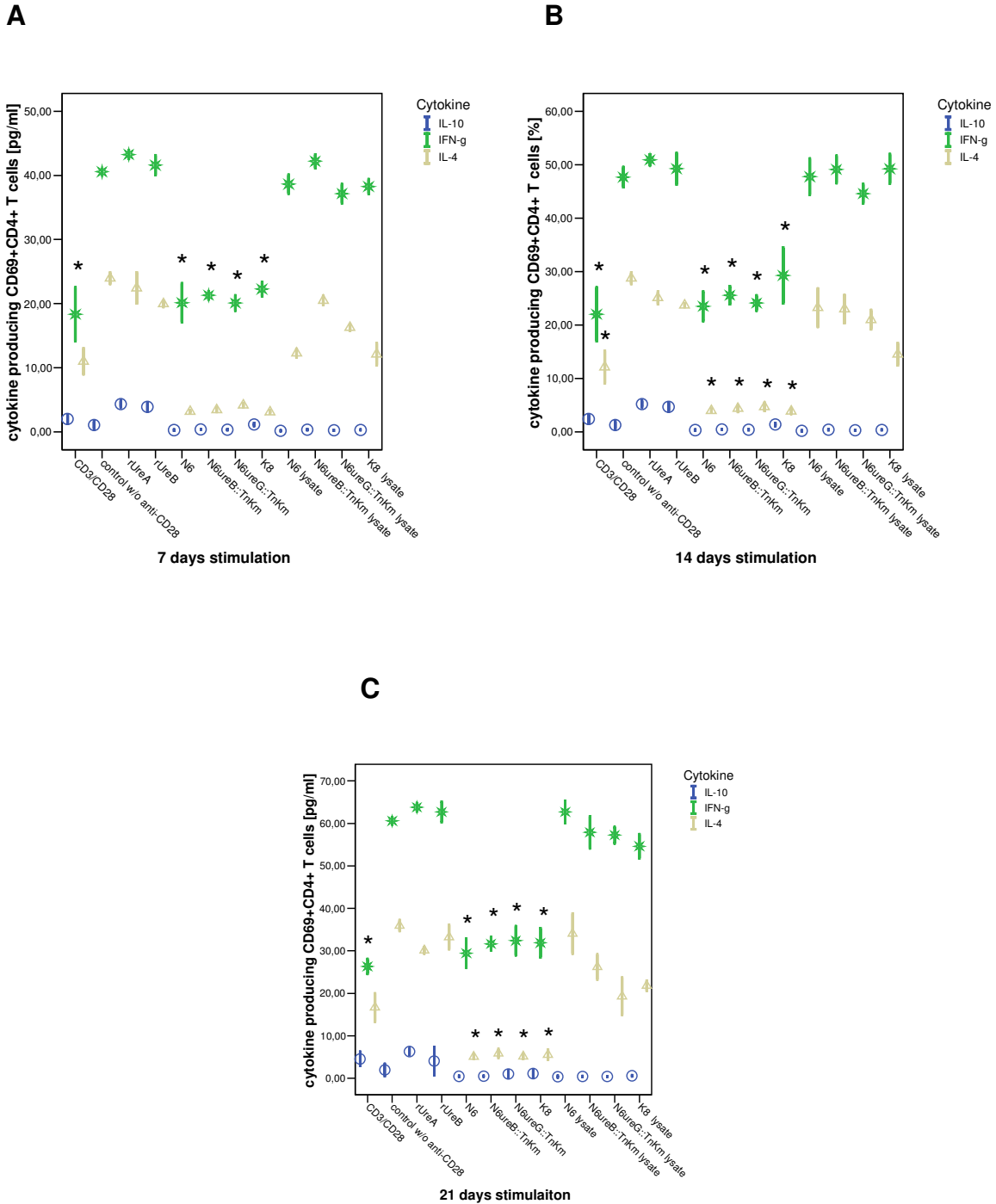


Figure 51 Statistical analysis of the percentage of intracellular IL-10, IL-4 or IFN γ producing CD69⁺CD4⁺ T cell subsets after (A) 7 days, (B) 14 days and (C) 21 days of stimulation with rUreA, rUreB, isogenic *H. pylori* strains, and bacterial lysates. Data shows mean \pm standard deviation. *P < 0.05, n = 3.

Regarding to IL-10 production, low level of IL-10 could be detected and no significant differences could be observed between the different stimuli (Figure 51). Cells stimulated with live bacteria, had a significant by ($P < 0.05$) lower percentage of IFN γ or IL-4 producing CD69⁺CD4⁺ T cells than the untreated control cells. Cells treated with rUreA, rUreB, or bacterial lysates had similar percentages of IFN γ or IL-4 producing CD69⁺CD4⁺ T cells. Addition of anti-CD28 to control cells as costimulator molecule did not affect the IFN γ or IL-4 positive CD69⁺CD4⁺ T cell subsets. Elongation of the stimulation period to 14 or 21 days showed slightly higher percentage levels but similar differences between samples as after 7 days.

6.6.3 Extracellular cytokine detection

In parallel experiments, cells were treated with the same stimuli under the same experimental conditions but in the absence of Brefeldin A. Supernatants were collected after 7, 14 and 21 days and analyzed by BioPlex triplex assay detecting IL-10, IFN γ and IL-4. IL-4 concentration was under the system's detection level (data not shown). With regard to IL-10, low levels (3-24 pg/ml) of this cytokine could be detected in the supernatants of stimulated cells. Untreated cells produced statistically significantly higher amounts of IL-10 ($P < 0.05$) than those of any other sample including the positive control sample. Values obtained with N6 and K8 were significantly higher than those obtained with N6*ureB*:TnKm ($P < 0.05$), whereas cells stimulated with the latter produced the lowest amount of IL-10 than any other sample.

With respect to IFN γ , irrespective of the strain, cells stimulated with live bacteria produced significantly lower amounts of the cytokine than those of any other sample ($P < 0.05$). Figure 52 shows data obtained for IL-10 and IFN γ after 7 days of stimulation. Similar results were obtained after longer periods of stimulation (14 and 21 days, data not shown).

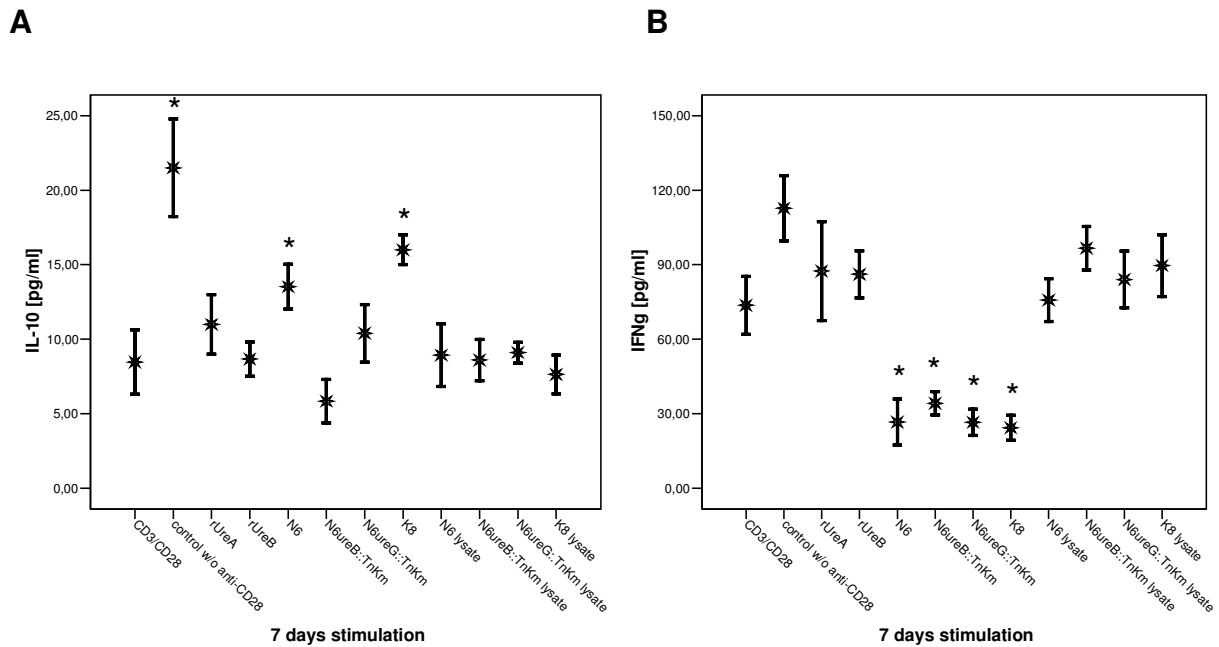


Figure 52 IL-10 (A) and IFN γ (B) detection in the supernatants of PBMCs stimulated for 7 days with anti-CD3+anti-CD28 (positive control), rUreA, rUreB, viable isogenic strains, and bacterial and lysates. Before cytokine detection, PMA/Ionomycin was added for 6 h. Data shows mean \pm standard deviation. *P < 0.05 untreated controls vs. all other samples, and N6 and K8 vs. N6ureB::TnKm, n=5.

6.7 Monocyte derived dendritic cells

After 5 days of incubation in the presence of GM-CSF and IL-4, monocytes (CD14⁺) become immature cells. During maturation, due to stimulation with either LPS (positive control), rUreA, rUreB, live bacteria, or bacterial lysates, morphological changes were observed, which were visualized by microscopy. Untreated negative control cells (immature dendritic cells) remained round shaped.

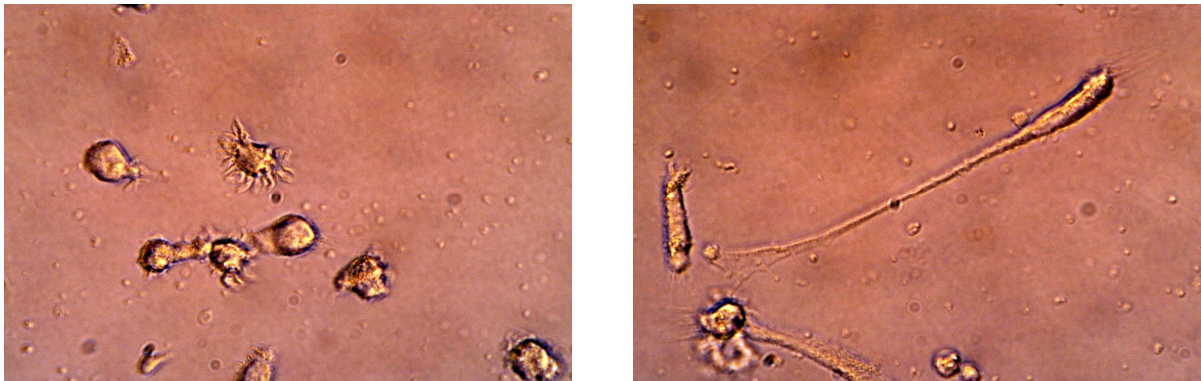


Figure 53 (A), Microscopic pictures of the “round” morphology of immature dendritic cells and (B), the “stick” morphology of maturing dendritic cells.

6.7.1 Surface staining of dendritic cells

The potential of *H. pylori* to induce DC maturation was investigated by stimulating immature DCs with *H. pylori* (viable and lysed bacteria), rUreA, or rUreB. Phenotypic changes of immature dendritic cells (iDCs) turning into mature DCs (mDCs) were also monitored using flow cytometry after 6, 24 and 48 h of stimulation. Untreated cells and *E. coli* LPS treated cells were as negative and positive controls respectively.

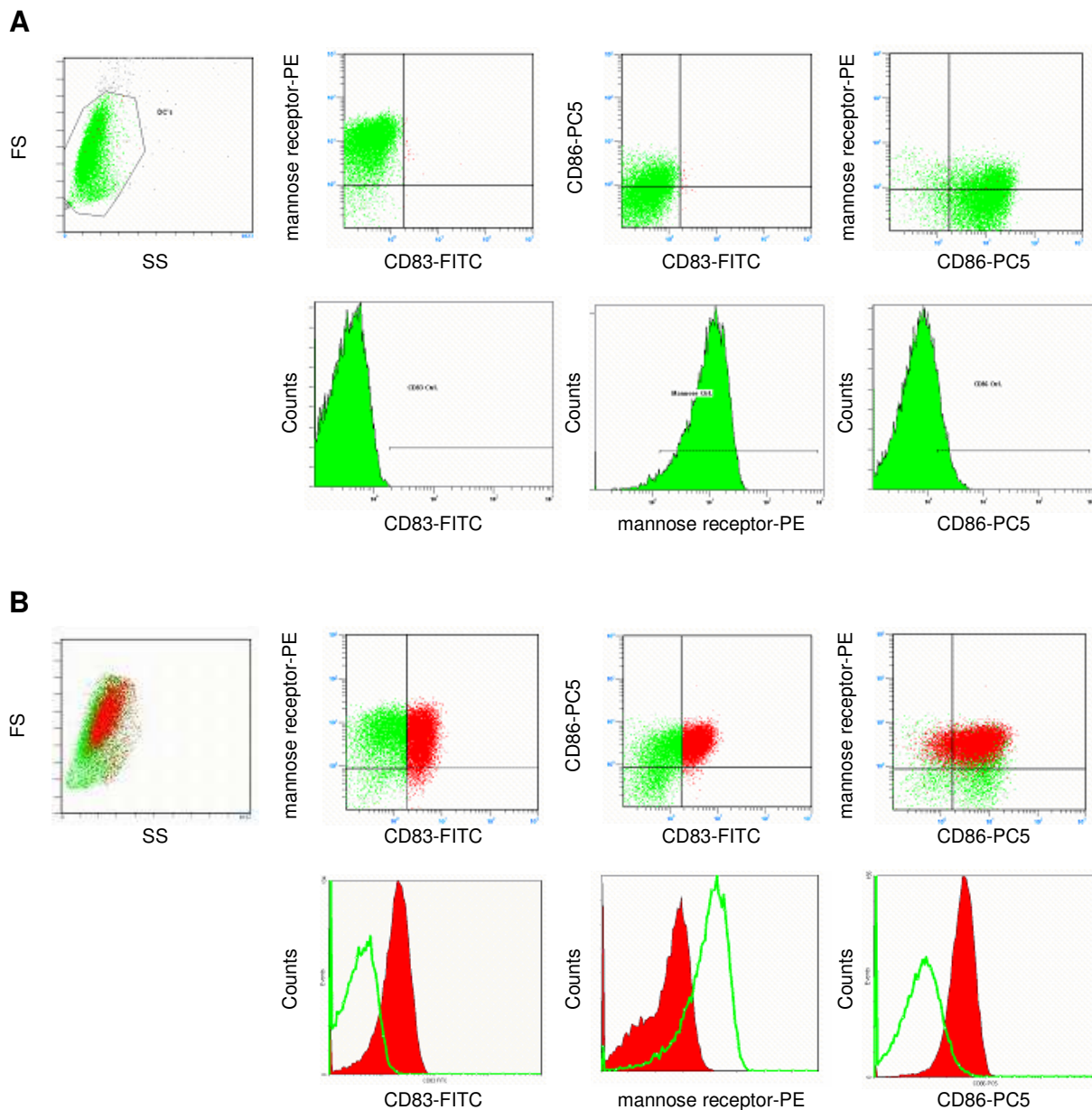


Figure 54 Cell surface markers on untreated cells (iDCs, A) and LPS treated cells (mDCs, B) after 48 h of incubation. Value of iDC was set as control (green line).

As shown in Figure 54 and Figure 55, mannose receptor expression decreased, while CD83 and CD86 expression increased on the cell surface of monocyte derived dendritic cells during maturation.

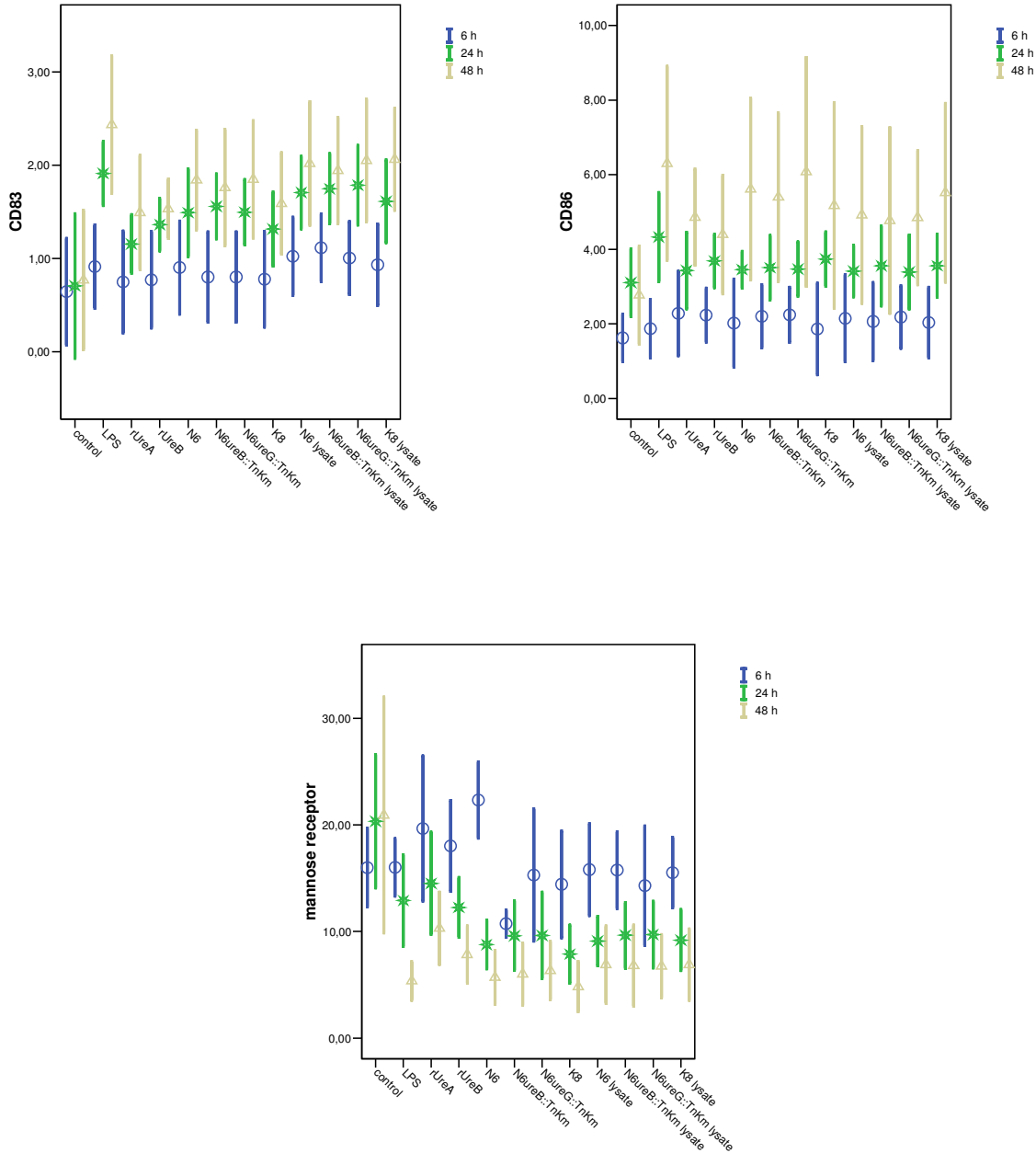


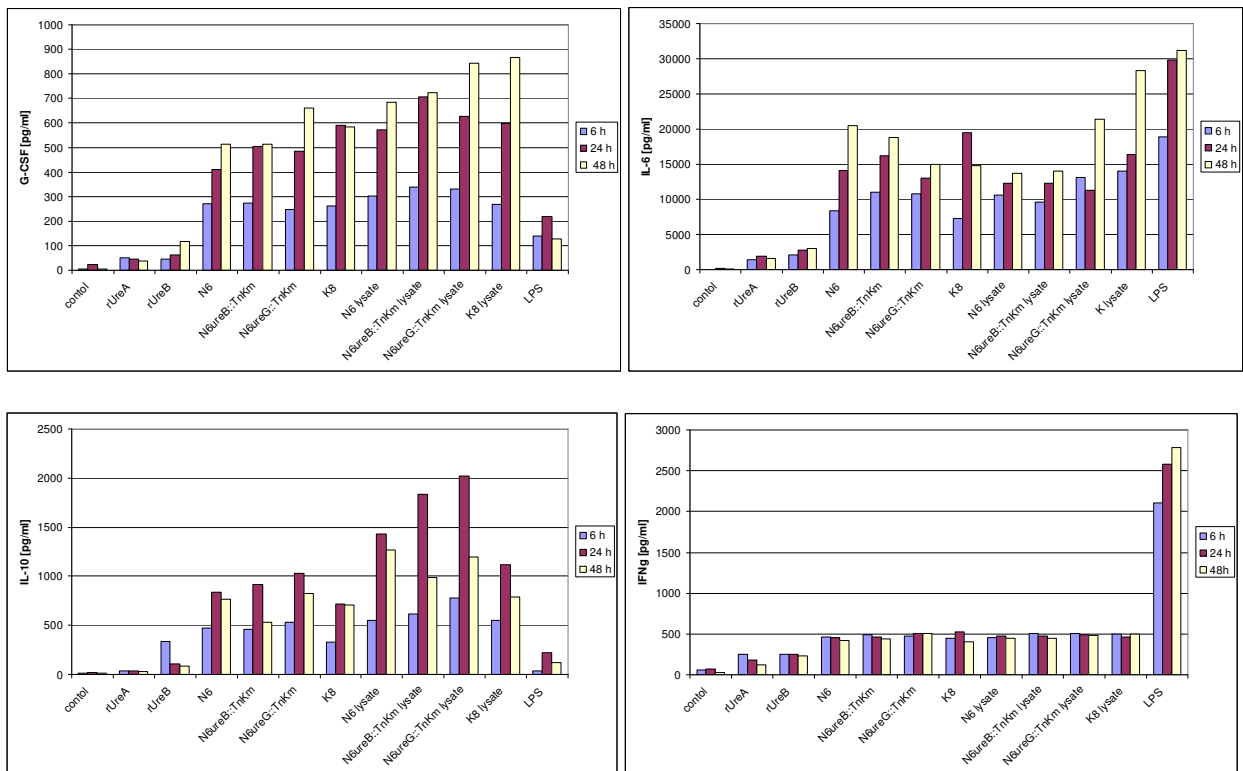
Figure 55 Comparison of phenotypic changes of DCs during maturation upon stimulation for up to 48 h with LPS, rUreA, rUreB, live bacteria and bacterial lysates. Data represents means \pm standard deviation (n = 5).

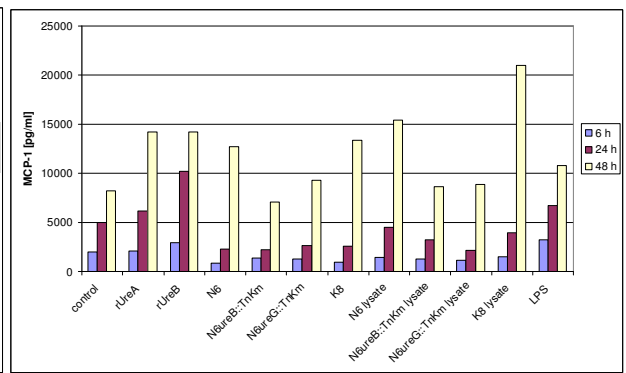
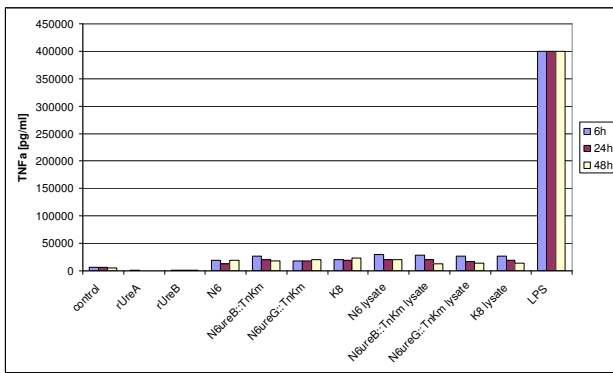
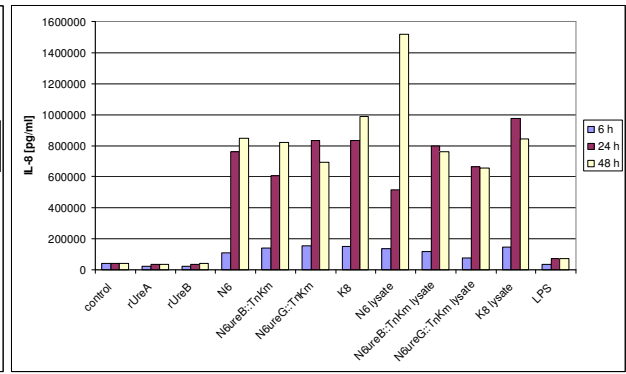
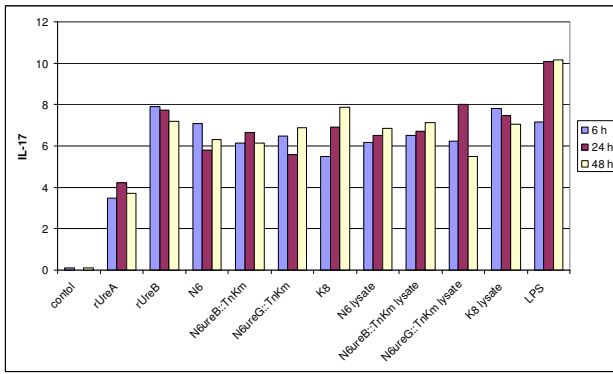
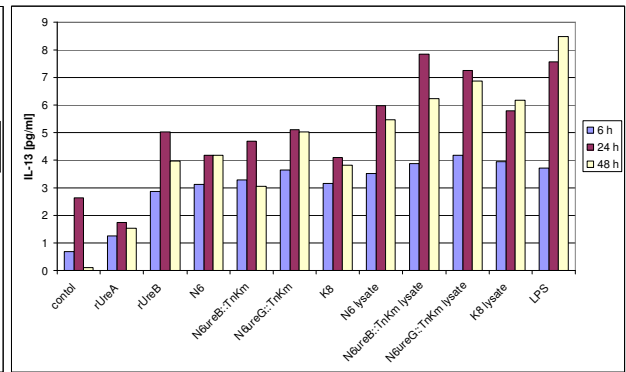
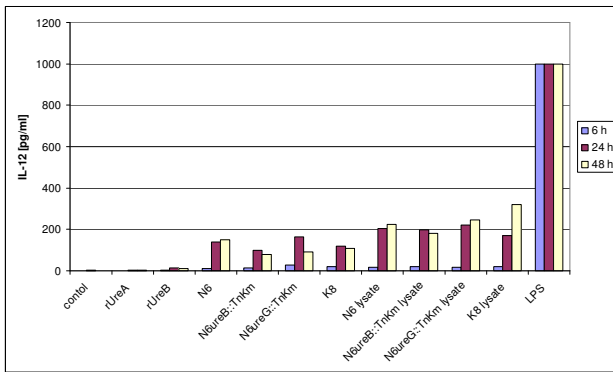
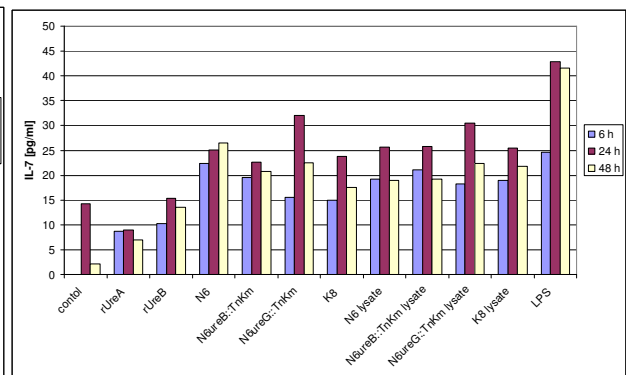
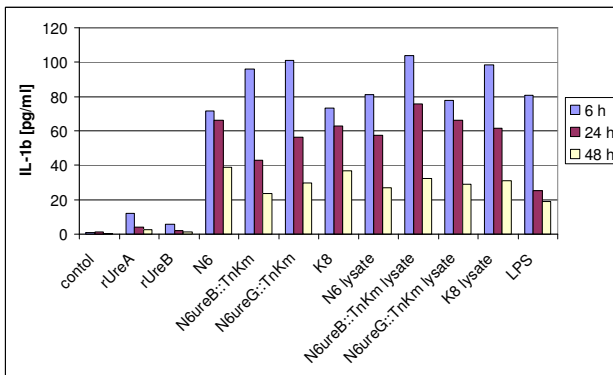
Expression of CD83 and CD86 were up regulated by stimulation with different *H. pylori* bacteria, bacterial lysates, rUreA, or rUreB as compared to basal expression in particular

after 48 h of incubation. Furthermore there was no considerable difference in the expression of CD86 and CD83 in comparison to LPS stimulated cells. Mannose receptor was downregulated during the maturation process indicating lower phagocytic ability of mature DCs. In contrast to untreated cells, mannose receptor expression was decreased in all the treated cells during the stimulation period. In contrast to other samples, in cells stimulated with *N6ureB::TnKm* live bacteria mannose receptor expression was considerably decreased as soon as after 6 h of stimulation. No considerable differences were observed between N6, *N6ureG::TnKm* or K8 treated cells as well as between those treated with the different bacterial lysates with respect to the expression of the mannose receptor (Figure 55).

6.7.2 Cytokine production by dendritic cells

First, the cytokine expression profile of DCs in response to the different stimuli was screened by the 17-Plex system of BioRad using pooled supernatants collected of 5 independent experiments after 6, 24 and 48 h of stimulation (Figure 56).





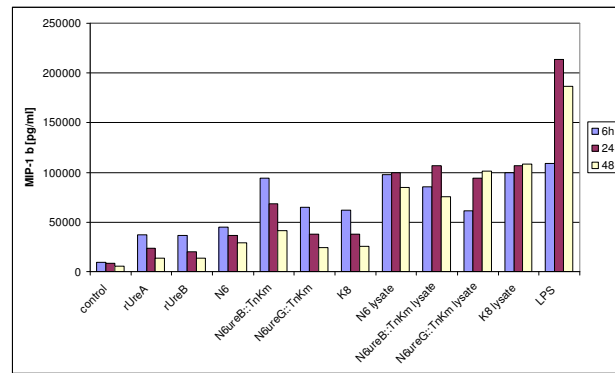


Figure 56 Cytokine expression profile of DCs after 6, 24, and 48 h of stimulation with rUreA, rUreB, live bacteria, bacterial lysates or LPS. Values correspond to pooled samples of 5 independent experiments.

Only very low amount of IL-13 and IL-17 could be detected and IL-5 could not be detected at all. Levels of G-CSF, IL-6, IL-12, IL-8, and MCP-1 increased during the 48 h incubation period. On the other hand, values for IL-1 β decreased during the 48 h incubation. IL-10 reached a peak after 24 h of incubation.

H. pylori live bacteria and bacterial lysates but in particular rUreA and rUreB induced considerably lower amounts of IL-12, IFN γ and TNF α as compared to LPS. LPS also showed to be more effective with respect to the induction of IL-6, IL-7, TNF α , IL-12 and MIP-1 β . On the other hand, bacteria and bacterial lysates were more effective in inducing IL-10, IL-8 and G-CSF than LPS.

Bacterial lysates induced higher amounts of IL-10 and MIP-1 β than the corresponding live bacteria with the exception of MIP-1 β induction by live N6ureB::TnKm after 6 h of stimulation. As a matter of fact, a different MIP-1 β production kinetic was observed between cells stimulated with live bacteria and those stimulated with bacterial lysates. So, in contrast to cells treated with live bacteria, MIP-1 β production did not decrease during the 48 h incubation period.

N6ureB::TnKm induced higher amounts of MIP-1 β , than the other live bacteria including N6. On the other hand, stimulation with N6 for 48 h induced higher levels of MCP-1, IL-10 and IL-12 secretion than N6ureB::TnKm.

In order to analyze whether these differences are of statistical significance, of the 5 independent experiments every single sample obtained after 6 and 24 h of stimulation

was tested for MIP-1 β , whereas every single sample obtained after 48 h of stimulation was tested for IL-10, IL-12 and MCP-1.

Recombinant proteins rUreA and rUreB did not induce IL-10 secretion at all eliciting values similar to those of the control. With the exception of N6ureB::TnKm and K8, all other stimuli delivered values, which were significantly higher ($P < 0.05$) than those of the control, rUreA, or rUreB (Figure 57).

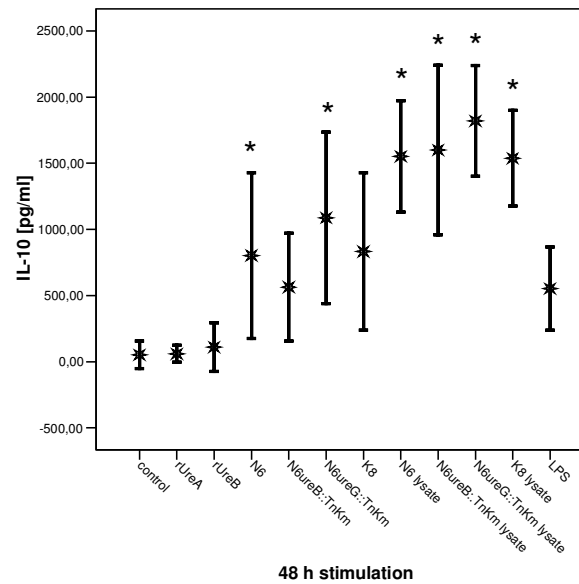


Figure 57 IL-10 content of supernatants of DCs stimulated for 48 h stimulation. Data show mean \pm standard deviation, * $P < 0.05$ compared to control, rUreA, and rUreB; $n = 5$.

With respect to IL-12, LPS was the most effective stimulus inducing statistically significantly higher amounts ($P < 0.05$) than any other of the stimuli. However, N6 and N6ureG::TnKm but not N6ureB::TnKm or any other stimulus, showed values significantly higher ($P < 0.05$) than that of the control (Figure 58).

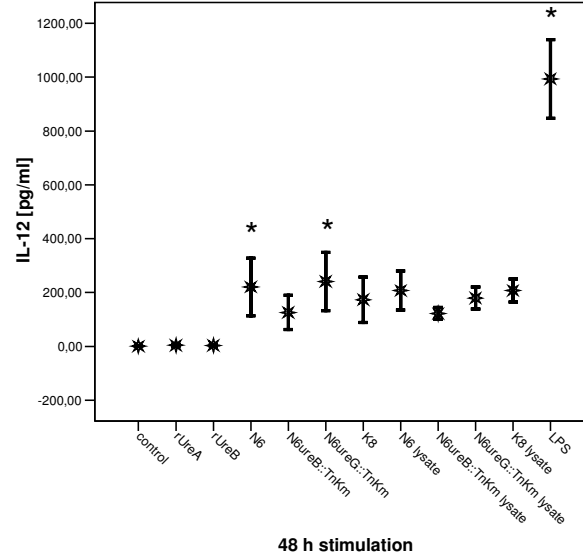


Figure 58 IL-12 content of supernatants of DCs stimulated after 48 h of stimulation. Data show mean \pm standard deviation. *P < 0.05 compared to control, n = 5.

MCP-1 production of cells stimulated for 48 h with N6ureB::TnKm or N6ureG::TnKm (live bacteria or bacterial lysates) was similar to that of untreated controls. All other stimuli with the exception of LPS induced significantly higher MCP-1 levels (P < 0.05) than that of the control Figure 59. Interestingly, rUreA and rUreB induced similar or even higher levels of MCP-1 in comparison to LPS, which is shown also in Figure 56.

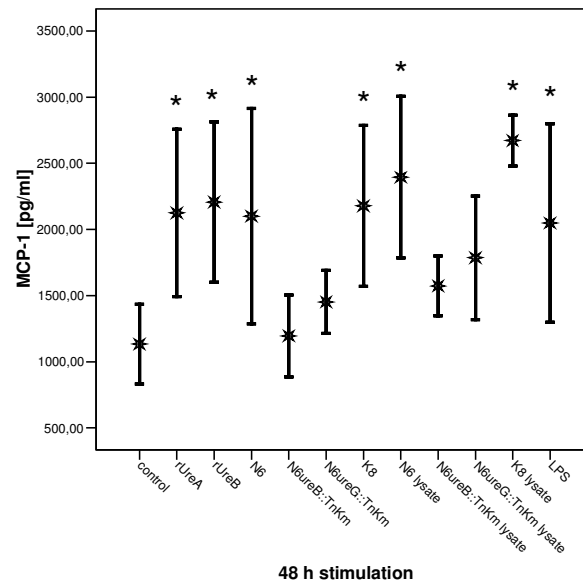


Figure 59 MCP-1 content of supernatants of DCs stimulated for 48. Data show mean \pm standard deviation.) *P < 0.05 significance compared to control and N6 and K8 lysates vs. N6ureB::TnKm live bacteria, n = 5.

Cells stimulated with LPS and bacterial lysates produced significantly higher amounts of MIP-1 β than untreated control cells ($P < 0.05$). With regard to stimulation with live bacteria,

N6*ureB*::TnKm but not N6 or K8 stimulated cells produced significantly higher amounts of MIP-1 β than the controls ($P < 0.05$) Figure 60.

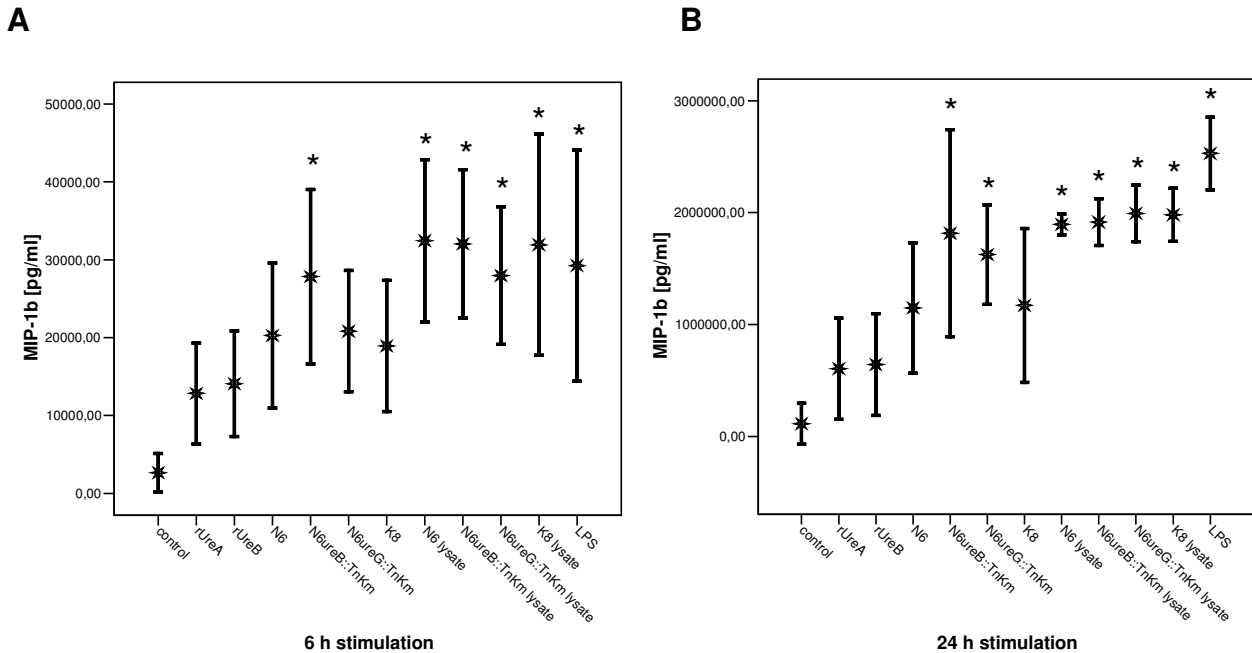


Figure 60 MIP-1 β content of supernatants of DCs stimulated for 6 h (A) and 24 h (B). Data show mean \pm standard deviation * $P < 0.05$ compared to control n = 5.

In addition, TGF- β 1 production of stimulated DCs was measured after 6, 24 and 48 h of stimulation (Figure 61). Cells stimulated with rUreA, rUreB or bacterial lysates produced similar amounts of TGF- β 1 as the untreated control cells. Compared to the control, significantly higher TGF- β 1 production was observed in all samples stimulated with live bacteria ($P < 0.001$). However values obtained with, N6*ureB*::TnKm were significantly ($P < 0.05$) lower than those obtained with N6, N6*ureG*::TnKm or K8 ($P < 0.05$).

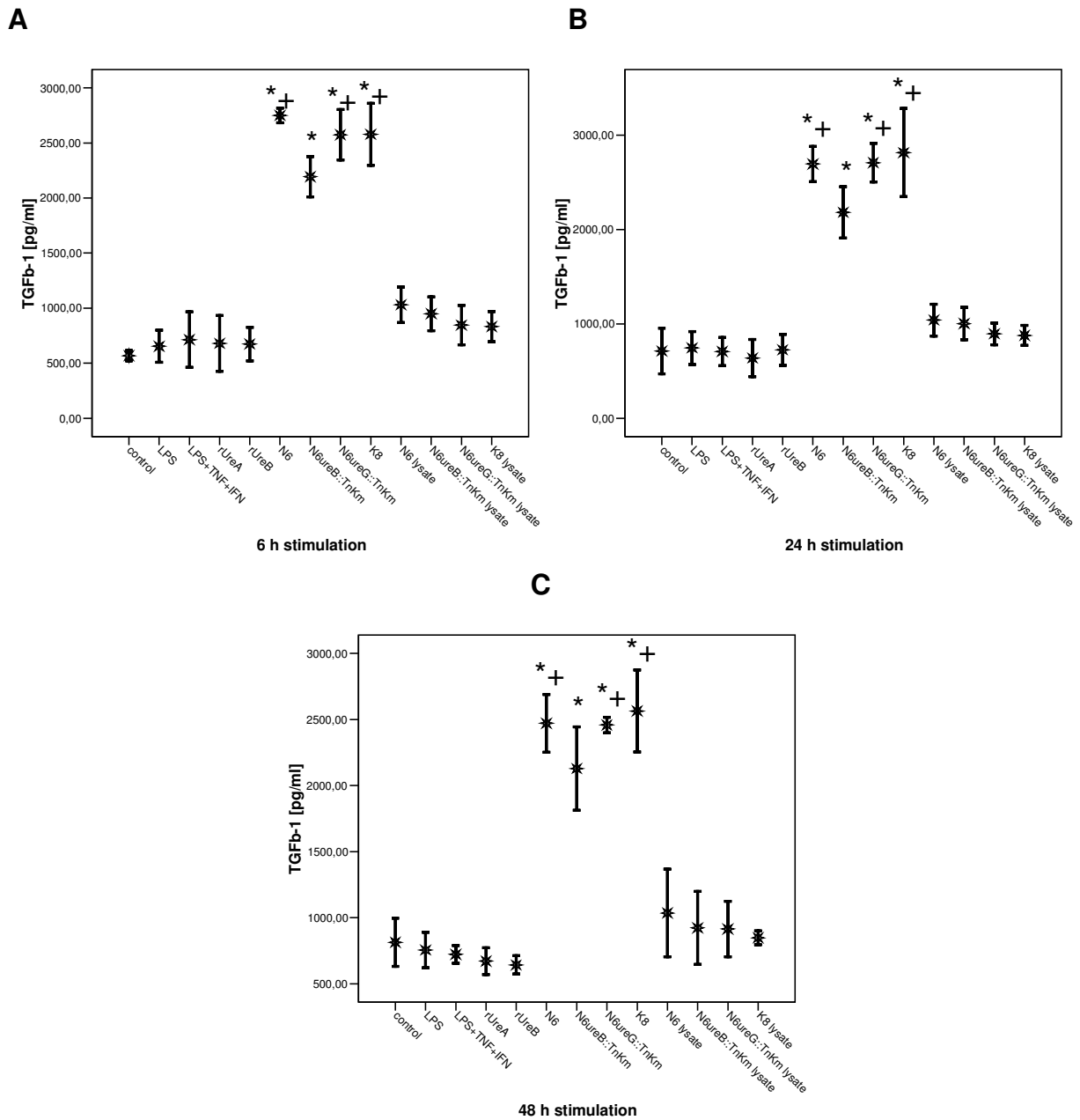


Figure 61 TGF-β1 content of DCs supernatants for 6 h (A), 24 h (B) and 48 h (C) stimulation. Data show mean ± standard deviation *P < 0.001 compared to control +P < 0.05 N6, N6ureG::TnKm, and K8 vs. N6ureB::TnKm; n = 5

7 Discussion

The healing process of peptic ulcer is accomplished by regulating luminal factors like H⁺-ions and pepsin, stimulating growth factors for cell proliferation, and migrating cells from the healing zone for reconstruction of the glandular structure. In addition, the granulation tissue supplies connective tissue and microvessels for the reconstruction process. A number of studies reported that EGF-receptor related peptides like EGF, TGF α , HB-EGF and amphiregulin play pivotal roles in gastrointestinal physiology and pathophysiology like tissue repair and ulcer healing [216]. The predominant effects of these peptides include suppression of gastric acid secretion, gastric cytoprotection, and stimulation of cell proliferation.

Previous studies could clearly demonstrate that *H. pylori* infection results in delayed ulcer healing and is the main cause of ulcer recurrence [217]. Bacterial virulence factors like the *cag* pathogenicity island or the vacuolating cytotoxin VacA have been associated with antiproliferative effects and apoptosis of gastric epithelial cells, ulcer disease, delay of ulcer healing and ulcer recurrence [218], [219]. On the other hand, Romano et al. [220] showed an effect of *H. pylori* on proliferation of gastric epithelial cells by a mechanism related to the expression of HB-EGF and amphiregulin.

In the present study, it has been shown that *H. pylori* urease specifically and in a statistically significant manner induces the expression of HB-EGF at the transcriptional level (Figure 43). Moreover, the fact that the HB-EGF polyA⁺-RNA concentration in samples obtained from cells stimulated with N6ureB::TnKm was similar to that in uninfected cells (Figure 43) indicates that urease may be the main bacterial factor responsible for HB-EGF expression during *H. pylori* infection. The fact that HB-EGF polyA⁺-RNA was also elevated in cells stimulated with purified urease (Figure 44) suggests that the protein must not necessarily be associated to the bacterial surface to exhibit such effects.

Induction of HB-EGF due to *H. pylori* urease was also confirmed at the protein level as shown in Figure 45 and Figure 46. Since values obtained with N6ureG::TnKm were similar to those obtained with wild-type N6 – and considerably higher than those

obtained with N6*ureB*::TnKm at both the transcriptional and the translational level – the enzymatic activity of the urease only seems to play a minor role with regard to HB-EGF expression. At the functional level, using a cell proliferation assay, both *H. pylori* associated as well as purified urease enhanced Kato III cell proliferation in a statistically significant manner (Figure 49). With this assay, values obtained with N6*ureG*::TnKm also showed only minor differences to those obtained with the wild-type.

Cell proliferation is one of the key cellular functions regulated at least in part by MAP kinase signaling. Three main groups of MAP kinases have been characterized to date: the extracellular signal-regulated kinases (ERK) 1/2 also known as p44/p42, the isoforms p54/p46 of the c-Jun N-terminal kinases (JNK), and the p38 MAP kinase [221], [222], [223]. These MAP kinase subfamilies form three parallel cascades that can be activated simultaneously or independently. ERK MAP kinases are strongly activated by growth factors; in contrast, JNK and p38 MAP kinases are mainly stimulated by inflammatory cytokines and stress stimuli, but show only minimal activation by growth factors. In this study, using Western blot analysis, *H. pylori* urease - both bacterial surface-associated and purified – was shown to induce phosphorylation (activation) of p44/p42 (Figure 48), but not of p54/p46 or p38 MAP kinases (data not shown).

The role of MAP kinases was also confirmed by the use of PD98059 and U0126, which are specific inhibitors of MEK, the kinase that catalyzes p44/p42 phosphorylation, and of SB203580, a selective p38 MAP kinase inhibitor. Unfortunately, no specific inhibitor for p54/p46 was available. As shown by real time RT-PCR, in the presence of PD98059 and U0126, HB-EGF gene expression due to *H. pylori* urease was completely inhibited, while SB203580 did not affect the effect of the urease.

After 1 h of stimulation, *H. pylori* urease was found to induce both selective activation of p44/p42 MAP kinases and HB-EGF gene expression, the latter being inhibited by specific p44/p42 inhibitors; therefore, it is reasonable to assume that the ERK MAP kinases cascade is required for HB-EGF induction through *H. pylori* urease. This is consistent with a recent report [224] suggesting that activation of p44/p42 MAP kinases is responsible for HB-EGF gene induction in wounded cell cultures. In addition, urease induced cell proliferation was completely abolished in the presence of the p44/p42

inhibitors providing additional evidence that this effect of the urease is due to activation of p44/p42 resulting in HB-EGF gene expression and release. Because HB-EGF potentially activates cell migration as well as cell proliferation [225], [226], this factor could provide a dual stimulus for the key events of epithelial repair, since growth factors being normally delivered to deeper wounds might not be readily available in the absence of vascular involvement. In such a setting, the local induction of HB-EGF expression within the damaged epithelium could be of particular importance [227].

With respect to the type of the host immune response to *H. pylori*, a predominantly Th1 response, characterized by high IFN γ , TNF α , and IL-12 production, has been reported [228], [229], [230]. In a more recent study, however, the authors showed that the Th1 immune response associates with peptic ulcer, whereas in uncomplicated gastritis secretion to almost the same extent of both Th1- and Th2-type cytokines was found [231]. Furthermore, some studies suggest that a Th2 response to *H. pylori* infection leads to a less severe inflammation or even protects against a persistent infection [232], [233], [234].

In the present study, the possible influence of *H. pylori* urease on the type of immune response (Th1/Th2) was investigated by stimulation of PBMCs followed by incubation over a longer period of time in order to induce Th1- or Th2-type specific T cell clones and allow their proliferation. After restimulation of PBMCs, detection of IFN γ , IL-4, or IL-10 producing T cells should then be indicative for the type of T cells, which has been activated in association with urease. Intracellular cytokine production could sufficiently be detected by flow cytometry only through additional activation by PMA/Ionomycin. In this setting, values for IL-10 were at basal levels irrespective of the stimulus. Interestingly, values for IFN γ and IL-4 were considerably lower in samples stimulated with the anti-CD3/anti-CD28 (positive control) or live bacteria than in the untreated negative control sample or those treated with other stimuli (Figure 51). This suggests that live bacteria and of course the positive control represent stronger stimuli, which may have caused desensitization of cells upon the first stimulation. If this assumption should be correct, rUreA and rUreB as well as bacterial lysates would represent only weak

stimuli. Furthermore, results obtained with strains producing urease did not differ considerably from those obtained with the isogenic mutant strains.

Analysis of the cytokine content of the supernatants by ELISA confirmed to a large extent flow cytometric findings. Negative control samples revealed cytokine levels higher than those of all other samples, which was of statistical significance in case of IL-10 (Figure 52). The urease negative mutant N6*ureB*::TnKm induced significantly lower levels of IL-10 than the parental strain N6 or K8, a isogenic clone producing similar amounts of urease as N6 (Figure 36, Figure 37 and Table 4), which according to the above assumption suggests that the mutant may be a stronger stimulus for cytokine production than urease producing strains.

In the following, dendritic cells (DCs), which are the key link between innate and adaptive immunity, were stimulated in order to investigate whether *H. pylori* urease may to some extent influence adaptive immunity by affecting cytokine production of DCs. As mentioned already, certain features of DCs, including their presence at sites of antigen entry and their ability to migrate from peripheral sites to secondary lymphoid organs, their ability to stimulate naive T cells, and to drive Th1/Th2 polarisation, and Treg induction, illustrate their pivotal role in the generation of adaptive immune responses [235]. Since cytokine release by dendritic cells also depends on their status of maturation, the effect of urease on maturation of monocyte derived dendritic cells was also investigated.

H. pylori both live bacteria and bacterial lysates induced within 48 h strong maturation of immature DCs, which was comparable to that induced by LPS (Figure 55). Preliminary experiments revealed that stimulation periods longer than 48 h did not alter the maturation status of DCs any more, as shown via monitoring of cell surface expression of CD83, CD86, and mannose receptor (data not shown). Presence or absence of urease on bacterial cells did not show to play a role in the expression of CD83 and CD86, although recombinant proteins rUreA and rUreB were capable themselves to cause similar levels of expression of these surface markers as bacteria or LPS. However, with respect to mannose receptor loss as sign of maturation, in contrast to

other stimuli including N6, N6*ureB*::TnKm caused receptor loss as soon as within 6 h of stimulation.

Screening of cytokine production by DCs using pooled samples, revealed differences due to the urease by IL-10, IL-12, MCP-1, and MIP-1 β , which were confirmed during subsequent testing of the corresponding individual samples for the purpose of statistical analysis (Figure 56).

After 48 h of stimulation when maturation of DCs was completed, in contrast to live N6*ureB*::TnKm live N6 induced IL-10 and IL-12 levels, which were statistically significantly higher than those of the negative control (Figure 57 and Figure 58). This effect was more prominent in case of MCP-1, where values obtained with N6*ureB*::TnKm were barely higher than those of untreated cells. Most importantly, rUreA and rUreB (2.5 μ g/ml each) showed MCP-1 values which were similar if not higher than those obtained with 100 ng/ml LPS (Figure 56 and Figure 59), a concentration, which was 10-times higher than the one needed to induce complete activation of DCs within 48 h as shown in preliminary experiments (data not shown).

LPS was shown to be a strong stimulus for IL-12 but not for IL-10 secretion (Figure 56, Figure 57 and Figure 58). In contrast, *H. pylori* induced only low levels of IL-12 but high levels of IL-10 as compared to LPS. This finding suggests that the interaction of *H. pylori* with DCs may induce polarization towards Th2 immune response and, furthermore, Tr1 regulatory T cell clones. This would result in immune tolerance towards *H. pylori* and persistence of the infection.

Induction of MCP-1 release by urease (rUreA, rUreB, N6 and K8 vs. N6*ureB*::TnKm; (Figure 59) may also be of importance, since MCP-1 is a chemokine signaling through CCR2, which is expressed on activated and memory T cells, and act to promote Th2 effector cell development. This is characterized by reduction of IL-12 production by antigen presenting cells and enhancement of IL-4 /IL-10 production by activated T cells [244]. On the other hand, the presence of urease affected to some extent release of MIP-1 β , since values obtained with the urease lacking mutant were considerably higher than those obtained with the urease producing isogenic strains N6 and K8 (Figure 60). Considering the fact, that the chemokine MIP-1 β signals through CCR5, which is

expressed on Th1 cells [236], again this finding suggests that urease may promote Th2 immune response. Data shown in Figure 59 suggests that the enzymatic activity of the urease may play a role with respect to MCP-1 release, since values obtained with N6ureB::TnKm were similar to those obtained with N6ureG::TnKm. In contrast, enzymatic activity seems to be of minor importance with respect to MIP-1 β production (Figure 60).

The fact, that intact *H. pylori* bacteria induce significant amounts of TGF- β 1 may be of crucial importance. Furthermore, surface-associated urease was shown to influence TGF- β 1 production, since strains producing the protein delivered statistically significantly higher values than those obtained with the urease lacking isogenic mutant, whereas the recombinant urease proteins did not show any effect (Figure 61). As mentioned in the section Introduction, TGF- β 1 which in the stomach is produced by parietal and neck cells, but not by epithelial cells, is a multifocal peptide growth factor. It has a special role in gastrointestinal mucosal healing as it stimulates fibroblasts, induces cell migration, angiogenesis, and enhances cellular matrix production. Furthermore, TGF- β 1 downregulates the tissue damaging Th1 response amongst others through the induction of CD4⁺CD25^{high} regulatory T cells [237], [238].

Thus, on the one hand *H. pylori* virulence factors like VacA were shown to cause gastric epithelial cell damage and apoptosis [239]. On the other hand, this data clearly demonstrate a significant effect of urease in the induction of HB-EGF expression, possibly via the p44/p42 pathway, resulting in a considerable increase of epithelial cell proliferation in-vitro. Furthermore, urease may at least to some extent influence the release of key cytokines and chemokines by dendritic cells such as IL-10, MCP-1, and MIP-1 β , which may favor the Th2 immune response in the in-vivo situation. In addition, the possible role of urease in the induction of TGF- β 1 by dendritic cells together with its importance in HB-EGF expression by epithelial cells may be of particular interest in terms of ulcer healing.

Although these findings seem to be controversial on first sight, they may not be surprising for a microorganism which causes an infection being characterized by its high prevalence, chronicity of carriage, lifelong persistence and generally low level of disease

[240]. All of these phenomena are markers for a relatively benign co-existence of *H. pylori* with its host, and *H. pylori* associated diseases have been described as accidents of bacterial persistence [241]. Thus, *H. pylori* urease may, at least in part, counteract the apoptotic, and Th1-related tissue damaging effects of other bacterial factors, and the extent of urease production of clinical isolates may influence the course of the infection. In that context, in order for *H. pylori* to adapt to changing host conditions, it would not be surprising if – apart from alterations at the genomic level – the expression of bacterial factors like urease is regulated at the transcriptional or the translational level in response to pathophysiological changes.

8 References

- 1 Konno M, Fujii N, Yokota S, Sato K, Takahashi M, Sato K, Mino E, Sugiyama T. Five-year follow-up study of mother-to-child transmission of *Helicobacter pylori* infection detected by a random amplified polymorphic DNA fingerprinting method. *J Clin Microbiol.* 2005 May;43(5):2246-50.
- 2 Buckolm G, Tannaes T, Nederrskov P, et al. Colony variation of *Helicobacter pylori*: pathogenic potential is correlated to cell wall lipid composition. *Scand J Gastroenterol Immunol*, 1997; 32: 445-54.
- 3 Cellini L, Allocati N, Di Campli E, Dainelli B. *Helicobacter pylori*: a fickle germ. *Microbiol Immunol* 1994; 38: 25-30).
- 4 Fawcett PT, Gibney KM, Vinette KM. *Helicobacter pylori* can be induced to assume the morphology of *Helicobacter heilmannii*. *J Clin Microbiol* 1999; 37: 1045-8.
- 5 Akopyanz N, Bukanov NO, Westblom TU, Kresovich S, Berg DE. DNA diversity among clinical isolates of *Helicobacter pylori* detected by PCR-based RAPD fingerprinting. *Nucleic Acids Res* 1992;20; 5137-42
- 6 Alm RA, Trust TJ. Analysis of the genetic diversity of *Helicobacter pylori*: the tale of two genomes. *J Mol Med* 1999; 77: 834-46
- 7 Ge Z Taylor DE. Contributions of genome sequencing to understanding the biology of *Helicobacter pylori*. *Annu Rev Microbiol* 1999; 53: 353-87
- 8 Jie Wang¹, David S. Chi¹, John J. Laffan², Chuanfu Li³, Donald A. Ferguson Jr², Peter Litchfield² and Eapen Thomas¹ Comparison of Cytotoxin Genotypes of *Helicobacter pylori* in Stomach and Saliva. *Annu. Rev. Microbiol.*, 1999 vol. 53, p. 353-387,
- 9 Buck GE, *Campylobacter pylori* and gastroduodenal disease. *Clin Microbiol Rev* 1990; 3: 1-12
- 10 Forbes KJ, Fang Z, Pennington TH. Allelic variation in the *Helicobacter pylori* flagellin genes *flaA* and *flab*: its consequences for strain typing schemes and population structure. *Epidemiol Infect* 1995; 114: 257-66
- 11 Evans DJ,Jr, Evans DJ, Engstrand L, Graham DY. Urease-associated heat shock protein of *Helicobacter pylori*. *Infect Immun* 1992; 60: 2125-7
- 12 Evans DG, Queiroz DM, Mendes EN, Svennerholm AM, Evans DJ, Jr. Differences among *Helicobacter pylori* strains isolated from three different populations and demonstrated by restriction enzyme analysis of an internal fragment of the conserved gene *hpaA*. *Helicobacter* 1999; 4: 82-8
- 13 Satin B, Del Giudice G, Della Bianca V, et al. The neutrophil-activating protein (HP-NAP) of *Helicobacter pylori* is a protective antigen and a major virulence factor. *J Exp med* 2000; 191: 1467-76
- 14 O'Toole PW, Logan SM, Kostrzynska M, Wadstrom T, Trust TJ. Isolation and biochemical and molecular analyses of a species-specific protein antigen from the gastric pathogen *Helicobacter pylori*. *J. Bacteriol* 1991; 173: 505-13

References

- 15 Lundström Am, Bölin I. A 26 kDa protein of *Helicobacter pylori* shows alkyl hydroperoxide reductase (AhpC) activity and the mono-cistronic transcription of the gene is affected by pH. *Microb Pathog* 2000; 29: 257-66
- 16 Evans DG, Evans DJ, Jr, Moulds JJ, Graham DY. N-acetylneuraminyllactose-binding fibrillar hemagglutinin of *Campylobacter pylori*: a putative colonization factor antigen. *Infect Immunol* 1988; 56: 2896-906
- 17 Kuipers EJ., et al. Long-term sequelae of *Helicobacter pylori* gastritis. *Lancet*, 1995. 345: 1525-1528.
- 18 Yamaji Y. et al. Inverse background of *Helicobacter pylori* antibody and pepsinogen in reflux oesophagitis compared with gastric cancer: analysis of 5732 Japanese subjects. *Gut*, 2001. 49: 335-340.
- 19 Koike T., *Helicobacter pylori* infection prevents erosive reflux oesophagitis by decreasing gastric acid secretion. *Gut*, 2001. 49: 330-334.
- 20 El-Omar E. et al. Interleukin-1 polymorphisms associated with increased risk of gastric cancer. *Nature*, 2000. 404: 398-402.
- 21 Beales IL and Calam. Interleukin 1 beta and tumor necrosis factor alpha inhibit acid secretion in cultured rabbit parietal cells by multiple pathways. *Gut*. 1998, 42: 227-234.
- 22 Podolsky DK. Mucosal immunity and inflammation. V. Innate mechanisms of mucosal defense and repair: the best offense is a good defense. *Am J Physiol*. 1999 Sep;277(3 Pt 1):G495-9.
- 23 Jones MK, Tomikawa M, Mohajer B, Tarnawski AS. Gastrointestinal mucosal regeneration: role of growth factors. *Front Biosci*. 1999 Mar 15;4:D303-9.
- 24 Tarnawski AS. Cellular and molecular mechanisms of gastrointestinal ulcer healing. *Dig Dis Sci*. 2005 Oct;50 Suppl 1:S24-33.
- 25 Podolsky DK. Healing the epithelium: solving the problem from two sides. *J Gastroenterol*. 1997 Feb;32(1):122-6.
- 26 Monteleone G, DeIvecchio Blanco G, Palmieri G, Vavassori P, Monteleone I, Colantoni A, Battista S, Spagnoli LG, Romano M, Borrelli M, MacDonald TT, Pallone F. Induction and regulation of Smad7 in the gastric mucosa of patients with *Helicobacter pylori* infection. *Gastroenterology*, 2004, march (126);3:674-682.
- 27 Roberts AB, Lamb LC, Newton DL, et al. Transforming growth factors: isolation of polypeptides from virally and chemically transformed cells by acid/ethanol extraction. *Proc Natl Acad Sci USA*, 1980;77:3494—3498.
- 28 Massague J. The transforming growth factor-beta family. *Annu Rev Cell Biol*. 1990;6:597-641.
- 29 Naef M, Ishiwata T, Friess H, Buchler MW, Gold LI, Korc M. Differential localization of transforming growth factor-beta isoforms in human gastric mucosa and overexpression in gastric carcinoma. *Int J Cancer*. 1997;71:131-137.
- 30 Mizoi T, Ohtani H, Miyazono K, Miyazawa M, Matsuno S, Nagura H. Immunoelectron microscopic localization of transforming growth factor beta 1 and latent transforming growth factor beta 1 binding protein in human gastrointestinal

References

- carcinomas: qualitative difference between cancer cells and stromal cells. *Cancer Res.* 1993;53:183-190.
- 31 Tanigawa T, Pai R, Arakawa T, Higuchi K, Tarnawski A.S. TGF- β signaling pathway: its role in gastrointestinal Pathophysiology and modulation of ulcer healing. *J. Pathophys and Pharmacol.* 2005; 56(1):3-13
- 32 Bulus N, Barnard JA. Heparin binding epidermal growth factor-like growth factor is a transforming growth factor beta-regulated gene in intestinal epithelial cells. *Biochem Biophys Res Commun.* 1999 Nov 2;264(3):808-12.
- 33 Higashiyama S., Lau K., Besner GE., Abraham JA., Klagsbrun M., Structure of heparin-binding EGF-like growth factor: Multiple forms, primary structure, and glycosylation of the mature protein. *J Biochem* 1992;267:6205-6212.
- 34 Murayma Y., Miyagawa JI., Higashiyama S., Kondo M., yabu K., Isozaki Y., Kayanoki S., Kanayama Y., Shinomura N., Tnguchi Y., Matsuzawa Y. Localisation of Heparin-binding epidermal growth factor-like growth factor in human gastric mucosa. *Gastroenterol* 1995;109:1051-1059.
- 35 Romano M, Ricci V, DiPopolo A, Sommi P, DelVecchio Blanco C, Bruni CB, Ventura F, Cover TL, Mlaser M, Cofey RJ, Zarrilli R. Helicobacter pylori upregulates expression of epidermal growth factor-related peptides, but inhibits their proliferative effect in MKN 28 gastric mucosal cells. *J Clin Invest* 1998;101:1604-1613.
- 36 Schreeiber S, Bucker R, Groll C, Azevedo-Vethacke M, Garten D, Scheid P, Friedrich S, Gatermann S, Josenhaus C, Suerbaum S. Rapid loss of motility of Helicobacter pylori in the gastric lumen in vivo. *Infect Immun* 2005 Mar, 73(3):1584-9.
- 37 Kirschner DE and Blaser MJ. The dynamics of Helicobacter pylori infection of the human stomach. *J. Theor. Biol.* 176 (1995), pp. 281–290
- 38 Meisser M, Lowe G, Berg HC. The proton flux through the bacterial flagellar motor. *Cell* 1987. Jun 5;49(5):643-50.
- 39 Minamino T, Imae Y, Oosawa F, Kobayashi Y, Oosana K. Effect of intracellular pH on rotation speed of bacterial flagellar motors. *J. Bacteriol* 2003 Feb, 185 (4):1190-4.
- 40 Czajkowsky DM, Iwamoto H, Cover TL, Shao Z (1999) The vacuolating toxin from Helicobacter pylori forms hexameric pores in lipid bilayers at low pH. *Proc Natl Acad Sci USA* 1999, 96:2001-2006; Iwamoto et al 1999
- 41 Szabo I, Brutsche S, Tombola F, Moschiono M, Satin B, Telford JL, Rappuoli R, Montecucco C, Papini E et al. Formation of anion-selective channels in the cell plasma membrane by the toxin VacA of Helicobacter pylori is required for its biological activity. *EMBO J.*1999,18:5517-5527.
- 42 Iwamoto H, Czajkowsky DM, Cover TL, Szabo G, shao Z. VacA from Helicobacter pylori: a hexameric chloride channel. *FEBS LETT* 1999, 450:101-104.
- 44 Vinion-Dubiel AD, McClain MS, Czajkowsky DM, Iwamoto H, Ye D, Cao P, Schraw W, Szabo G. Blanke Sr. et al. A dominant negative mutant of

References

- Helicobacter pylori Vacuolating toxin (VacA) inhibits VacA-induced cell vacuolation. *J Biol Chem* 2003, 274:37736-37742.
- 45 Amieva MR, Salama NR, Tompkins LS, Falkow S. Helicobacter pylori enter and survive within multivesicular vacuoles of epithelial cells. *Cell Microbiol* 2002, 4:677-690.
- 46 Zheng PY and Jones NL. Helicobacter pylori strains expressing the Vacuolating cytotoxin interrupt phagosome maturation in macrophages by recruiting and retaining TACO (coronin 1) protein. *Cell Microbiol* 2003, 5:25-40.
- 47 Odenbreit S, et al. Translocation of Helicobacter pylori CagA into gastric epithelial cells by type IV secretion. *Science*, 2000. 287:1497-1500.
- 48 Selbach M, Moese S, Hauck CR, Meyer TF, and Backert S. Src kinase of Helicobacter pylori CagA protein in vitro and in vivo. *J. Biol. Chem.* 2002, 277:6775-6778,
- 49 Perez-Perez GI, et al. Evidence that cagA+ Helicobacter pylori strains are disappearing more rapidly than cagA- strains. *Gut*, 2002; 50:295-298.
- 50 Guillemin K, Salama N, Tompkins L, and Falkow S. CagA pathogenicity island-specific responses of gastric epithelial cells to Helicobacter pylori infection. *Proc. Natl. Acad. Sci. U.S.A.* 2002; 99:15136-15141.
- 51 Mimuro H, et al. Grb2 is a key mediator of Helicobacter pylori CagA protein activities. *Mol. Cell.* 2002;10:745-775.
- 52 Tsutsumi R., Higashi H, Higuchi M, Okada M, and Hatakeyama M. Attenuation of Helicobacter pylori CagA x SHP-2 signaling by interaction between CagA and C-terminal Src kinase. *J. Biol. Chem.* 2003; 278:3664-3670
- 53 Selbach M et al. The Helicobacter pylori CagA protein induces cortactin dephosphorylation and actin rearrangement by c-Src inactivation. *EMBO J.*2003;22:515-528.
- 54 Atherton J et al Mosaicism in vacuolating cytotoxin alleles of Helicobacter pylori: association of specific vacA types with cytotoxin production and peptic ulceration. *J. Biol. Chem.* 1995; 270:17771-17777.
- 55 Weel, J. F., R. W. van der Hulst, Y. Gerrits, P. Roorda, M. Feller, J. Dankert, G. N. Tytgat, and A. van der Ende. 1996. The interrelationship between cytotoxin-associated gene A, vacuolating cytotoxin, and Helicobacter pylori-related diseases. *J. Infect. Dis.* 173:1171-1175.
- 56 Cover T.L. The vacuolating cytotoxin of Helicobacter pylori. *Mol. Microbiol* 1996, 20; 241-246.
- 57 Mahdavi J, Sondeń B, Hurtig M, Olfat FO, Forsberg L, Roche N, Ångstrońm J, Larsson T, Teneberg S, Anders Karlsson K, Altraja S, Wadstrońm T, Kersulyte. Berg D.E, Dubois A, Petersson C, Magnusson KE, Norberg T, Lindh F, Lundskog BB, Arnqvist A, Hammarstrońm L, Boreń T. Helicobacter pylori SabA Adhesin in Persistent Infection and Chronic Inflammation, *Scand. J. Gastroenterol.* 24, 581 (1989).

References

- 58 Clausen H, Hakomori S. I. ABH and related histo-blood group antigens; immunochemical differences in carrier isotypes and their distribution *Vox Sang.* 1989, 1:56, 1-20.
- 59 Sakamoto J S, Watanabe T, Tokumaru T, Takagi H, Nakazato H, Lloyd KO. Expression of Lewisa, Lewisb, Lewisx, Lewisy, sialyl-Lewisa, and sialyl-Lewisx blood group antigens in human gastric carcinoma and in normal gastric tissue. *Cancer Res* 1989. 49; 745.
- 60 Boren T, Falk P, Roth KA, Larson G, Normark S. Attachment of *Helicobacter pylori* to human gastric epithelium mediated by blood group antigens. *Science* 1993, 262; 1892.
- 61 Hakomori S. I., in *Gangliosides and Cancer*, H. F. Oettgen, Ed. (VCH Publishers, New York, 1989), pp. 58–68.
- 62 Madrid JF, Ballesta J, Castells MT, Hernandez F. Glycoconjugate distribution in the human fundic mucosa revealed by lectin- and glycoprotein-gold cytochemistry. *Histochemistry* 1990, 95, 179-187.
- 63 Alper J. Searching for Medicine's Sweet Spot, *Science* 2001 291:2338-2343.
- 64 Falk P, Roth KA, Boren T, Westblom TU, Gordon JI, Normark S. An in vitro adherence assay reveals that *Helicobacter pylori* exhibits cell lineage-specific tropism in the human gastric epithelium. *Proc. Natl. Acad. Sci. U.S.A.* 1993, 90, 2035-2039.
- 65 Karlsson KA. Meaning and therapeutic potential of microbial recognition of host glycoconjugates. *Mol Microbiol.* 1998 Jul;29(1):1-11.
- 66 Odenbreit S., Till M., Hofreuter D., Faller G. and Haas R. Genetic and functional characterization of the *alpAB* gene locus essential for the adhesion of *Helicobacter pylori* to human gastric tissue. *Mol. Microbiol* 1999, 31:1637-48.
- 67 Odenbreit S. Adherence properties of *Helicobacter pylori*: impact on pathogenesis and adaptation to the host. *Int J Med Microbiol.* 2005 Sep;295 (5):317-24
- 68 Tsuda M, Karita M, Morshed MG, Okita K, Nakazawa T. A urease-negative mutant of *Helicobacter pylori* constructed by allelic exchange mutagenesis lacks the ability to colonize the nude mouse stomach. *Infect Immun* 1994; 62:3586-9.
- 69 Eaton KA, Krakowka S. Effect of gastric pH on urease-dependent colonization of gnotobiotic piglets by *Helicobacter pylori*. *Infect Immun* 1994; 62:3604-7.
- 70 Peek RM, Jr., Miller GG, Tham KT, Perez Perez GI, Cover TL, Atherton JC, Dunn GD, Blaser MJ. Detection of *Helicobacter pylori* gene expression in human gastric mucosa. *J Clin Microbiol* 1995; 33:28-32.
- 71 Harris PR, Mobley HL, Perez Perez GI, Blaser MJ, Smith PD. *Helicobacter pylori* urease is a potent stimulus of mononuclear phagocyte activation and inflammatory cytokine production. *Gastroenterology* 1996; 111:419-25.
- 72 Harris PR, Ernst PB, Kawabata S, Kiyono H, Graham MF, Smith PD. Recombinant *Helicobacter pylori* urease activates primary mucosal macrophages. *J Infect Dis* 1998; 178:1516-20.
- 73 Mobley HL. The role of *Helicobacter pylori* urease in the pathogenesis of gastritis and peptic ulceration. *Aliment Pharmacol Ther* 1996; 10 Suppl 1:57-64.

References

- 74 Smoot DT, Mobley HL, Chippendale GR, Lewison JF, Resau JH. Helicobacter pylori urease activity is toxic to human gastric epithelial cells. *Infect Immun* 1990; 58:1992-4.
- 75 Tsujii M, Kawano S, Tsuji S, Fusamoto H, Kamada T, Sato N. Mechanism of gastric mucosal damage induced by ammonia. *Gastroenterology* 1992; 102:1881-1888.
- 76 Triebling AT, Korsten MA, Dlugosz JW, Paronetto F, Lieber CS. Severity of Helicobacter-induced gastric injury correlates with gastric juice ammonia. *Dig Dis Sci* 1991; 36:1089-96.
- 77 Gladziwa U, Haase G, Handt S, Riehl J, Wietholtz H, Dakshinamurty KV, Glockner WM, Sieberth HG. Prevalence of Helicobacter pylori in patients with chronic renal failure. *Nephrol Dial Transplant* 1993; 8:301-6.
- 78 Cover TL, Puryear W, Perez Perez GI, Blaser MJ. Effect of urease on HeLa cell vacuolation induced by Helicobacter pylori cytotoxin. *Infect Immun* 1991; 59:1264-70.
- 79 Andersen LP, Blom J, Nielsen H. Survival and ultrastructural changes of Helicobacter pylori after phagocytosis by human polymorphonuclear leukocytes and monocytes. *APMIS* 1993; 101:61-72.
- 80 Kist M, Spiegelhalder C, Moriki T, Schaefer HE. Interaction of Helicobacter pylori (strain 151) and Campylobacter coli with human peripheral polymorphonuclear granulocytes. *Int J Med Microbiol Virol Parasitol Infect Dis* 1993; 280:58-72.
- 81 Williams CL, Preston T, Hossack M, Slater C, McColl KE. Helicobacter pylori utilises urea for amino acid synthesis. *FEMS Immunol Med Microbiol* 1996; 13:87-94
- 82 Nakamura H, Yoshiyama H, Takeuchi H, Mizote T, Okita K, Nakazawa T. Urease plays an important role in the chemotactic motility of Helicobacter pylori in a viscous environment. *Infect Immun* 1998; 66:4832-7.
- 83 Makristhatis A, Rokita E, Labigne A, Willinger B, Rotter ML, Hirschl AM. Highly significant role of Helicobacter pylori urease in phagocytosis and production of oxygen metabolites by human granulocytes. *J Infect Dis* 1998;177:803-806.
- 84 Rokita E, Makristhatis A, Presterl E, Rotter ML, Hirschl AM. Helicobacter pylori urease significantly reduces opsonisation by human complement. *J Infect Dis* 1998; 178:1521-1525.
- 85 Clyne, M, Labigne A, and Drumm B. Helicobacter pylori requires an acidic environment to survive in the presence of urea. *Infect Immun* 1995, 63: 1669-1673.
- 86 Akada JK, Shirai M, Takeuchi H, Nakazawa T. Transcriptional analysis of urease accessory genes of Helicobacter pylori. *Gut* 1999; 45:A19.
- 87 Bauerfeind P, Garner R, Dunn BE, Mobley HL. Synthesis and activity of Helicobacter pylori urease and catalase at low pH. *Gut* 1997; 40:25-30.
- 88 Mobley HL, Island MD, Hausinger RP. Molecular biology of microbial ureases. *Microbiol Rev* 1995; 59:451-80

References

- 89 Brayman, TG, and Hausinger RP. Purification, characterization, and functional analysis of a truncated *Klebsiella aerogenes* UreE urease accessory protein lacking the histidine-rich carboxyl terminus. *J Bacteriol* 178: 5410-5416, 1996
- 90 Moncrief, MB, and Hausinger RP. Purification and activation properties of UreD-UreF-urease apoprotein complexes. *J Bacteriol* 1996 178: 5417-5421.
- 91 Mulrooney, SB, and Hausinger RP. Sequence of the *Klebsiella aerogenes* urease genes and evidence for accessory proteins facilitating nickel incorporation. *J Bacteriol* 1990, 172: 5837-5843.
- 92 Park, IS, Carr MB, and Hausinger RP. In vitro activation of urease apoprotein and role of UreD as a chaperone required for nickel metallocenter assembly. *Proc Natl Acad Sci USA* 1994, 91: 3233-3237.
- 93 Park, IS, and Hausinger RP. Evidence for the presence of urease apoprotein complexes containing UreD, UreF, and UreG in cells that are competent for in vivo enzyme activation. *J Bacteriol* 1995, 177: 1947-1951.
- 94 Skouloubris S, Thiberge JM, Labigne A, De Reuse H. The *Helicobacter pylori* Urel protein is not involved in urease activity but is essential for bacterial survival in vivo. *Infect Immun* 1998; 66:4517-21.
- 95 Chebrou H, Bigey F, Arnaud A, Galzy P. Study of the amidase signature group. *Biochim Biophys Acta*. 1996 Dec 5;1298(2):285-93.
- 96 Weeks, DL, Eskandari S, Scott DR, and Sachs G. A H⁺-gated urea channel: the link between *Helicobacter pylori* urease and gastric colonization. *Science* 2000, 287: 482-485.
- 97 Athmann, C, Zeng N, Kang T, Marcus EA, Scott DR, Rektorschek M, Buhmann A, Melchers K, and Sachs G. Local pH elevation mediated by the intrabacterial urease of *Helicobacter pylori* cocultured with gastric cells. *J Clin Invest* 2000, 106: 339-347.
- 98 Scott, DR, Marcus EA, Weeks DL, Lee A, Melchers K, and Sachs G. Expression of the *Helicobacter pylori* urel gene is required for acidic pH activation of cytoplasmic urease. *Infect Immun* 2000, 68: 470-477,
- 99 Skouloubris, S, Thiberge JM, Labigne A, and De Reuse H. The *Helicobacter pylori* Urel protein is not involved in urease activity but is essential for bacterial survival in vivo. *Infect Immun* 1998, 66: 4517-4521.
- 100 Clyne, M, Labigne A, and Drumm B. *Helicobacter pylori* requires an acidic environment to survive in the presence of urea. *Infect Immun* 1995, 63: 1669-1673.
- 101 Eaton, KA, and Krakowka S. Effect of gastric pH on urease-dependent colonization of gnotobiotic piglets by *Helicobacter pylori*. *Infect Immun* 1994, 62: 3604-3607.
- 102 Eaton, KA, Brooks CL, Morgan DR, and Krakowka S. Essential role of urease in pathogenesis of gastritis induced by *Helicobacter pylori* in gnotobiotic piglets. *Infect Immun* 1991, 59: 2470-2475.

References

- 103 Mollenhauer-Rektorschek M, Hanauer G, Sachs G, Melchers K. Expression of Urel is required for intragastric transit and colonization of gerbil gastric mucosa by *Helicobacter pylori*. *Res Microbiol.* 2002 Dec;153(10):659-66.
- 104 Marshall, BJ, Barrett LJ, Prakash C, McCallum RW, and Guerrant RL. Urea protects *Helicobacter* (*Campylobacter*) *pylori* from the bactericidal effect of acid. *Gastroenterology* 1990, 99: 697-702.
- 105 Tsuda, M, Karita M, Mizote T, Morshed MG, Okita K, and Nakazawa T. Essential role of *Helicobacter pylori* urease in gastric colonization: definite proof using a urease-negative mutant constructed by gene replacement. *Eur J Gastroenterol Hepatol* 6 Suppl1: S49-S52, 1994, 36
- 106 Tsuda, M, Karita M, Morshed MG, Okita K, and Nakazawa T. A urease-negative mutant of *Helicobacter pylori* constructed by allelic exchange mutagenesis lacks the ability to colonize the nude mouse stomach. *Infect Immun* 1994, 62: 3586-3589.
- 107 Hu LT, Mobley HL. Purification and N-terminal analysis of urease from *Helicobacter pylori*. *Infect Immun* 1990; 58:992-8.
- 108 Dunn BE, Campbell GP, Perez Perez GI, Blaser MJ. Purification and characterization of urease from *Helicobacter pylori*. *J Biol Chem* 1990; 265:9464-9.
- 109 Evans DJ, Jr., Evans DG, Kirkpatrick SS, Graham DY. Characterization of the *Helicobacter pylori* urease and purification of its subunits. *Microb Pathog* 1991; 10:15-26
- 110 Austin JW, Doig P, Stewart M, Trust TJ. Macromolecular structure and aggregation states of *Helicobacter pylori* urease. *J Bacteriol* 1991; 173:5663-7.
- 111 Heimer, SR, and Mobley HL. Interaction of *Proteus mirabilis* urease apoenzyme and accessory proteins identified with yeast two-hybrid technology. *J Bacteriol* 2001, 183: 1423-1433.
- 112 Bode G, Malfertheiner P, Lehnhardt G, Nilius M and Ditschuneit H, Ultrastructural localization of urease of *Helicobacter pylori*. *Med. Microbiol. Immunol. (Berl.)* 1993, 182: 233–242.
- 113 Mobley HL, Island MD and Hausinger RP, Molecular biology of microbial ureases. *Microbiol. Rev.* 1995, 59: 451–480.
- 114 Dunn BE, Campbell GP, Perez-Perez GI and Blaser MJ, Purification and characterization of urease from *Helicobacter pylori*. *J. Biol. Chem* 1990, 265: 9464–9469.
- 115 Evans DG Jr., Evans DG, Kirkpatrick SS and Graham DY, Characterization of the *Helicobacter pylori* urease and purification of its subunits. *Microb. Pathog.* 1991, 10: 15–26
- 116 Mobley HLT, Ernst PB, Michetti P, Smith PD. *The Immunology of H. pylori: From Pathogenesis to Prevention.* 1st ed Philadelphia: Lippincott-Raven Publishers, 1997:59-74.
- 118 Dunn BE, Phadnis SH. Structure, function and localization of *Helicobacter pylori* urease. *Yale J Biol Med.* 1998 Mar-Apr;71(2):63-73.

References

- 119 Berry AM, Paton JC, Hansman D. Effect of insertional inactivation of the genes encoding pneumolysin and autolysin on the virulence of *Streptococcus pneumoniae* type 3. *Microb Pathog* 1992; 12:87-93.
- 120 Jonsson AB, Nyberg G, Normark S. Phase variation of gonococcal pili by frameshift mutation in *pilC*, a novel gene for pilus assembly. *EMBO J* 1991; 10:477-88.
- 121 Lopez R, Garcia E, Garcia P, Garcia JL. The pneumococcal cell wall degrading enzymes: a modular design to create new lysins? *Microb Drug Resist* 1997; 3:199-211.
- 122 Vanet A, Labigne A. Evidence for specific secretion rather than autolysis in the release of some *Helicobacter pylori* proteins. *Infect Immun* 1998; 66:1023-7.
- 124 Catrenich CE, Makin KM. Characterization of the morphologic conversion of *Helicobacter pylori* from bacillary to coccoid forms. *Scand J Gastroenterol Suppl* 1991; 181:58-64.
- 125 Weeks DL, Eskandari S, Scott DR and Sachs G. A H⁺-gated urea channel: the link between *Helicobacter pylori* urease and gastric colonization. *Science* 2000, 287: 482–485.
- 126 Krishnamurthy P, Parlow M, Zitzer JB, Vakil NB, Mobley HL, Levy M, Phadnis SH, Dunn BE. *Helicobacter pylori* containing only cytoplasmic urease is susceptible to acid. *Infect Immun* 1998; 66:5060-6.
- 127 Machado, J.C. et al. A proinflammatory genetic profile increases the risk for chronic atrophic gastritis and gastric carcinoma. *Gastroenterology*. 2003, 125:364-371.
- 128 El-Omar E. et al. Interleukin-1 polymorphisms associated with increased risk of gastric cancer. *Nature*.2000, 404:398-402
- 129 El-Omar E. et al. Increased risk of noncardia gastric cancer associated with proinflammatory cytokine gene polymorphisms. *Gastroenterology*. 2003, 124:1193-1201
- 130 Lindholm, C., M. Quiding-Jarbrink, H. Lonroth, A. Hamlet, and A. M. Svennerholm. Local cytokine response in *Helicobacter pylori*-infected subjects. *Infect. Immun*. 1998, 66:5964-5971.
- 131 Crowe, S. E., L. Alvarez, M. Dytoc, R. H. Hunt, M. Muller, P. Sherman, J. Patel, Y. Jin, and P. B. Ernst. Expression of interleukin 8 and CD54 by human gastric epithelium after *Helicobacter pylori* infection in vitro. *Gastroenterology* 1995, 108:65-74.
- 132 Huang, J., P. W. O'Toole, P. Doig, and T. J. Trust. Stimulation of interleukin-8 production in epithelial cell lines by *Helicobacter pylori*. *Infect. Immun* 1995, 63:1732-1738.
- 133 Jung, H. C., J. M. Kim, I. S. Song, and C. Y. Kim. *Helicobacter pylori* induces an array of pro-inflammatory cytokines in human gastric epithelial cells: quantification of mRNA for interleukin-8, -1 alpha/beta, granulocyte-macrophage colony-stimulating factor, monocyte chemoattractant protein-1 and tumour necrosis factor-alpha. *J. Gastroenterol. Hepatol* 1997, 12:473-480.

References

- 134 Zhannat Z. Nurgalieva, Margaret E. Conner, Antone R. Opekun, Carl Q. Zheng, Susan N. Elliott, Peter B. Ernst, Michael Osato, Mary K. Estes, and David Y. Graham. B-Cell and T-Cell Immune Responses to Experimental *Helicobacter pylori* Infection in Humans *Infection and Immunity*, May 2005, 73 (5): 2999-3006.
- 135 Kavermann, H., B. P. Burns, K. Angermuller, S. Odenbreit, W. Fischer, K. Melchers, and R. Haas. Identification and characterization of *Helicobacter pylori* genes essential for gastric colonization. *J. Exp. Med.* 2003, 197:813-822.
- 136 Lock, R. A., G. W. Coombs, T. M. McWilliams, J. W. Pearman, W. B. Grubb, G. J. Melrose, and G. M. Forbes. Proteome analysis of highly immunoreactive proteins of *Helicobacter pylori*. *Helicobacter* 2002, 7:175-182.
- 137 E-Rokita, A. Makristathis, E. Presterl, M. Rotter and A.M.Hirschl. *Helicobacter pylori* urease significant reduces opsonization by human complement. *J Infect Dis.* 1998 Nov;178(5):1521-5.
- 138 Kozol R, Donmanowski A, Jaszewski R., Czanko R., McCurdy B., Prasad M., Fromm B., Calzada R. Neutrophil chemotaxis in gastric mucosa. A signal-to response comparison. *Dig Dig Sci* 1991. Sep;36 (9):1277-80.
- 139 Yoshida N., Granger DN, Evans DJ Jr, Evans DG, Graham DY, Anderson DC, Wolf RE, Kviety PR. Mechanisms involved in *Helicobacter pylori*-induced inflammation. *Gastroenterology*, 1993 Nov; 105(5):1431-40.
- 140 Hida, N., T. Shimoyama, Jr., P. Neville, M. F. Dixon, A. T. Axon, T. Sr. Shimoyama, and J. E. Crabtree. Increased expression of IL-10 and IL-12 (p40) mRNA in *Helicobacter pylori* infected gastric mucosa: relation to bacterial cag status and peptic ulceration. *J. Clin. Pathol.* 1999, 52:658-664.
- 141 Lindholm, C., M. Quiding-Jarbrink, H. Lonroth, A. Hamlet, and A.-M. Svennerholm. Local cytokine response in *Helicobacter pylori*-infected subjects. *Infect Immun.* 1998, 66:5964-5971.
- 142 Orsini B, Ottanelli B, Amedei A, Surrenti E, Capanni M, Del Prete G, Amorosi A, Milani S, Délios MM, surrenti C. *Helicobacter pylori* cag pathogenicity island is associated with reduced expression of interleukin-4 (IL-4) mRNA and modulation of the IL-4delta2 mRNA isoform in human gastric mucosa. *Infect. Immun.* 2003, Nov;71(11):6664-7.
- 143 Zabaleta, J., D. J. McGee, A. H. Zea, C. P. Hernandez, P. C. Rodriguez, R. A. Sierra, P. Correa, and A. C. Ochoa. *Helicobacter pylori* arginase inhibits T cell proliferation and reduces the expression of the TCR zeta-chain (CD3zeta). *J. Immunol.* 2004, 173:586-593.
- 144 D'Elis MM, Manghetti M, Almerigogna F, Amedei A, Costa F, Burrioni D, Baldari CT, Romagnani S, Telford JL, Del Prete G. Different cytokine profile and antigen-specificity repertoire in *Helicobacter pylori*-specific T cell clones from the antrum of chronic gastritis patients with or without peptic ulcer. *Eur J Immunol.* 1997 Jul;27(7):1751-5.
- 145 Banchereau J, and Steinman RM. Dendritic cells and the control of immunity. *Nature* 1998, 392: 245-252.
- 146 Hart DN. Dendritic cells: unique leukocyte populations which control the primary immune response. *Blood* 1997, 90: 3245-3287.

References

- 147 De Smedt T, Van Mechelen M, De Becker G, Urbain J, Leo O, and Moser M. Effect of interleukin-10 on dendritic cell maturation and function. *Eur J Immunol* 1997, 27: 1229-1235.
- 148 Kalinski P, Schuitemaker JH, Hilkens CM, and Kapsenberg ML. Prostaglandin E2 induces the final maturation of IL-12-deficient CD1a+CD83+ dendritic cells: the levels of IL-12 are determined during the final dendritic cell maturation and are resistant to further modulation. *J Immunol*. 1998, 161: 2804-2809.
- 149 Kuroda E, Sugiura T, Zeki K, Yoshida Y, and Yamashita U. Sensitivity difference to the suppressive effect of prostaglandin E2 among mouse strains: a possible mechanism to polarize Th2 type response in BALB/c mice. *J Immunol*. 2000, 164: 2386-2395.
- 150 Liu L, Rich BE, Inobe J, Chen W, and Weiner HL. A potential pathway of Th2 development during primary immune response. IL-10 pretreated dendritic cells can prime naive CD4+ T cells to secrete IL-4. *Adv Exp Med Biol*. 1997, 417: 375-381.
- 151 Peguet-Navarro J, Moulon C, Caux C, Dalbiez-Gauthier C, Banchereau J, and Schmitt D. Inhibitory effect of IL-10 on human Langerhans cell antigen presenting function. *Adv Exp Med Biol*. 1995, 378: 359-361.
- 152 Van der Pouw Kraan TC, Snijders A, Boeijs LC, de Groot ER, Alewijnse AE, Leurs R, and Aarden LA. Histamine inhibits the production of interleukin-12 through interaction with H2 receptors. *J Clin Invest* 102: 1866-1873, 1998
- 153 Vieira PL, de Jong EC, Wierenga EA, Kapsenberg ML, and Kalinski P. Development of Th1-inducing capacity in myeloid dendritic cells requires environmental instruction. *J Immunol* 2000, 164: 4507-4512.
- 154 Cyster JG. Chemokines and the homing of dendritic cells to the T cell areas of lymphoid organs. *J Exp Med* 1999, 189: 447-450.
- 155 Homey B, and Zlotnik A. Chemokines in allergy. *Curr Opin Immunol* 1999, 11: 626-634.
- 156 Sallusto F, and Lanzavecchia A. Efficient presentation of soluble antigen by cultured human dendritic cells is maintained by granulocyte/macrophage colony-stimulating factor plus interleukin 4 and downregulated by tumor necrosis factor alpha. *J Exp Med* 1994, 179: 1109-1118.
- 157 Zlotnik A, and Yoshie O. Chemokines: a new classification system and their role in immunity. *Immunity* 2000, 12: 121-127.
- 158 Caux C, Dezutter-Dambuyant C, Schmitt D, and Banchereau J. GM-CSF and TNF-alpha cooperate in the generation of dendritic Langerhans cells. *Nature* 2002, 360: 258-261.
- 159 Inaba K, Inaba M, Romani N, Aya H, Deguchi M, Ikehara S, Muramatsu S, and Steinman RM. Generation of large numbers of dendritic cells from mouse bone marrow cultures supplemented with granulocyte/macrophage colony-stimulating factor. *J Exp Med* 1992, 176: 1693-1702.
- 160 Maraskovsky E, Brasel K, Teepe M, Roux ER, Lyman SD, Shortman K, and McKenna HJ. Dramatic increase in the numbers of functionally mature dendritic

References

- cells in Flt3 ligand-treated mice: multiple dendritic cell subpopulations identified. *J Exp Med* 1996, 184: 1953-1962.
- 161 Pulendran B, Lingappa J, Kennedy MK, Smith J, Teepe M, Rudensky A, Maliszewski CR, and Maraskovsky E. Developmental pathways of dendritic cells in vivo: distinct function, phenotype, and localization of dendritic cell subsets in FLT3 ligand-treated mice. *J Immunol* 1997, 159: 2222-2231.
- 162 Romani N, Gruner S, Brang D, Kampgen E, Lenz A, Trockenbacher B, Konwalinka G, Fritsch PO, Steinman RM, and Schuler G. Proliferating dendritic cell progenitors in human blood. *J Exp Med* 1994, 180: 83-93.
- 163 Strobl H, Bello-Fernandez C, Riedl E, Pickl WF, Majdic O, Lyman SD, and Knapp W. flt3 ligand in cooperation with transforming growth factor-beta1 potentiates in vitro development of Langerhans-type dendritic cells and allows single-cell dendritic cell cluster formation under serum-free conditions. *Blood* 1997, 90: 1425-1434.
- 164 Zhang Y, Zhang YY, Ogata M, Chen P, Harada A, Hashimoto S, and Matsushima K. Transforming growth factor-beta1 polarizes murine hematopoietic progenitor cells to generate Langerhans cell-like dendritic cells through a monocyte/macrophage differentiation pathway. *Blood* 1999, 93: 1208-1220.
- 165 Borkowski TA, Letterio JJ, Farr AG, and Udey MC. A role for endogenous transforming growth factor beta in Langerhans cell biology: the skin of transforming growth factor beta null mice is devoid of epidermal Langerhans cells. *J Exp Med* 1996, 184: 2417-2422.
- 166 Grouard G, Risoan MC, Filgueira L, Durand I, Banchereau J, and Liu YJ. The enigmatic plasmacytoid T cells develop into dendritic cells with interleukin (IL)-3 and CD40-ligand. *J Exp Med* 1997, 185: 1101-1111.
- 167 Maraskovsky E, Daro E, Roux E, Teepe M, Maliszewski CR, Hoek J, Caron D, Lebsack ME, and McKenna HJ. In vivo generation of human dendritic cell subsets by Flt3 ligand. *Blood* 2000, 96: 878-884.
- 168 Pulendran B, Banchereau J, Burkeholder S, Kraus E, Guinet E, Chalouni C, Caron D, Maliszewski C, Davoust J, Fay J, and Palucka K. Flt3-ligand and granulocyte colony-stimulating factor mobilize distinct human dendritic cell subsets in vivo. *J Immunol* 2000, 165: 566-572.
- 169 Rescigno M, Granucci F, and Ricciardi-Castagnoli P. Dendritic cells at the end of the millennium. *Immunol Cell Biol* 1999, 77: 404-410.
- 170 Sallusto F, and Lanzavecchia A. Understanding dendritic cell and T-lymphocyte traffic through the analysis of chemokine receptor expression. *Immunol Rev* 2000, 177: 134-140.
- 171 Sallusto F, Mackay CR, and Lanzavecchia A. The role of chemokine receptors in primary, effector, and memory immune responses. *Annu Rev Immunol* 2000, 18: 593-620.
- 172 Mary F., Lipscomb and Barbara J. Masten. Dendritic cells: Immune Regulators in Health and Disease. *Physiol. Rev.* 2002; 82:97-130.

References

- 173 Steinman RM, and Swanson J. The endocytic activity of dendritic cells. *J Exp Med* 1995, 182: 283-288.
- 174 Harshyne LA, Watkins SC, Gambotto A, and Barratt-Boyes SM. Dendritic cells acquire antigens from live cells for cross-presentation to CTL. *J Immunol* 2001, 166: 3717-3723.
- 175 Larsson M, Fonteneau JF, and Bhardwaj N. Dendritic cells resurrect antigens from dead cells. *Trends Immunol* 2001, 22: 141-148.
- 176 Geissmann F, Launay P, Pasquier B, Lepelletier Y, Leborgne M, Lehuen A, Brousse N, and Monteiro RC. A subset of human dendritic cells expresses IgA Fc receptor (CD89), which mediates internalization and activation upon cross-linking by IgA complexes. *J Immunol* 2001, 166: 346-352.
- 177 Dixon, G. L., P. J. Newton, B. M. Chain, D. Katz, S. R. Andersen, S. Wong, P. van der Ley, N. Klein, and R. E. Callard. Dendritic cell activation and cytokine production induced by group B *Neisseria meningitidis*: interleukin-12 production depends on lipopolysaccharide expression in intact bacteria. *Infect. Immun.* 2001, 69:4351-4357.
- 178 Verhasselt, V., C. Buelens, F. Willems, D. De Groote, N. Haeflner-Cavaillon, and M. Goldman. Bacterial lipopolysaccharide stimulates the production of cytokines and the expression of costimulatory molecules by human peripheral blood dendritic cells: evidence for a soluble CD14-dependent pathway. *J. Immunol.* 1997, 158:2919-2925.
- 179 Galgani M, Busiello I, Censini S, Zappacosta S, Racioppi L, Zarrilli E. *Helicobacter pylori* induces apoptosis of human monocytes but not monocyte-derived dendritic cells: role of the cag pathogenicity island. *Infect Immun.* 2004 Aug;72(8): 4480-5.
- 180 Hafsi N., Volland P., Schwendy S., Rad R., Reindl W., Gerhard M. And Princ C. Human dendritic cells repond to *Helicobacter pylori*, promoting NK cell and Th1-effector responses in vitro. *J. Immunol* 2004. 173: 1249-57.
- 181 Carson BD, Lopes JE, Soper DM, Ziegler SF. Insights into transcriptional regulation by FOXP3. *Front Biosci.* 2006 May 1;11:1607-19.
- 182 Allan SE, Passerini L, Bacchetta R, Crellin N, Dai M, Orban PC, Ziegler SF, Roncarolo MG, Levings MK. The role of 2 FOXP3 isoforms in the generation of human CD4 Tregs. *J Clin Invest.* 2005 Nov 1;115(11):3276-3284. Epub 2005 Oct 6.
- 183 Levings MK, Sangregorio R, Sartirana C, Moschin AL, Battaglia M, Orban PC, Roncarolo MG. Human CD25+CD4+ T suppressor cell clones produce transforming growth factor beta, but not interleukin 10, and are distinct from type 1 T regulatory cells. *J Exp Med.* 2002 Nov 18;196(10):1335-46.
- 184 Kirkland T, Viriyakosol S, Pérez-Pérez GI, and Blaser MJ. 1997. *Helicobacter pylori* lipopolysaccharide can activate 70Z/3 cells via CD14. *Infect. Immun.* 1997, 65:604–608.
- 185 Muotiala, A., Helander, I.M., Pyhala, L., Kosunen, T.U., and Moran, A.P. Low biological activity of *Helicobacter pylori* lipopolysaccharide. *Infect. Immun.* 1992, 60:1714–1716.

References

- 186 Ogawa, T., et al. Endotoxic and immunobiological activities of a chemically synthesized lipid A of *Helicobacter pylori* strain 206-1. *FEMS Immunol. Med. Microbiol.* 2003, 36:1–7.
- 187 Gewirtz, A.T., et al. 2003. *Helicobacter pylori* evades toll like receptor 5 in innate immunity. *Gastroenterology*. 4:A592. (Abstr.)
- 188 Krieg, A.M. 2002. CpG motifs in bacterial DNA and their immuneeffects. *Annu. Rev. Immunol.* 20:709–760.
- 189 Kao JY, Pierzchala A., Rathinavelu S., Zavros Y., Tessier A., Merchant JI. Somatostatin inhibit dendritic cell responsiveness to *Helicobacter pylori*. *Regul Pept.* 2005 Dec 19.
- 190 Molinari M, Salio M, Galli C, Norais N, Rappuoli R, Lanzavecchia A, Montecucco C. Selective inhibition of li-dependent antigen presentation by *Helicobacter pylori* toxin VacA. *K Exp Med* 1998, 187:135-140.
- 191 Gerbert G, Fischer W, Weiss E, Hoffmann R, Haas R. *Helicobacter pylori* Vacuolating cytotoxin inhibits T lymphocyte activation. *Science* 2003, 301:1099-1102.
- 192 Boncristiano M, Paccani SR, Barone S, Ulivieri C, Patrussi L, Ilver D, Amedei A, Délios MM, Telford JL at al. The *Helicobacter pylori* vacuolating toxin inhibits T cell activation by two independent mechanisms. *J. Exp Med* 2003, 198:1887-1897.
- 193 Neu B, Randlkofer P, Neuhofer M, Voland P, Mayerhofer A, Gerhard M, Schepp W, Prinz C. *Helicobacter pylori* induces apoptosis of rat gastric parietal cells. *Am J Physiol Gastroinvest Liver Physiol* 2002, 283:G309-G318.
- 194 Boncristiano M, Paccani SR, Barone S, Ulivieri C, Patrussi L, Ilver D, Amedei A, Délios MM, Telford JL at al. The *Helicobacter pylori* vacuolating toxin inhibits T cell activation by two independent mechanisms. *J. Exp Med* 2003, 198:1887-1897.
- 195 Lee-Ann H. Allena,b, Larry S. Schlesingera, and Byoung Kanga Virulent Strains of *Helicobacter pylori* Demonstrate Delayed Phagocytosis and Stimulate Homotypic Phagosome Fusion in Macrophages *The Journal of Experimental Medicine*, Volume 191, Number 1, January 3, 2000 115-128.
- 196 Andersen, L.P., Blom, J., Nielsen, H. Survival and ultrastructural changes of *Helicobacter pylori* after phagocytosis by human polymorphonuclear phagocytes and monocytes. *APMIS.* 1993, 101:61-72.
- 197 Engstrand, L., Graham, D., Scheynius, A., Genta, R.M., El-Zaatari, F. Is the sanctuary where *Helicobacter pylori* avoids antibacterial treatment intracellular? *Am. J. Clin. Pathol.* 1997, 108:504-509.
- 198 Ramarao N, Gray-Owen SD, Meyer TF. *Helicobacter pylori* induces but survives the extracellular release of oxygen radicals from professional phagocytes using its catalase activity *Mol Microbiol.* 2000 Oct; 38(1):103-13.
- 199 Gerhard M, Schmees C, Voland P, Endres N, Sander M, Reindl W, Rad R, Oelsner M, Decker T, Mempel M, Hengst L, Prinz C. A secreted low-molecular-

References

- weight protein from *Helicobacter pylori* induces cell-cycle arrest of T cells. *Gastroenterology* 2005 May; 128(5):1327-39.
- 200 Makristathis A, Rokita E, Labigne A, Willinger B, Rotter ML, Hirschl AM. Highly significant role of *Helicobacter pylori* urease in phagocytosis and production of oxygen metabolites by human granulocytes. *J Infect Dis* 1998; 177:803-6.
- 201 Rokita E, Makristathis A, Presterl E, Rotter ML, Hirschl AM. *Helicobacter pylori* urease significantly reduces opsonization by human complement. *J Infect Dis* 1998; 178:1521-5
- 202 A. Makristathis, E Rokita, E Pasching, P Apfalter, B Willinger, M Rotter and AM Hirschl Urease prevents adherence of *Helicobacter pylori* to KatIII gastric epithelial cells. *Journal of Infectious Diseases* 2001; 184:439-45.
- 203 St. Geme JW, Cutter D. Influence of pili, fibrils, and capsule on in vitro adherence by *Haemophilus influenzae* type b. *Mol Microbiol* 1996; 21:21-31.
- 204 Hammerschmidt S, Hilse R, van Putten JP, Gerardy Schahn R, Unkmeir A, Frosch M. Modulation of cell surface sialic acid expression in *Neisseria meningitidis* via a transposable genetic element. *EMBO J* 1996; 15:192-8.
- 205 Makristathis A, Rokita E, Labigne A, Willinger B, Rotter ML, Hirschl AM. Highly significant role of *Helicobacter pylori* urease in phagocytosis and production of oxygen metabolites by human granulocytes. *J Infect Dis* 1998; 177:803-6.
- 206 Rokita E, Makristathis A, Presterl E, Rotter ML, Hirschl AM. *Helicobacter pylori* urease significantly reduces opsonization by human complement. *J Infect Dis* 1998; 178:1521-5.
- 207 Bortolussi R, Ferrieri P, Quie PG. Influence of growth temperature of *Escherichia coli* on K1 capsular antigen production and resistance to opsonization. *Infect Immun* 1983; 39:1136-41.
- 208 Domenico P, Tomas JM, Merino S, Rubires X, Cunha BA. Surface antigen exposure by bismuth dimercaprol suppression of *Klebsiella pneumoniae* capsular polysaccharide. *Infect Immun* 1999; 67:664-9.
- 209 Lundgreen A, Stromberg E, Sjolting A, Lindholm C, Enarsson K, Edebo A, Johnsson E, Suri-Payer E, Larsson P, Rudin A, Svennerholm AM, Lundin BS. Mucosal FOXP3-expressing CD4+ CD25high regulator T cells in *Helicobacter pylori*-infected patients. *Infect Immunol* 2005 Jan; 73 (1)
- 210 Romano M., Ricci A. Di Popolo, Sommi P, Del Vecchio B C., Bruni C.B., Ventura U., Cover T.L., Blaser M.J. Coffey R.J. and Zarrilli R. *Helicobacter pylori* upregulates expression of epidermal growth factor-related peptides, but inhibits their proliferative effect in MKN 28 gastric mucosal cells. *J Clin Invest.* 1998 Apr 15;101(8):1604-13.
- 211 Ferrero RL, Cussac V, Courcoux P, Labigne A. Construction of isogenic urease-negative mutants of *Helicobacter pylori* by allelic exchange. *J Bacteriol* 1992; 174:4212-7.
- 212 Cussac V, Ferrero RL, Labigne A. Expression of *Helicobacter pylori* urease genes in *Escherichia coli* grown under nitrogen-limiting conditions. *J Bacteriol* 1992; 174:2466-73.

References

- 213 McGee, D. J., C. A. May, R. M. Garner, J. M. Himpel, and H. L. Mobley. Isolation of *Helicobacter pylori* genes that modulate urease activity. *J. Bacteriol.* 1999, 181:2477-2484.
- 214 Weatherburn, MW Phenol-hypochlorite reaction for determination of ammonia. *Anal. Chem.* 1967, 39:971-974,
- 215 Ellis, PD, KM Hadfield, JC Pascall, and KD Brown. Heparin-binding epidermal-growth-factor-like growth factor gene expression is induced by scrape-wounding epithelial cell monolayers: involvement of mitogen-activated protein kinase cascade. *J. Biochem.* 2001, 354:99-106.
- 216 Barnard, JA, RD Beauchamp, WE Russell, RN Dubois, and R. J. Coffey. Epidermal growth factor-related peptides and their relevance to gastrointestinal pathophysiology. *Gastroenterol.* 1995, 108:564-580.
- 217 Labenz, J., and G. Borsch. Highly significant change of the clinical course of relapsing and complicated peptic ulcer disease after cure of *Helicobacter pylori* infection. *Am. J. Gastroenterol.* 1994, 89:1785-1788.
- 218 Peek, R. M. Jr., M. J. Blaser, D. J. Mays, M. H. Forsyth, T. L. Cover, S. Y. Song, U . Krishna, and J. A. Pietenpol. *Helicobacter pylori* strain-specific genotypes and modulation of the gastric epithelial cell cycle. *Cancer Res.* 1999, 59:6124-6131.
- 219 Konturek SJ, T Brzozowski, PC Konturek, S Kwiecien, E Karczewska, D Drozdowicz, J Stachura, and EG Hahn. *Helicobacter pylori* infection delays healing of ischaemia-reperfusion induced gastric ulcerations: new animal model for studying pathogenesis and therapy of *H. pylori* infection. *Eur. J. Gastroenterol. Hepatol.* 2000, 12:1299-1313.
- 220 Romano M., V Ricci, A Di Popolo, P Sommi, BC Del Vecchio, CB Bruni, U Ventura, TL Cover, MJ Blaser, RJ Coffey, and R Zarrilli. *Helicobacter pylori* upregulates expression of epidermal growth factor-related peptides, but inhibits their proliferative effect in MKN 28 gastric mucosal cells. *J. Clin. Invest.* 1998, 101:1604-1613.
- 221 Han J, J D Lee, L Bibbs, and RJ Ulevitch. A MAP kinase targeted by endotoxin and hyperosmolarity in mammalian cells. *Science* 1994, 265:808.
- 222 Kyriakis JM, P Bonlyee, E Nikolakoki, T Dai, EA Rubie, M F Ahmad, J Avruck, and JR Woodgett. The stress-activated protein kinase subfamily of c-Jun kinases. *Nature* 1994, 369:156.
- 223 Lee JC, JT Laydon, PC McDonnell, TF Gallagher, S Kumar, D Green, D McNulty, MJ Blumenthal, JR Heys, and SW Landvatter. A protein kinase involved in the regulation of inflammatory cytokine biosynthesis. *Nature* 1994, 372:739.
- 224 Ellis PD, KM Hadfield, JC Pascall, and KD Brown. Heparin-binding epidermal-growth-factor-like growth factor gene expression is induced by scrape-wounding epithelial cell monolayers: involvement of mitogen-activated protein kinase cascade. *J. Biochem.* 2001, 354:99-106.
- 225 Wilson SE, YG He, J Weng, JD Zieske, JV Jester, and GS Schultz. Effect of epidermal growth factor, hepatocyte growth factor, and keratinocyte growth factor, on proliferation, motility and differentiation of human corneal epithelial cells. *Exp. Eye Res.* 1994, 59:665-678.

References

- 226 Barnard, JA, R Gravesdeal, MR Pittelkow, RN Dubois, P Cook, GW. Ramsey, P R Bishop, L Damstrup, and RJ Coffey. Auto-induction and cross-induction within the mammalian epidermal growth factor-related peptide family. *J. Biol. Chem.* 1994, 269:22817-22822.
- 227 Murayama, Y, J Miyagawa, S Higashiyama, S Kondo, M Yabu, K Isozaki, Y Kayanoki, S Kanayama, Y Shinomura, and N Taniguchi. Localisation of heparin-binding epidermal growth factor-like growth factor in human gastric mucosa. *Gastroenterol.* 1995, 109:1051-1059.
- 228 Bamford KB, X Fan, SE Crowe, JF Leary, WKGourley, GK Luthra, EG Brooks, DY Graham, V.E. Reyes and P.B. Ernst. Lymphocytes in the human gastric mucosa during *Helicobacter pylori* have a T helper cell 1 phenotype. *Gastroenterology* 1998, 114:482-492.
- 229 Lindholm C, M Quiding-Jarbrink, H Lonroth, A Hamlet and AM svennerholm. Local cytokine response in *Helicobacter pylori*-infected subjects. *Infect. Immun.* 1998, 66:5864-71.
- 230 Mohammadi M, SJ Czinn, R Redline and J Nedrud. *Helicobacter*-specific cell-mediated immune responses display a predominant Th1 phenotype and promote a delayed-type hypersensitivity response in the stomachs of mice. *J.Immunol.* 1996, 156:4729-38.
- 231 Délios MM, Amedei A, Benagiano M, Azzuri A, Del Prete G. *Helicobacter pylori*, T cells and cytokines: the "dangerous Liaisons". *FEMS Immunol Med Microbiol.* 2005 May 1;44(2):113-9.
- 232 Mohammadi M, J Nedrud, R Redline, N Lycke and SJ Czinn. Murine CD4+ Tcell response to *Helicobacter* infection: TH1 cells enhance gastritis and TH2 cells reduce bacterial load. *Gastroenterology* 1997, 113:1848-57.
- 233 Smythies LE, KB Waites, JR Lindsey, PR Harris, P Ghiara and PD Smith. *Helicobacter pylori*-induced mucosal inflammation is TH1 mediated and exacerbated in IL-4, but not IFG-gamma, gene deficient mice. *J. Immunol.* 2000, 165:1022-29.
- 234 Sommer F, G Faller, M Rollinghoff, T Kirchner, TW Mark and M Lohoff. Lack of gastritis and of an adaptive immune response in infection regulatory factor-1 deficient mice infected with *Helicobacter pylori*. *Eur.J.Immunol.* 2002, 31:396-402.
- 235 Banchereau J, Briere F, Caux C, Davoust J, Lebecque S, Liu YJ, Pulendran B, Palucka K. Immunobiology of dendritic cells. *Annu Rev Immunol* 2000; 18:767-811.
- 236 Kim CH, Broxmeyer HE. Chemokines: Signal lamps for trafficking T and B cells for development and effector function. *J Leukoc Biol.* 1999, Jan;65(1):6-15
- 237 Chen W, Jin W, Hardegen N, Lei KJ, Li L, Marinos N, McGrady G, Wahl SM. Conversion of peripheral CD4+CD25- naive T cells to CD4+CD25+ regulatory T cells by TGF-beta induction of transcription factor Foxp3. *J Exp Med.* 2003 Dec 15;198(12):1875-86.
- 238 Park HB, Paik DJ, Jang E, Hong S, Youn J. Acquisition of anergic and suppressive activities in transforming growth factor-beta-costimulated CD4+CD25- T cells. *Int Immunol.* 2004 Aug;16(8):1203-13. Epub 2004 Jul 5.

References

- 239 Kuck D, B Kolmerer, C Iking-Konert, PH Krammer, W Stremmel, and J Rudi. Vacuolating cytotoxin of *Helicobacter pylori* induces apoptosis in the human gastric epithelial cell line AGS. *Infect. Immun.* 2001, 69:5080-5087.
- 240 Mendall MA, PM Goggin, and N Molineaux. Childhood living conditions and *Helicobacter pylori* seropositivity in adult life. *Lancet* 1992, 339:896-897.
- 241 Blaser MJ. The versatility of *Helicobacter pylori* in the adaption to the human stomach. *J. Physiol. Pharmacol.* 1997, 48:307-314.
- 242 Segal ED. Electroporation of *Helicobacter pylori*. *Methods Mol Biol* 1995; 47:179-84.
- 243 Ng PK, Mitra G, Lundblad JL. Simultaneous salt and ethanol removal from human serum albumin. *J Pharm Sci* 1978; 67:431-3
- 244 Luther SA, Cyster JG. Chemokines as regulators of T cell differentiation. *Nat Immunol.* 2001 Feb;2(2):102-7.

Abbreviations

AIX	anion exchange chromatography
cDNA	complemented DNA
DC	dendritic cell
DNA	deoxyribonucleic acid
EDTA	ethylenediaminetetraacetic acid
ELISA	enzyme linked immunoassay
FCS	fetal calf serum
FITC	fluoresce isothiocyanate
HIC	hydrophobic interaction chromatography
HRP	horseradish peroxidase
Ig	immunoglobulin
IL	interleukin
kb	kilobase
kDa	kilodalton
MAP	mitogen activated protein
mM	milimol
PAGE	polyacrylamide gel electrophoresis
PAI	pathogenicity island
PC5	phycoerythrin-cyanin 5.1
PE	phycoerythrin
PMN	polymorphonuclear
ROI	reactive oxygen ontermediates
PBS	phosphate salin buffer
PE	phycoerythrin
RNA	ribonucleic acid
RT	reverse transcriptase
SDS	sodium dodecyl sulphate
SEX	size exclusion chromatography

CURRICULLUM VITAE

NAME: KOVÁCH, Zsuzsanna

DATE OF BIRTH: 08.01.1977.

MARITAL STATUS: married (2005)

NATIONALITY: Hungarian

EDUCATION:

2001-2006 Studies for a doctor's degree (PhD), University of Technology, Vienna

1997-2000: Studies of Molecular Biology and immunology, Faculty of Biology of Eötvös Loránd University of Sciences

1999-2000 Labor experiences in University of Tampere Medical School, Finland

1995-1997: Studies of Biology, Eötvös Loránd University Faculty of Sciences, and German specialised translator Certificate

1991-1995: Berze Nagy János Secondary School, General Certificate of Secondary Education

1993: German language exam (middle level)

1983-1991 Elementary school in Gyöngyös

EXAMINATIONS AND DEGREES:

2006 Doctor's degree (Doctor of Science) in process

PhD-thesis: "In vitro investigation of the role of Helicobacter pylori urease in repair mechanisms of gastric epithelial cells and cytokine release by monocyte derived dendritic cells"

2000 Diploma in Molecular Biology and Immunology (Master of Science), Eötvös Loránd University Faculty of Sciences

Diploma thesis: "Polymorphisms of the genes of the inflammatory cytokines predict development of gastric cancer during Helicobacter pylori-infection"

2000 Diploma: Biology specialized german language translator, Eötvös Loránd University Faculty of Sciences

1997 Base level, general Biology exams, Eötvös Loránd University Faculty of Sciences

1995 Secondary school's leaving certificate

STUDIED BASIC SUBJECTS:

Mathematics, Anatomy, Biochemistry, Physical chemistry, Analytical chemistry, Organic and Inorganic chemistry, Atomic physics, Animal and Plant physiology, Animal and Plant organism, Computer technology, Ethology, Nature biology, Taxology, Genetics, Molecularbiology, Immunology

STUDIED SPECIAL SUBJECTS:

Immunology, Cell signal transfer, Protein science, Genetics, Microbiology, Medical Statistic.

PLACE OF WORK:

2001-2006 Hygiene-Institute, Dept. of Clinical Microbiology (Prof. A. Makristathis), University of Vienna

1999-2000 University of Tampere Medical School, Department of Microbiology and Immunology, (Laboratory of prof. Mikko Hurme) Tampere, FINLAND:

Polymorphisms of the genes of the inflammatory cytokines predict development of gastric cancer during *Helicobacter pylori*-infection

Ref: M.Hurme, Z. Kovách, H. Rautelin, O. P. Heinonen, J. Virtamo and T. U. Kosunen. Interleukin-10 haplotype is associated with increased risk for gastric cancer during *Helicobacter pylori*-infection. Manuscript.

REFERENCES:

2004 Novel real-time PCR assay for detection of *Helicobacter pylori* infection and simultaneous clarithromycin susceptibility testing of stool and biopsy specimens. Schabereiter-Gurtner C, Hirschl AM, Dragosics B, Hufnagl P, Puz S, Kovach Z, Rotter M, Makristathis A. *J Clin Microbiol.* 2004;42(10):4512-8.

2000 Z. Kovách, M. Hurme, TU Kosunen. IgA antibody levels against *Helicobacter pylori* are regulated by the IL-1 gene genotype. Manuscript.

LEBENS LAUF

NAME: Zsuzsanna Kovách
GEBURTSDATUM: 08.01.1977
FAMILIENSTAND: verheiratet (2005)
STAATSBÜRGERSCHAFT: Ungarin

AUSBILDUNG:

2001-2006 Doktoratstudium der Naturwissenschaften, Fakultät Technische Chemie, Technische Universität Wien
1997-2000 Studienabschnitt Molekularbiologie und Immunologie, Eötvös Lóránd Universität, Budapest
1999-2000 Laborpraktikum, Medizinische Universität Tampere, Finnland
1995-1997 Studienabschnitt Biologie, Eötvös Lóránd Universität, Budapest
Lóránd Universität, Budapest
1991-1995 Berze Nagy János Gymnasium
1983-1991 Volksschule in Gyöngyös

PRÜFUNGSNACHWEISE:

2006 Doktoratsprüfung, Verleihung des Titels Dr.rer.nat. (im Gange)
Doktorarbeit: "In vitro Untersuchung der Rolle von Helicobacter pylori urease in Reparaturmechanismen von Magenepithelzellen und die Freisetzung der Zytokine von Monocyte abgeleiteten Dendritische Zellen"
2000 2.Studienabschnitt Molekularbiologie und Immunologie, Verleihung des Titels Mag.rer.nat. Diplomarbeit: "Polimorfismen der inflammatorischen Zytokine gene verhindert Magenkarzinom Entwicklung während der Helicobacter pylori Infektion"
2000 Diplom: Fachübersetzerin der deutsche Sprache, Biologie, Eötvös Lóránd Universität, Budapest
1997 1.Studienabschnitt Biologie, Eötvös Lóránd Universität, Budapest
1995 Matura

GRUNDAUSBILDUNG:

Mathematik, Anatomie, Biochemie, Physische Chemie, Analytische Chemie, Organisch- und Unorganische Chemie, Atomphysik, Animal- und Pflanzenphysiologie, Taxonomie, Verhaltensforschung, Umweltforschung, Genetik, Molekularbiologie, Immunologie

SPEZIELLE AUSBILDUNG:

Immunologie, Signal Transduktion, Proteinforschung, Genetik, Mikrobiologie, Medizinische Statistika.

ARBEITSTELLEN:

2001-2006 Hygiene-Institut, Abt. Für Klinische Mikrobiologie (Prof. A. Makristathis), Medizinische Universität Wien

1999-2000 Abt. für Mikrobiologie und Immunologie (Prof. M. Hurme), Medizinische Universität Tampere

REFERENZEN:

2004 Novel real-time PCR assay for detection of *Helicobacter pylori* infection and simultaneous clarithromycin susceptibility testing of stool and biopsy specimens. Schabereiter-Gurtner C, Hirschl AM, Dragosics B, Hufnagl P, Puz S, Kovach Z, Rotter M, Makristathis A.J Clin Microbiol. 2004;42(10):4512-8.

2000 Z. Kovách, M. Hurme, TU Kosunen. IgA antibody levels against *Helicobacter pylori* are regulated by the IL-1 gene genotype. Manuscript.